



Červenka Consulting s.r.o.
Na Hřebenkách 55
150 00 Prague
Czech Republic
Phone: +420 220 610 018
E-mail: cervenka@cervenka.cz
Web: <http://www.cervenka.cz>

ATENA Program Documentation Part 4-7

ATENA Science – GiD FRC Examples & Tutorial

Example manual and step by step guide for
nonlinear analysis of fiber reinforced concrete
structures with ATENA Science

Written by

**Tereza Sajdlová, Petr Kabele, Jan Červenka,
Zdeněk Janda**

Prague, December 20, 2016



The manual and related program features/modules were developed during a research project TA03011564 “Computer model for high performance fibre reinforced concrete material” funded by Technology Agency of the Czech Republic:

Material model for high performance fibre reinforced concrete material - Nonlinear Cementitious HPFRC and FRC material

T A

Č R

Technology
Agency
of the Czech Republic

Trademarks:

ATENA is registered trademark of Vladimir Cervenka.

GiD is registered trademark of CIMNE of Barcelona, Spain.

Microsoft and Microsoft Windows are registered trademarks of Microsoft Corporation.

Other names may be trademarks of their respective owners.

Copyright © 2015-2016 Červenka Consulting s.r.o.

1 CONTENTS

1	CONTENTS	1
2	INTRODUCTION	1
3	BRIEF OVERVIEW	2
4	THE STEPS BEFORE MATERIAL MODEL DETERMINATION	3
4.1	Starting Program	3
4.2	Loading the Model	3
5	FRC MATERIAL MODEL	10
5.1	Necessary Information for Creating FRC Material Model	10
5.2	Determining the FRC Material Model Parameters	11
5.2.1	Modification of the Default Material Model	12
5.2.2	Running the Analysis	20
5.2.3	Load-Displacement Diagram and its export from ATENA to Excel File or Similar	21
5.2.4	Analysis of the results and subsequent material modification	28
5.2.5	General Instructions for Inverse Analysis	38
6	ANALYSIS OF SHORT TERM BEHAVIOR OF HIGH PERFORMANCE FIBER REINFORCED CONCRETE STRUCTURES	39
6.1	Simulation of SHCC shear beam test	39
6.1.1	Introduction	39
6.1.2	Material parameters	40
6.1.3	Results	42
6.2	Simulation of HSFRC shear beam test	46
6.2.1	Introduction	46
6.2.2	Material parameters	46
6.2.3	Results	47
7	ANALYSIS OF LONG TERM BEHAVIOR OF HIGH PERFORMANCE FIBRE REINFORCED CONCRETE STRUCTURES	51
7.1	Simulation of ECC creep test – bending specimen under sustained load	51
7.1.1	Introduction	51
7.1.2	Material parameters	52
7.1.3	Results	54
8	SIMULATION OF MOISTURE TRANSPORT AND DRYING SHRINKAGE PROPERTIES OF STEEL FIBRE REINFORCED CONCRETE	56
8.1	Material parameters	59
8.2	Results	60
9	THERMAL ANALYSIS OF HIGH PERFORMANCE FIBER REINFORCED CONCRETE STRUCTURES	64
9.1	Introduction	64
9.2	Thermal analysis	65

9.3	Stress analysis.....	67
8	APPLICATION OF FRC MATERIAL MODEL	71
8.1	Vault Bending Tests	71
8.2	Model of Segment (Keystone) in Compression.....	72
9	CONCLUSION.....	73
10	PROGRAM DISTRIBUTORS AND DEVELOPERS.....	74
11	LITERATURE.....	75

2 INTRODUCTION

Fiber reinforced concrete (FRC) composites are more and more often used in engineering practice, and therefore the need of numerical models describing these materials increases. Material behavior is more difficult to describe in comparison with ordinary concrete. Cementitious composites are combined with randomly oriented fibers made from different materials (steel, polymers, glass, etc.) and applied in different fractions.

The issue is to find the appropriate input material parameters to successfully model FRC. In particular, the tensile parameters that are important for FRC must be determined properly. The measured response of direct tensile test can serve for direct input of the parameters into the material model. Unfortunately, preparation of test sample is complicated and the test is not performed very often. The three or four point bending tests are more common. Results can be also used for the material model however they cannot be directly put into the model. Inverse analysis of the results must be performed to identify model parameters correctly.

This tutorial provides instructions regarding modeling of fiber reinforced concrete (FRC) materials using the programs **ATENA** and **GiD**. **ATENA-GiD** is a finite element based software system specifically developed for the nonlinear analysis of reinforced concrete structures. Besides the material models for ordinary reinforced concrete, **ATENA** offers special numerical models accounting for the FRC specifics such as shape of tensile softening branch, high toughness and ductility.

This tutorial contains a step by step explanation on how to obtain the input parameters of the FRC material model and its application for the analysis of the segmental tunnel lining. The four point bending test (simply supported beam loaded by two loads) is used for the determination of the material parameters, see Figure 1. Usually, results of this test are available for FRC together with those from a compressive test. It is also possible to use the three point bending test results, modify the geometry of the model, and follow the instructions in the tutorial. More details about the problem or experiment can be obtained from the program developer or distributor.

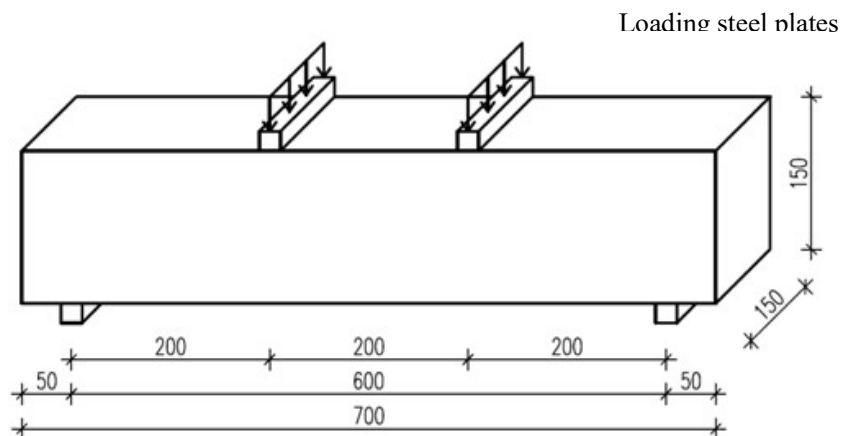


Figure 1: Geometry of the structure for inverse analysis of material model parameters

This manual is targeted for intermediate **ATENA-GiD** users who have already finished the basic **ATENA** and **GiD** tutorial. The preparation of the model is not described in detail, as it can be done according to the basic **ATENA-GiD** tutorial. This document is focused just on the material model determination and its application.

3 BRIEF OVERVIEW

To summarize this tutorial, basic steps of the procedure are highlighted now. The method how to obtain the material model for fiber reinforced concrete requires the knowledge of material model for ordinary concrete that is subsequently modified to FRC. To have an opportunity to define model more in the detail, **CC3DNonLinCementitious2User** is utilized and user can define his own laws in this fracture-plastic material model. Most important parameters for modeling FRC include:

- tensile stress – strain law (tensile function) – describes ductility in tension, it is the most important parameter for FRC modeling,
- tensile strength – tensile strength of FRC is usually higher than for ordinary concrete, thus it should be modified, this value also governs the y-axis of tensile function,
- compressive stress – strain law (compressive function) – describes ductility in compression,
- reduction of compressive strength due to cracks (Fc Reduction-COMPRED) – function describing how cracks reduce material compressive strength, default function drops sharply, for FRC it is recommended to keep the function constant with value 1 (it means no reduction of compressive strength due to cracks).

Procedure how to determine material model for FRC consists of following steps:

- initial setup of the tensile parameters (tensile strength, tensile function),
- running the analysis,
- export the load-displacement diagram from **ATENA** to excel file or similar,
- comparison of load-displacement diagram from calculation and laboratory test,
- if the difference between diagrams is within the user accuracy limits, the determination of FRC model is completed,
- if the difference between diagrams is not within the user accuracy limits, the input parameters must be modified in order to achieve better results, and again compare with the laboratory results. This step must be repeated until the results are satisfactory.

4 THE STEPS BEFORE MATERIAL MODEL DETERMINATION

4.1 Starting Program

After the installation of the programs **GiD** and **ATENA** during the basic tutorial [1], you can start a nonlinear analysis using the **ATENA-GiD** system. Firstly, the program **GiD** is started, e.g. from the start menu of your computer using the following menu path: **Start | All Programs | CervenkaConsulting | ATENA Science | GiD**. This opens the program **GiD** which is used for the preparation of the numerical model of the analyzed structure.

If you do not have installed the above mentioned programs yet, you can install them following the instructions from the ATENA-GiD manual [2].

4.2 Loading the Model

To start the model determination described in the following chapters, it is necessary to load the prepared model by selecting **Files | Open** in **GiD** and choosing the file: **%Public%\Documents\ATENA Examples\Science\GiD\Tutorial.FRC\FRC_4PBT_2D_initial model.gid**.

The prepared model contains beam loaded by two described displacement at the top plates and supported by two bottom plates, see Figure 2. The geometry corresponds to the beam in Figure 1. The top and bottom plates are connected to the beam through fixed contacts (Master-Slave). The reactions are monitored at the supports, both on the left (Reaction L) and the right (Reaction R) bottom plate. The displacement of the beam is monitored in the middle at the point under the beam by boundary condition **Monitor for Point Nearest Node IP**, see Figure 3.

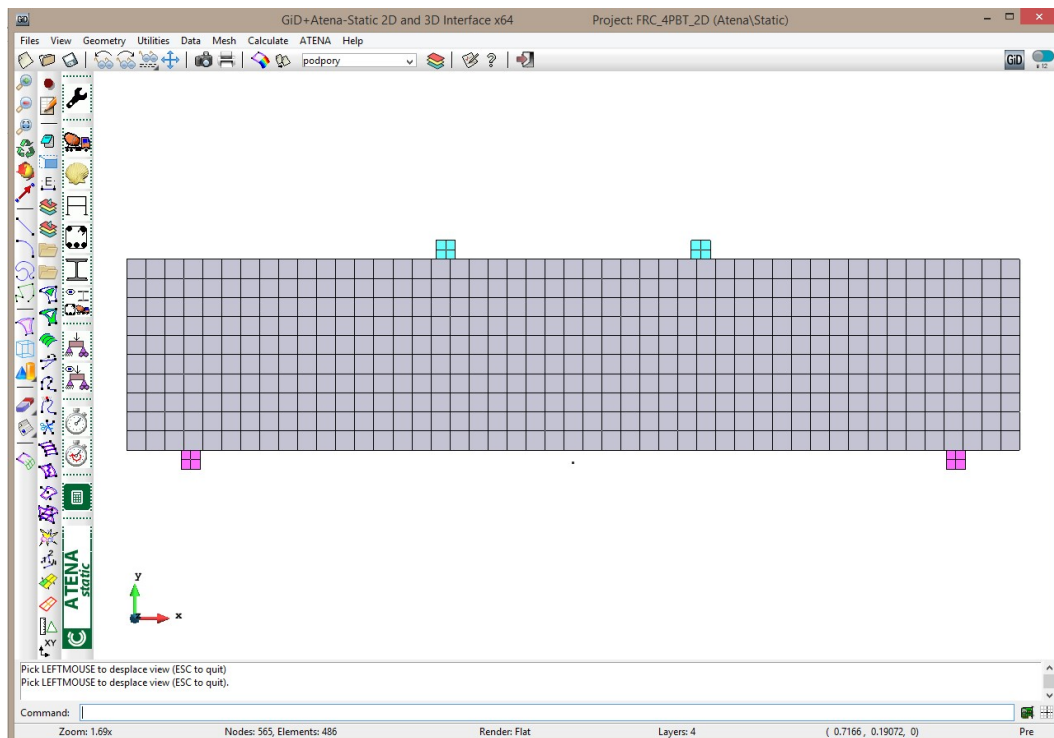


Figure 2: Prepared model of the four point bending test in GiD

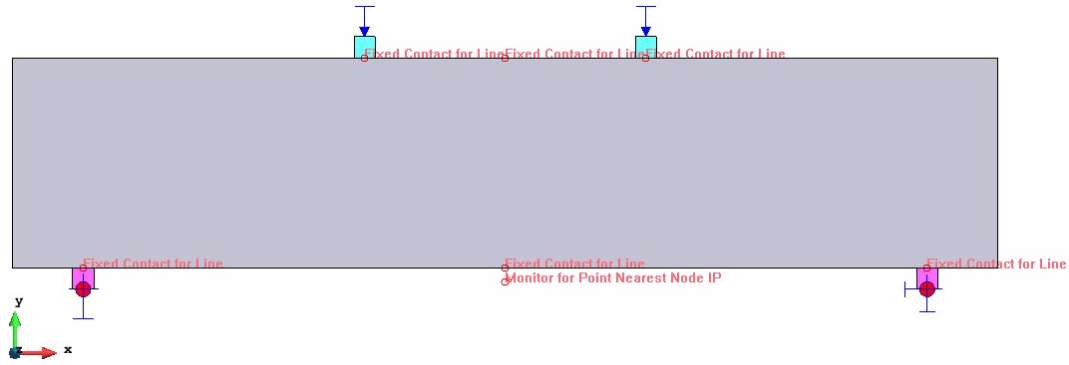


Figure 3: Boundary conditions

The size of the finite element mesh is 0.015 m (10 finite elements per height and 47 elements per length). The model consists of 486 finite elements (470 elements in beam and 16 elements in plates), see Figure 4. Two different materials are used in the model. The material named **Plates** is **SOLID Elastic** and it represents steel, the parameters are shown in the Figure 7 to Figure 9. The second material **FRC beam** is **SOLID Concrete** with the material prototype **CC3DNonLinCementitious2User** (see Figure 10 to Figure 16). At this stage, the material model has default values of its parameters. The process how to modify these parameters in order to model FRC successfully is described in the following sections.

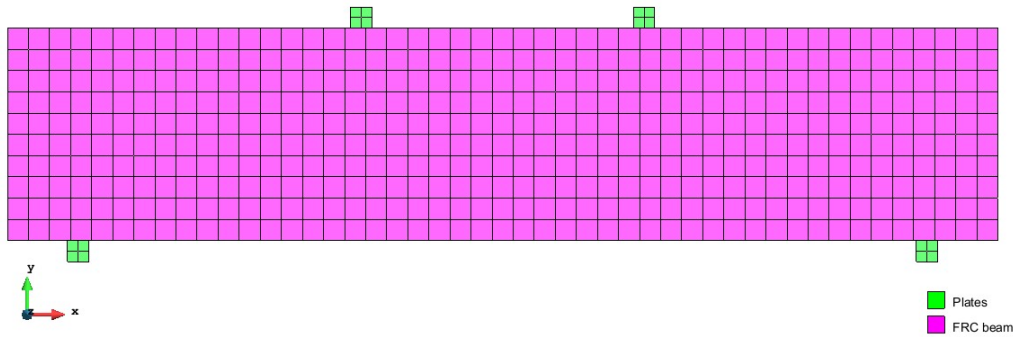


Figure 4: Finite element mesh and applied material models

Material model **CC3DNonLinCementitious2User** is the most sophisticated and most general model of FRC available in **ATENA** and it combines constitutive models for tensile (fracturing) and compressive (plastic) behavior. It describes the tensile behaviour according to the material response measured in tests point-wise in terms of the stress-strain relationship (Figure 5). The first part of the diagram is the usual stress-strain constitutive law. After exceeding the localization strain ε_{loc} the material law assumed for the characteristic crack band width L_{ch} is adjusted to the actual crack band width L_r . Usually, ε_{loc} is the strain after which the diagram is entering into the softening regime.

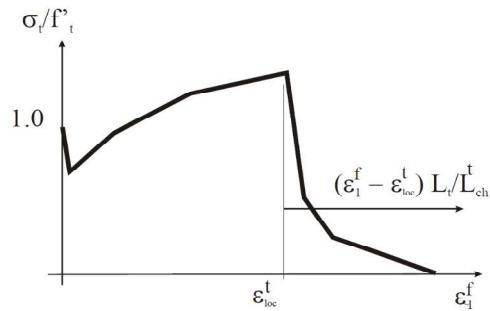


Figure 5: User defined tensile behavior [4]

The compressive stress-strain law of the mentioned material model is described in Figure 6. The softening law in compression is linearly descending and the end point of the softening curve is defined by plastic strain ϵ_d . By increasing material parameter ϵ_d the contribution of the fibers to the compressive behavior of concrete is considered. Another important compressive parameter for FRC modeling is reduction of compressive strength due to cracks (labeled as Fc Reduction-COMPRED, see Figure 14) which says how the strength is reduced while the material is subjected to lateral tension.

See also the ATENA Troubleshooting Manual [5], section 2.2.4 I want to use the user-defined stress-strain law of concrete to replace that used in ATENA program. How can I do it? for more information about the **CC3DNonLinCementitious2User** material model.

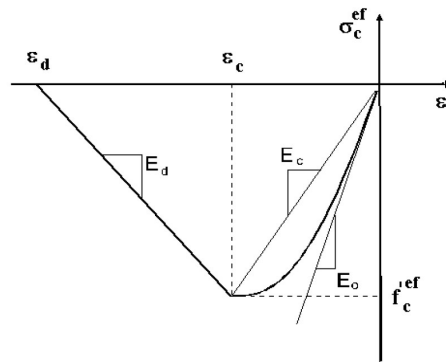


Figure 6: Compressive stress-strain law [4]

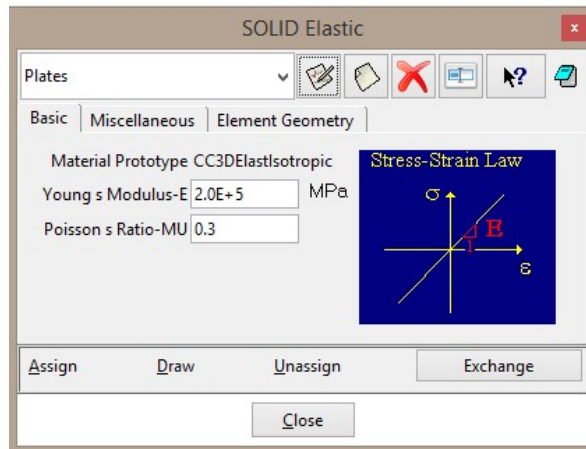


Figure 7: Material model of plates – Basic parameters

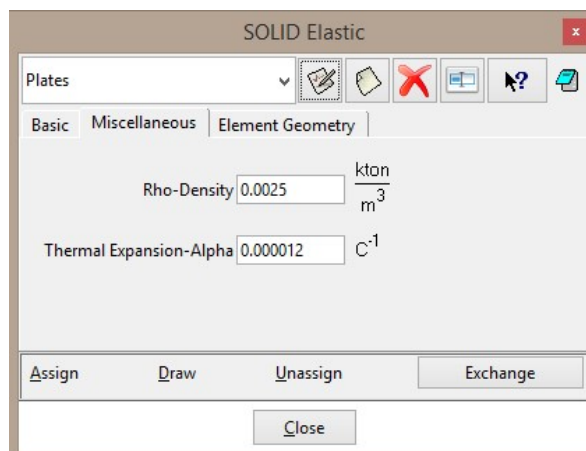


Figure 8: Material model of plates – Miscellaneous parameters

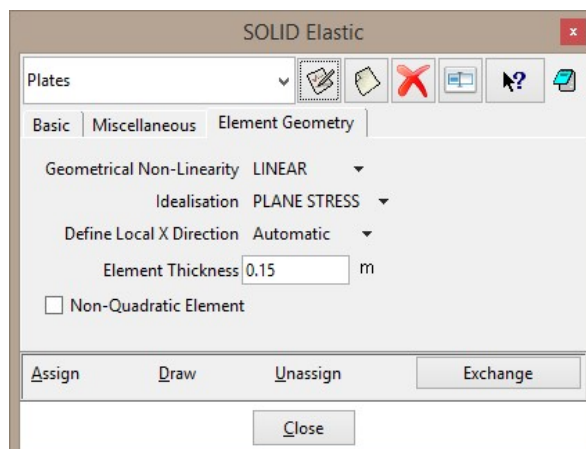


Figure 9: Material model of plates – Element geometry – plane stress idealization, element thickness 0.15 m according the geometry in Figure 1

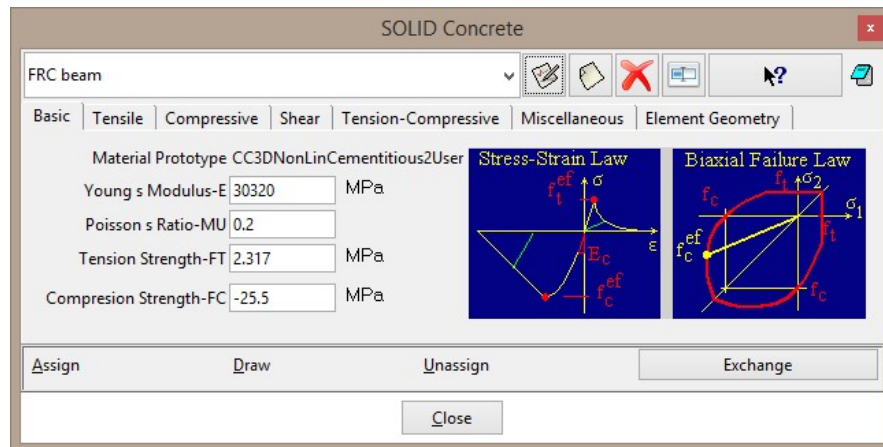


Figure 10: Material model of FRC – Default basic parameters

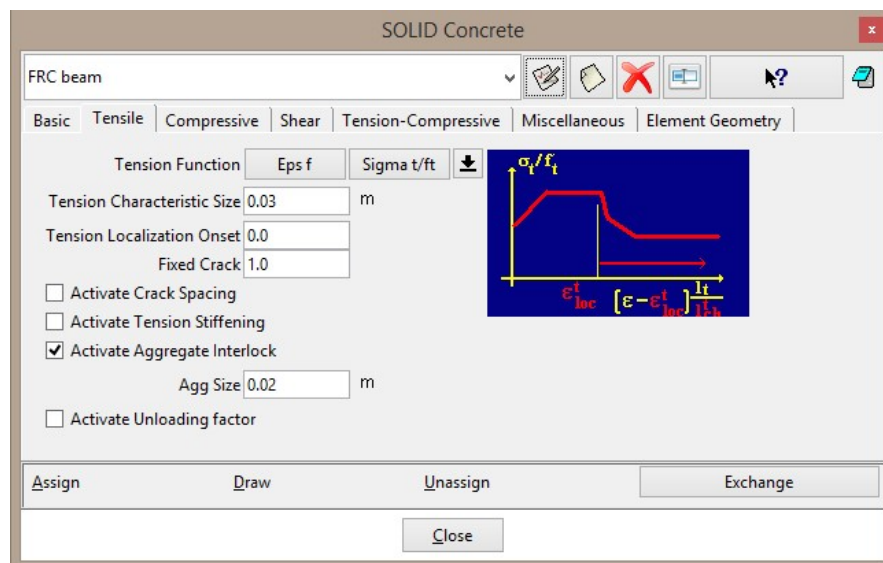


Figure 11: Material model of FRC – Default tensile parameters

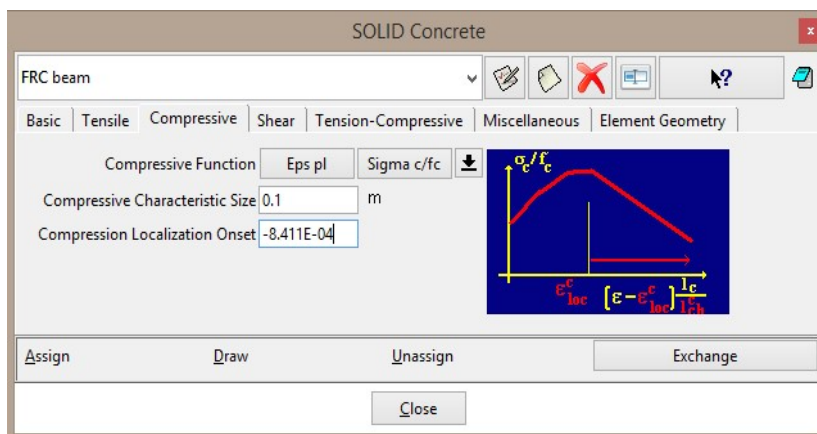


Figure 12: Material model of FRC – Default compressive parameters

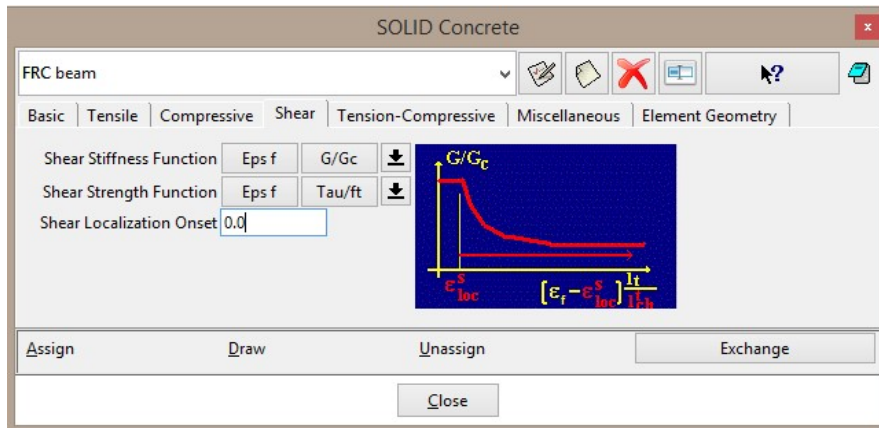


Figure 13: Material model of FRC – Default shear parameters

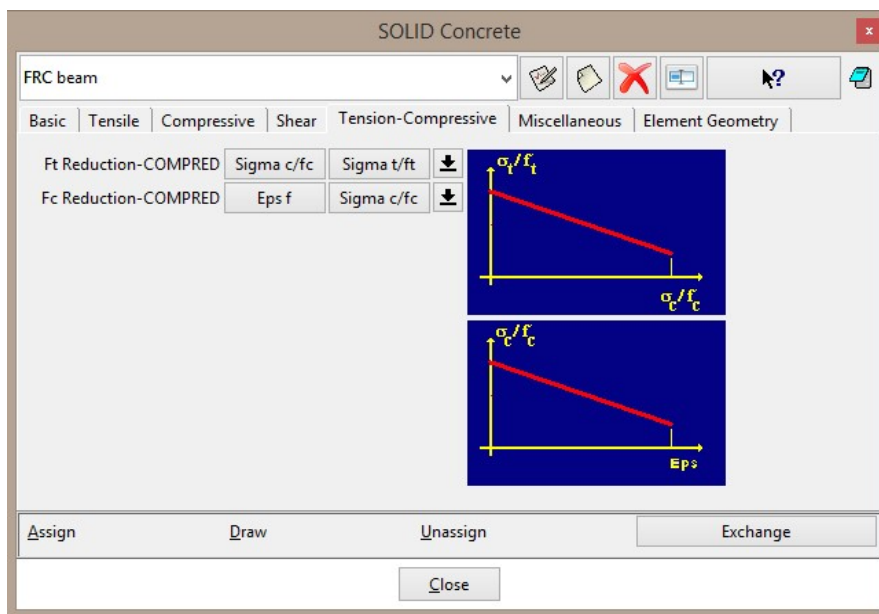


Figure 14: Material model of FRC – Default tension-compressive parameters

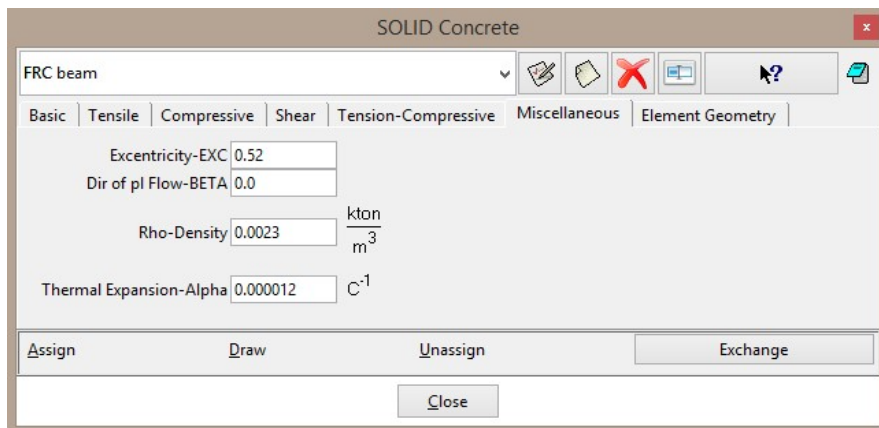


Figure 15: Material model of FRC – Default miscellaneous parameters

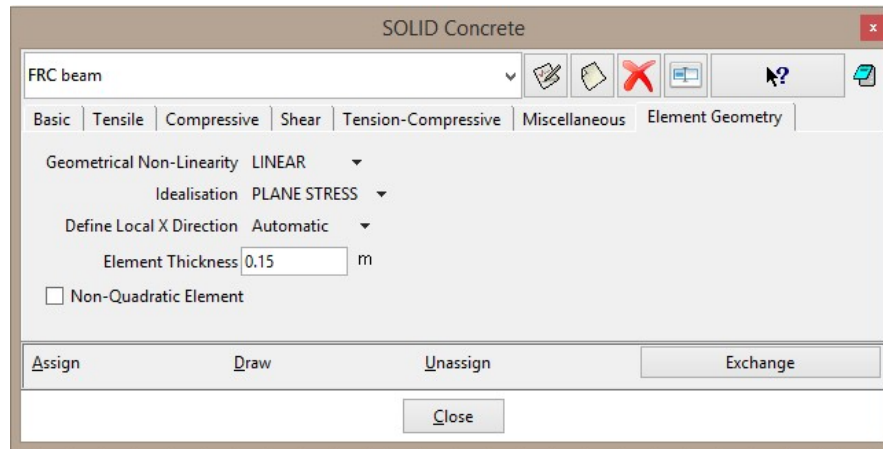


Figure 16: Material model of FRC – Element geometry – plane stress idealization, element thickness 0.15 m according the geometry in Figure 1

The last part of the prepared model is Interval data (Figure 17). The load is applied in the 70 steps with interval multiplier 70. It means that each step contains the assigned load multiplied by 1. The number of steps is based on the specific calculation which the user wants to provide. In the presented case, it is known from the experimental results that the beam should fail at the deflection of about 7 mm, see Figure 18. The prescribed displacement applied at the top plates is 0.1 mm. This means that the predefined displacement should be multiplied approximately 70 times to reach the failure. Based on this assumption, the load interval is multiplied by 70. Naturally, such a load should not be applied to the structure in one moment. Therefore, it is necessary to subdivide the interval in several load steps. In this case the interval will be divided in 70 load steps.

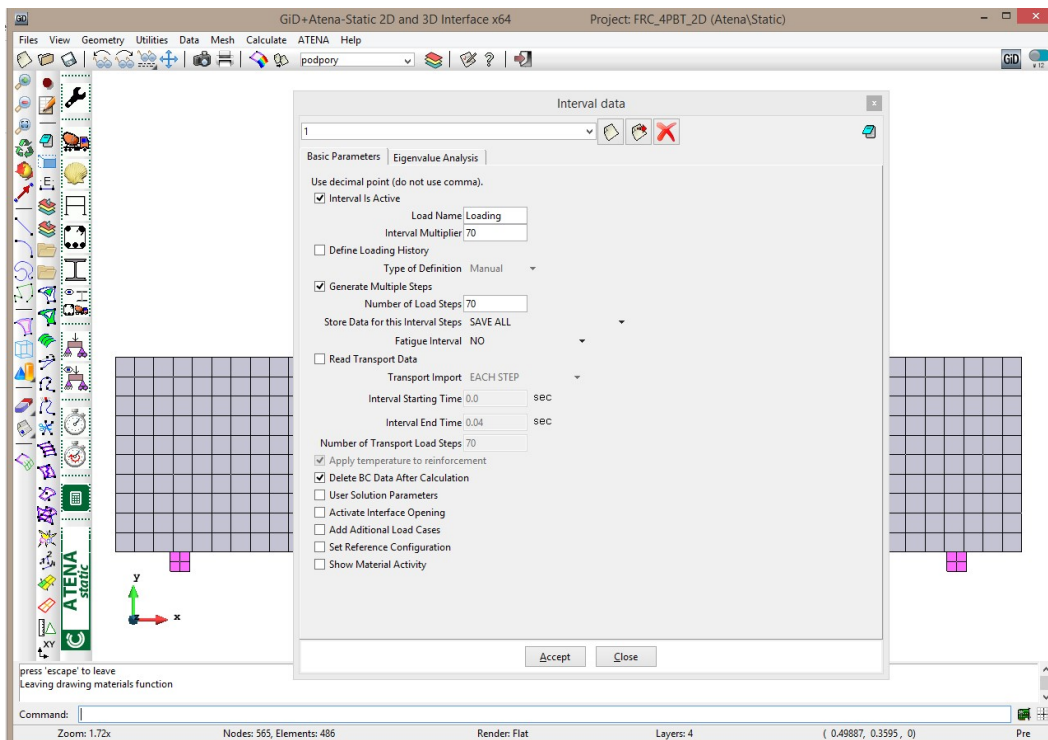


Figure 17: Interval data

5 FRC MATERIAL MODEL

5.1 Necessary Information for Creating FRC Material Model

For determining FRC parameters that serve as an input for material model in **ATENA**, it is necessary to use results from laboratory tests, e.g. three (3PBT) or (better) four point bending (4PBT) tests, compression tests on cubes or cylinders and test for the elastic (Young's) modulus.

The data from four point bending test (load-displacement diagrams, see Figure 18), compression test (compressive strength) and Young's modulus are available for the case presented in this tutorial and are summarized in Table 1. It is also known that concrete belongs to class C110/130 and it is reinforced by steel fibers BASF Masterfiber 482 in volume fraction 1.5 %. The fibers length is 13 mm and the diameter is 0.2 mm.

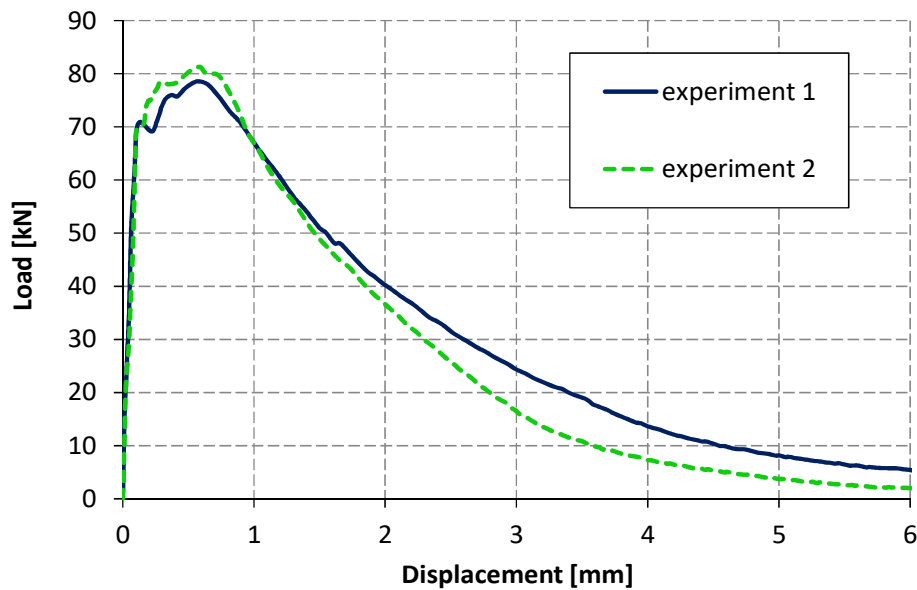


Figure 18: Measured load-displacement diagrams of laboratory tests

Table 1: Available material parameters

Material parameter [unit]	Value
Cylindrical compressive strength [MPa]	125
Young's modulus [MPa]	45000

5.2 Determining the FRC Material Model Parameters

Based on the available results from chapter 5.1 the material model for FRC can be determined. Clear parameters as compressive strength and Young's modulus are directly put into the model.

The issue is to obtain tensile parameters as tensile strength and tension function (Figure 11), i.e., the key FRC parameters. The measured response of direct tensile test can serve for direct input of the parameters into the material model. Unfortunately, preparation of test sample is complicated and the test is not performed very often. Therefore, the results of four point bending test are utilized for parameters determination but they cannot be directly put into the model. Inverse analysis of the load-displacement diagrams from Figure 18 needs to be performed to identify parameters correctly. There are two possible methods, the first one is manual inverse analysis which consists of following steps:

- initial setup of the tensile parameters (tensile strength, tensile function),
- running the analysis,
- export the load-displacement diagram from **ATENA** to excel file or similar,
- comparison of load-displacement diagram from calculation and laboratory test,
- if the difference between diagrams is within the user accuracy limits, the determination of FRC model is completed,
- if the difference between diagrams is not within the user accuracy limits, the input parameters must be modified in order to achieve better results, and again compare with the laboratory results. This step must be repeated until the results are satisfactory.

The step by step procedure of this method is described in chapter 5.2.1.

The second method utilizes a sophisticated program for inverse analysis instead of the manual approach. The program is called **Consoft** and it was developed by Prof. Dr.-Ing. Volker Slowik and his colleagues at the University of Applied Sciences in Leipzig, Germany (HTWK). Automatic analysis based on the evolutionary algorithms is used for determining the tensile function [6]. Before the Consoft analysis, it is necessary to specify the initial function parameters and their limits. The experiment is then numerically simulated and the initial parameters are modified during an iterative process to achieve the best possible agreement between the experimental results and the numerical model. As a result, **Consoft** gives the tensile strength and tensile function to the user and afterwards it can be used for **ATENA** simulations.

5.2.1 Modification of the Default Material Model

The material modification starts by selecting the **Define SOLID Concrete material** icon  or with the command **Data | Materials | SOLID Concrete** in main menu. After selecting this command, the window for the definition of the **SOLID Concrete** appears (see Figure 19). The prepared material called FRC beam should be selected (see Figure 20) and then its parameters can be changed.

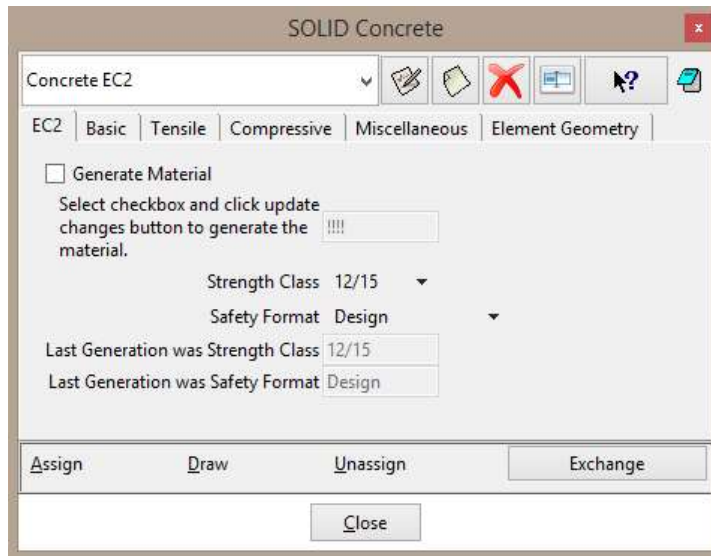


Figure 19: The window for the definition of the SOLID Concrete

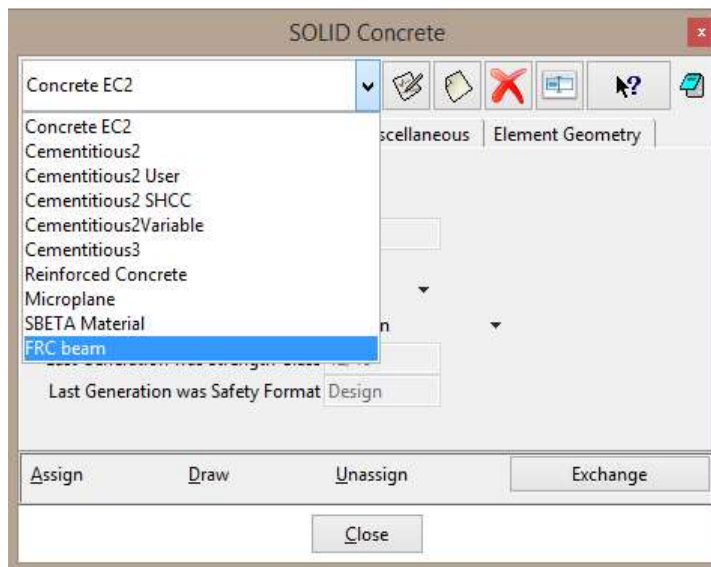
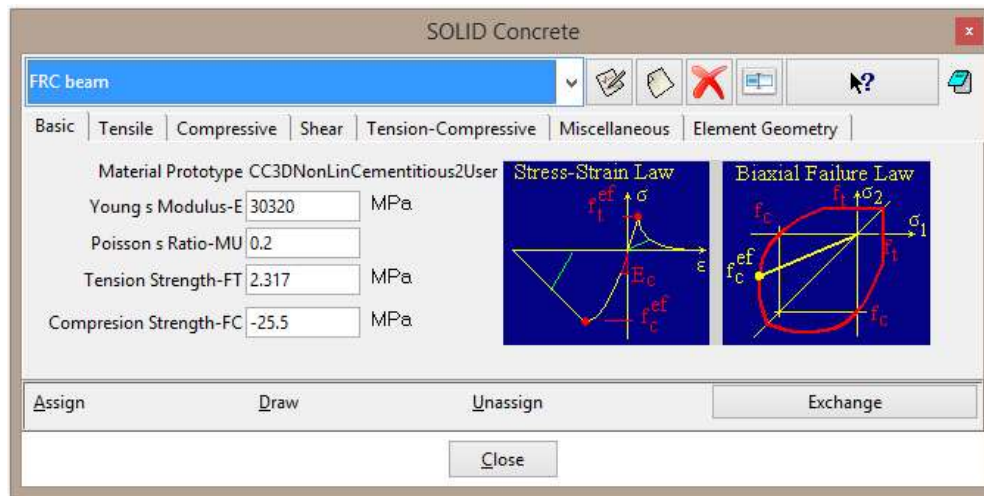


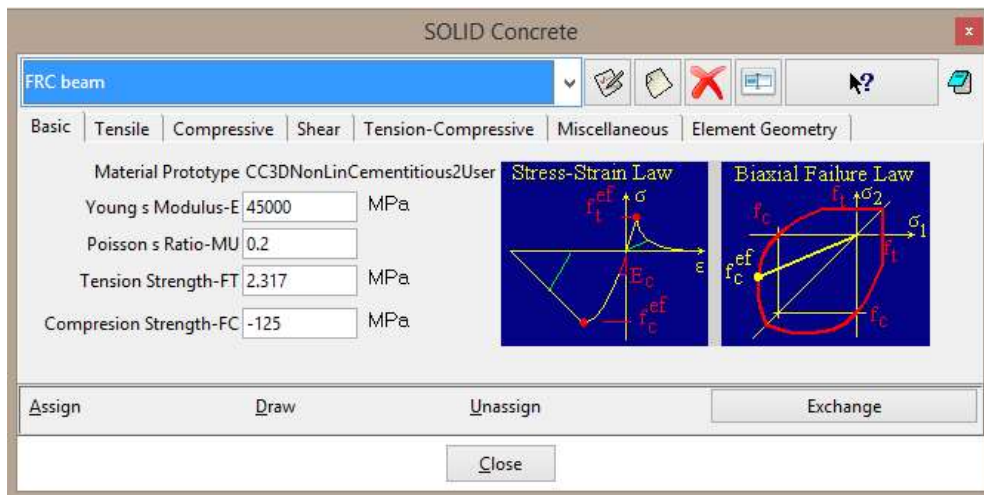
Figure 20: The selection of the FRC beam material

Firstly, parameters directly obtained by test results are modified in the material model. In this case, the compressive strength and Young's modulus are known and can be edited in the model according to the values in Table 1. The data before and after the modification

are depicted in Figure 21. The modified parameters are saved by clicking on the **Update Changes** icon .



(a)



(b)

Figure 21: The Basic parameters of the material FRC beam before (a) and after (b) modification

Secondly, other parameters must be estimated. Attention should be paid to the tensile parameters which are of crucial importance for FRC materials. The first peak of the Load - Displacement (L-D) diagram represents the formation of tensile crack and it is governed by the tensile strength. According to the assumptions of linear elastic behavior, the tensile strength F_t can be determined by formula for flexural stress σ :

$$\sigma = M/W \quad (1)$$

where M is bending moment at the central part of the beam loaded by four point bending test and it can be calculated as:

$$M = Fl/6 \quad (2)$$

where F is total load acting on the beam and l is the span of the beam.

The denominator of formula (1) is section modulus of the beam:

$$W = bh^2/6 \quad (3)$$

where b is the width of the beam cross section and h is the height of the beam cross section. By utilizing formulas (2) and (3) in the formula (1), the tensile strength F_t can be calculated as:

$$F_t = F_{max} l/bh^2 \quad (4)$$

where F_{max} is the load corresponding to the tensile strength (first peak in the L-D diagram).

Fib Model Code for Concrete Structures 2010[7] describes a procedure how to find the tensile stress – strain law (tensile function) based on the results of three point bending test on the notched beam according to EN 14651 [8]. The diagram of the applied force versus the crack mouth opening displacement is a required result of the test. Afterwards, residual flexural tensile strength can be calculated for individual crack openings by the formula (1) where the bending moment is adapted to the three point bending test. Thus obtained tensile function can serve as a first estimation of the function in the model.

As there is no information about crack opening from the four point bending test, the procedure described in *Fib* Model Code [7] can be used at least for determining the tensile strength. Load F_{max} corresponding to the tensile strength is approximately 70 kN, see the first peak in the Figure 18. The cross section dimensions are 150 x 150 mm and span of the beam is 600 mm, see Figure 1. The tensile strength calculated by formula (4) is 12.4 MPa and this value is used in the model, see Figure 22. The tensile strength is quite high but considering high compressive strength 125 MPa it is possible.

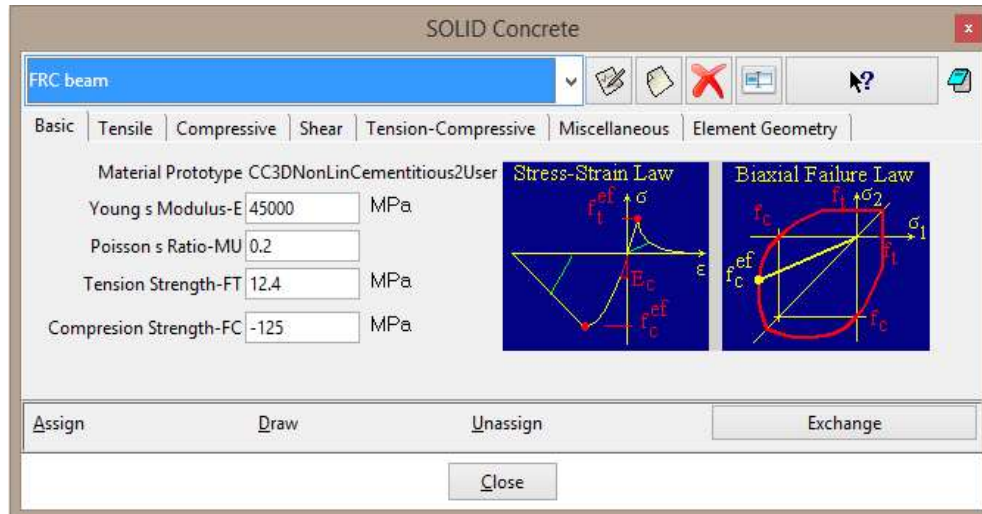


Figure 22: The modification of the tensile strength

Another important tensile parameter is the tensile function. In the fracture model, each crack is represented on the finite element level and its response is characterized by the traction-separation relationship (tensile function). A crack is perceived as a displacement discontinuity, which, however, is capable of transferring stress between its faces. This cohesive stress is related to the crack opening displacement through a traction-separation relationship. To this end, the crack band model is employed and the band width (characteristic length) is related to the element size to remain objective results with respect to the size of the finite elements.

The aforementioned tension function is specified in the model as relationship between fracture strain on the horizontal axis and tensile stress divided by tensile strength on the vertical axis. The fracture strain can be calculated by the following formula:

$$\varepsilon_f = w_c / L_t \quad (5)$$

where ε_f is fracture strain, w_c is crack opening and L_t is characteristic length. More information can be found at ATENA Theory Manual [4]. The characteristic length is a material parameter and it should be equal to the size of the element, in this case 0.015 m (Figure 24). Then, the tensile function describes the evolution of tensile stresses in one finite element after crack formation.

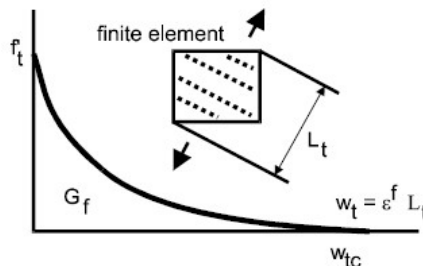


Figure 23: Tensile softening and characteristic length [4]

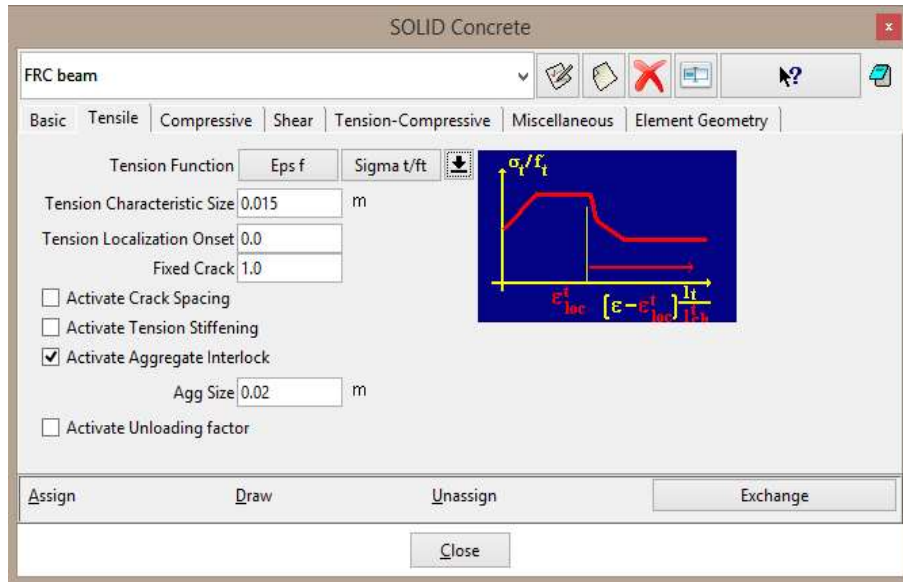


Figure 24: Modification of tension characteristic length

In other words, the post-peak behavior and the shape of diagram is governed by tensile function. In the **GiD**, the user can display function by opening the dialog for diagram input and clicking on the button . The results of four point bending tests do not provide information about crack propagation, crack widths and stresses that can be used for the first estimation of the function. Information that can help at this stage is that crack width in FRC during similar tests is usually in millimetres, and based on this fact the order of fracture strain can be at least determined according to the formula (5). Fracture strain corresponding to the crack width 1 mm is 0.07, therefore, the last point of the function, describing the maximal crack opening, is shifted to position [0.1, 0]. It means that initial value of strain is multiplied approximately 10 times. The second point is shifted with the same multiplier, see Figure 26. The horizontal values are maintained because it is not clear now how to modify them.

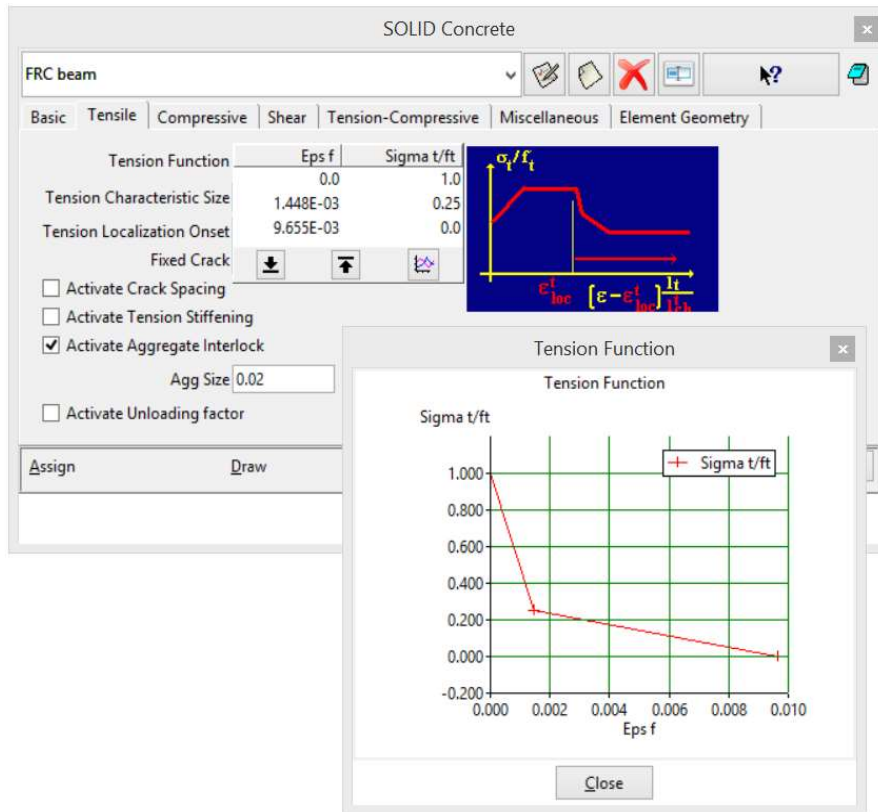


Figure 25: Default tensile function

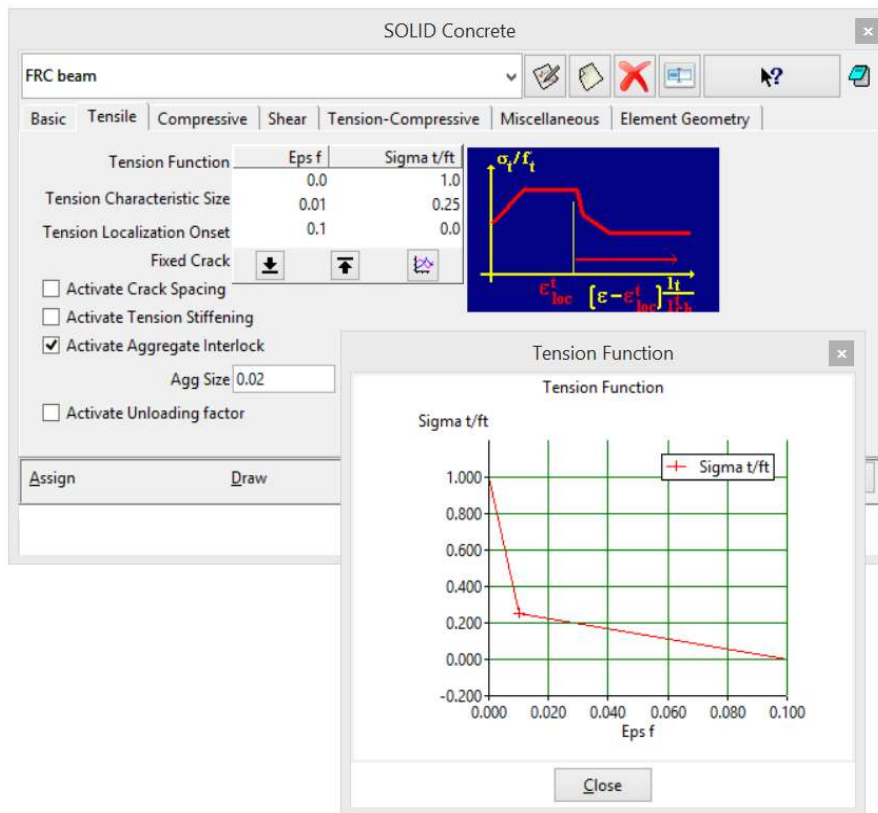


Figure 26: Modified tensile function

The last part of the material model that should be adapted to FRC behavior is compression. As it is known that FRC has higher ductility in tension in comparison with ordinary concrete, the compression ductility also increases. In the model **CC3DNonLinCementitious2User**, the ductility in compression is described by compressive function, the default function is depicted in Figure 27. In contrast to the tension, there is no result of compressive test that can help to determine the shape of compression function. Due to this fact, the first point of the diagram is just moved 100 times (the multiplier is based on the developers experience) to increase the ductility, see Figure 28.

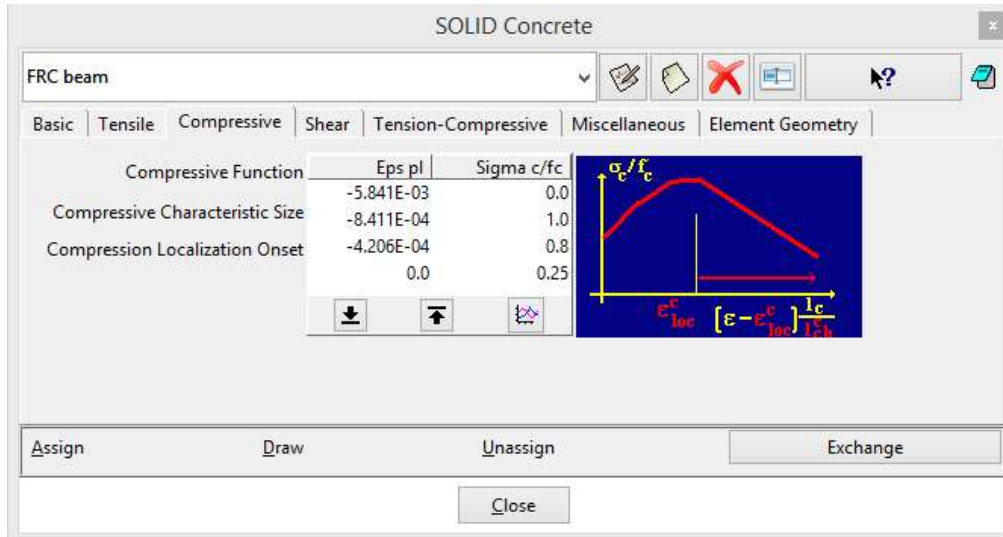


Figure 27: Default compressive function

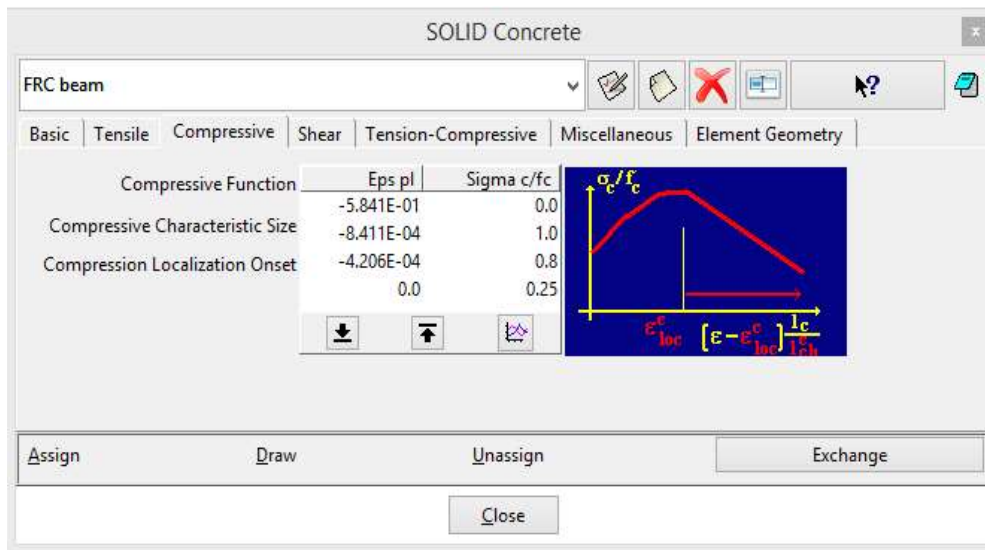


Figure 28: Modified compressive function

Second parameter connected with compression is Fc Reduction-COMPRED (reduction of compressive strength due to cracks) which says how the strength is reduced while the material is subjected to lateral tension. In the model **CC3DNonLinCementitious2User**, the parameter is described by function shown in Figure 29. Based on the developers

experience, this reduction should be deactivated by adjusting the function to the constant value 1, see Figure 30.

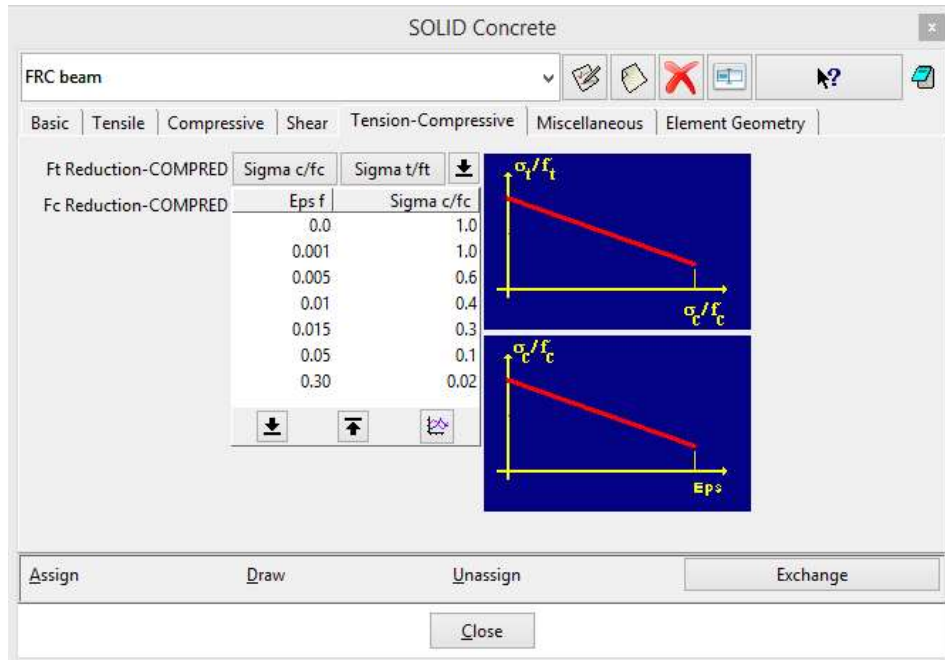


Figure 29: Default parameter Fc Reduction-COMPRED

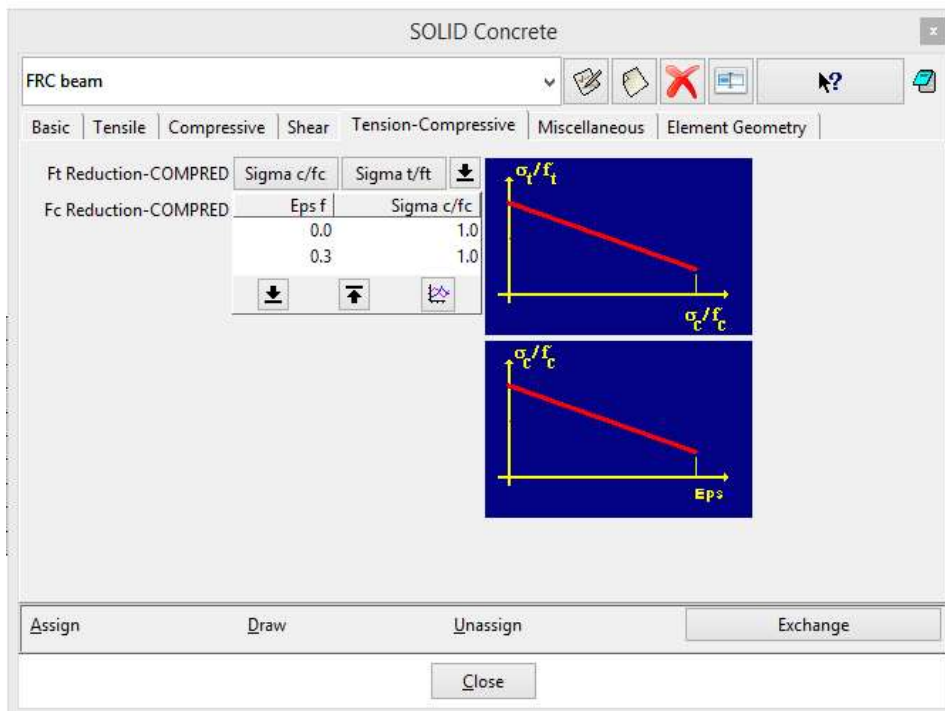


Figure 30: Modified parameter Fc Reduction-COMPRED

This is the initial model for the inverse analysis. Based on its results, material parameters will be modified to find the suitable model in accordance with experimental results.

5.2.2 Running the Analysis

After the material model modifications described in the previous chapter, the finite element analysis is started by clicking on the **Start ATENA static analysis** icon  or by the using of command **Calculate | Calculate** or **ATENA | ATENA Analysis**. After selecting this command, the program will start to generate the input file. This process is indicated by the dialog box (see Figure 31). Then, the **ATENA Studio** window appears and analysis is in progress (see Figure 32).

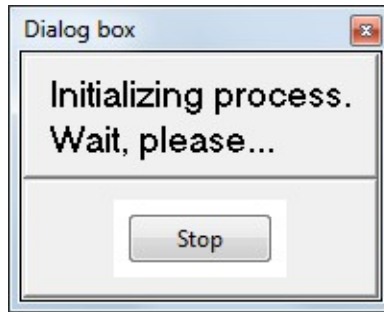


Figure 31: The initializing of the analysis

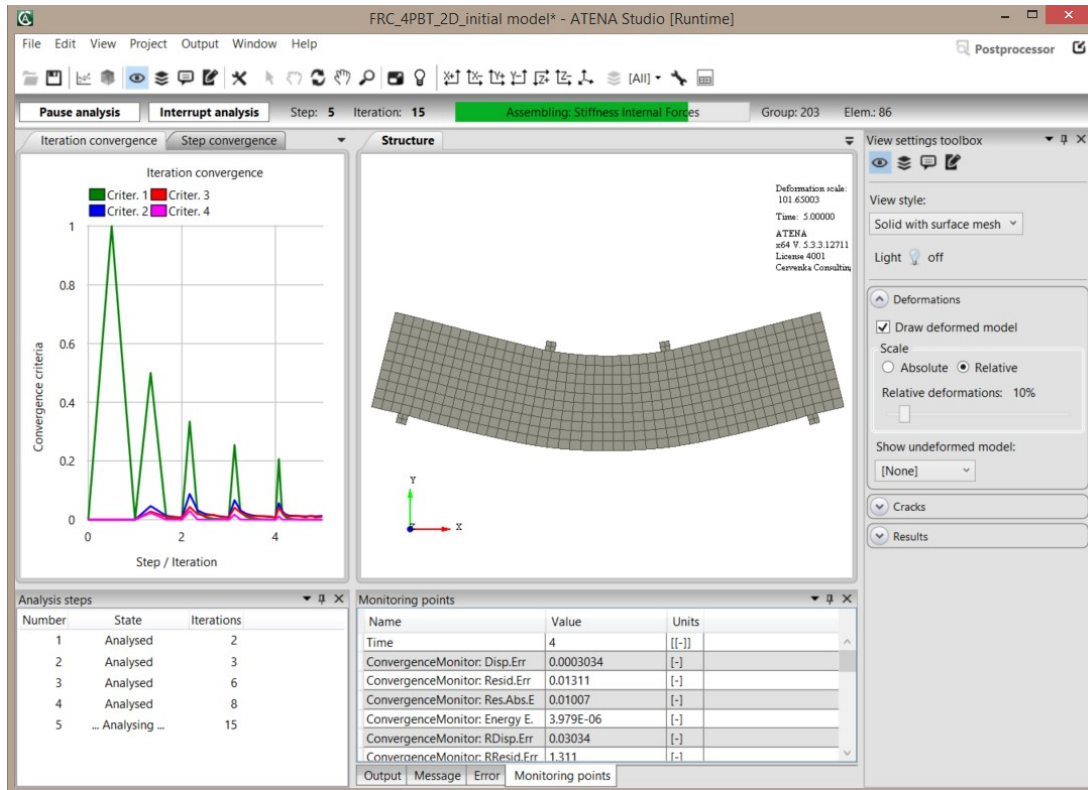


Figure 32: The ATENA Studio interface window

5.2.3 Load-Displacement Diagram and its export from ATENA to Excel File or Similar

During the analysis, it is very useful to see the evolution of the applied load and beam deflections. The progress of the load and deflection is available in the monitors that were defined in the model, see chapter 4.2 and Figure 3.

To visualize these monitors during the nonlinear analysis, new diagram window must be opened by the clicking on the icon . The empty window for the diagram and the diagram settings appears (see Figure 33). The new diagram is defined by diagram settings dialog (see Figure 34 to Figure 36). You may also wish to see the ATENA Studio User's Manual [3] for more options.

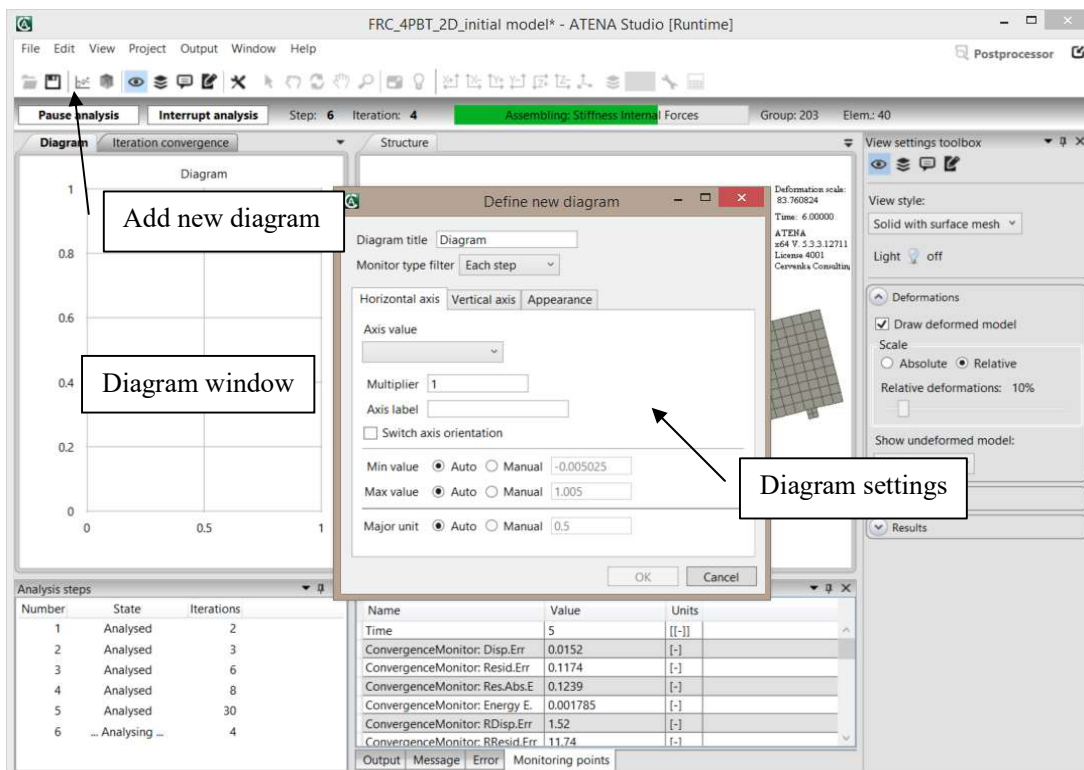


Figure 33: The execution of the graph

The diagram title can be **L-D** and the monitor type filter should be **Each step**. For the horizontal value the monitor labeled **displacement_DISPLACEMENTS** should be selected. The name of axis should be **Displacement [mm]** and the values are multiplied by -1000 to achieve switched orientation of the axis and millimetres instead of default meters, see Figure 34.

The vertical axis can display more series. Add new series, choose the **Reaction R_REACTIONS** for the right reaction and **Reaction L_REACTIONS** for the left reaction. Use multiplier 1000 to achieve reactions in the kilonewtons instead of meganewtons. The axis label can be **Reactions [kN]**. The series definition must be applied by the **OK** button above Axis label, see Figure 35 and Figure 36. The definition of the diagram parameters is finished by clicking on the **OK** button. After this, the L-D diagram is shown on the left side of the **ATENA Studio** interface, see Figure 37. This diagram is showing actual stage of the running analysis and it changes as the analysis progresses based on the current loads and deflections.

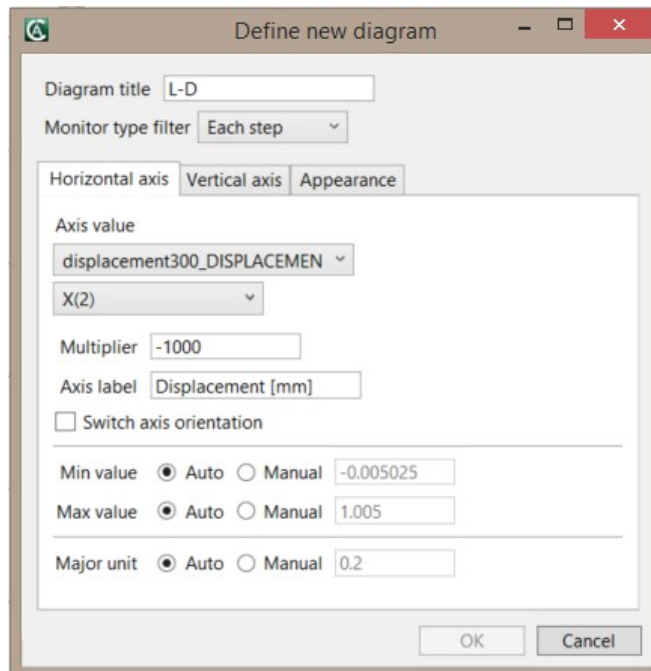


Figure 34: The diagram definition – properties of the horizontal axis

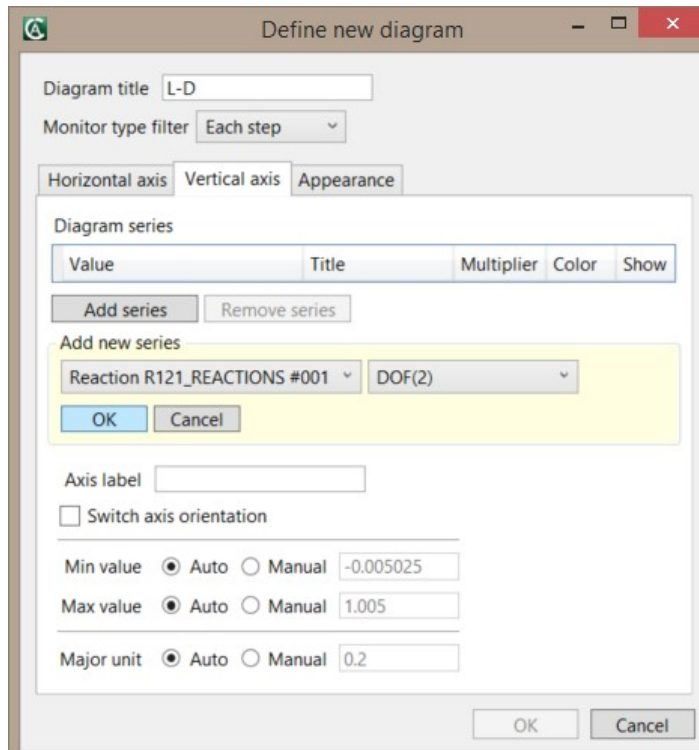


Figure 35: The diagram definition – selection of the series for vertical axis

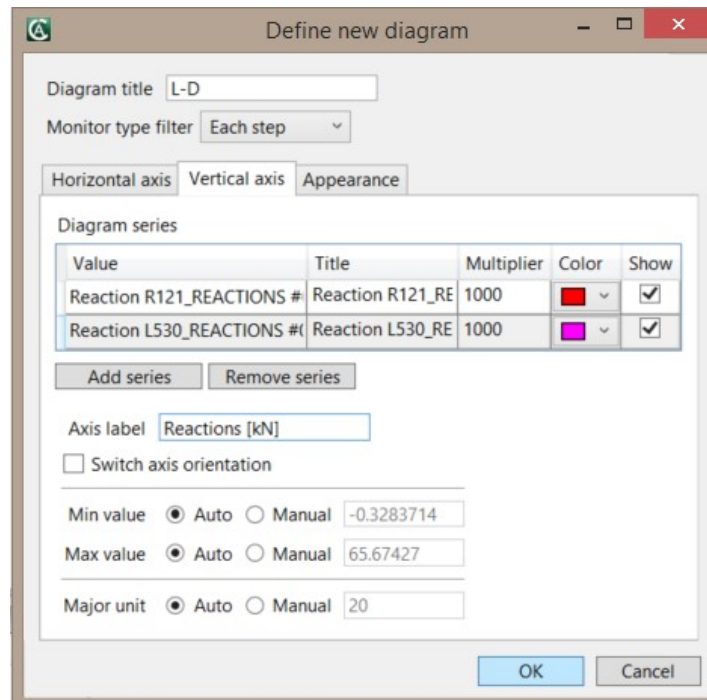


Figure 36: The diagram definition – properties of the vertical axis

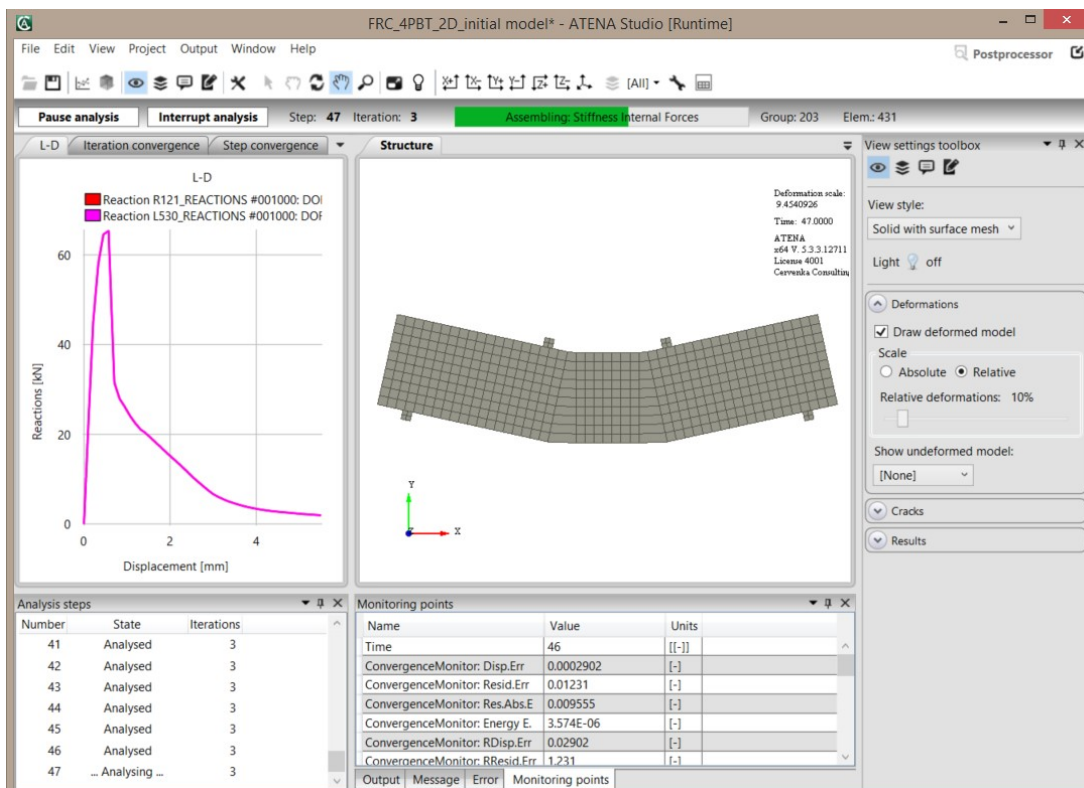


Figure 37: The L-D diagram showing stage of the running analysis

At the stage shown in the Figure 37, the calculation can be stopped. It is obvious from the L-D diagram that applied load decreases almost to the zero and the beam fails. The calculation is interrupted by clicking on the button **Interrupt analysis** above the

diagrams. The dialog appears and asks the user if the analysis should be stopped after the step, iteration or as soon as possible, see Figure 38. The third option is chosen in this case.

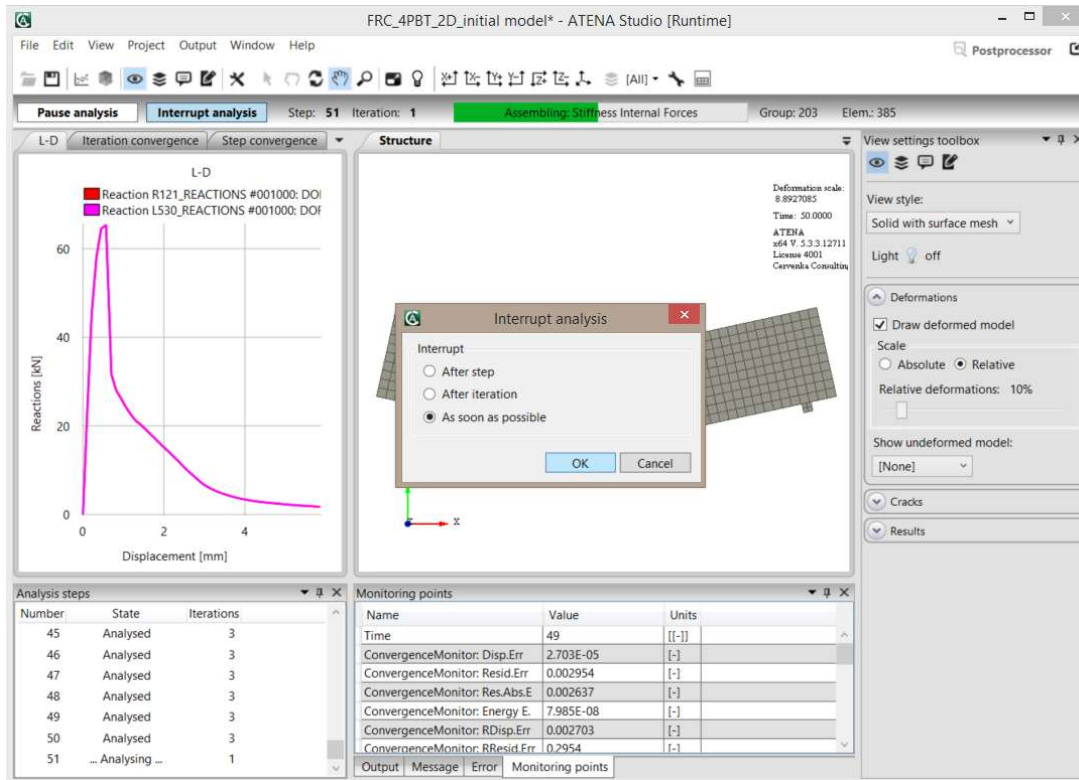


Figure 38: Dialog for interrupting the analysis

When the calculation is interrupted, the data from L-D diagram must be copied into the excel file or similar and compared with experimental data. It can be done at the runtime mode, it is not necessary to go to the postprocessor. Click on the window with L-D diagram and use Ctrl-C to copy the data. The dialog shown in Figure 39 appears, copy data by clicking on the OK button.

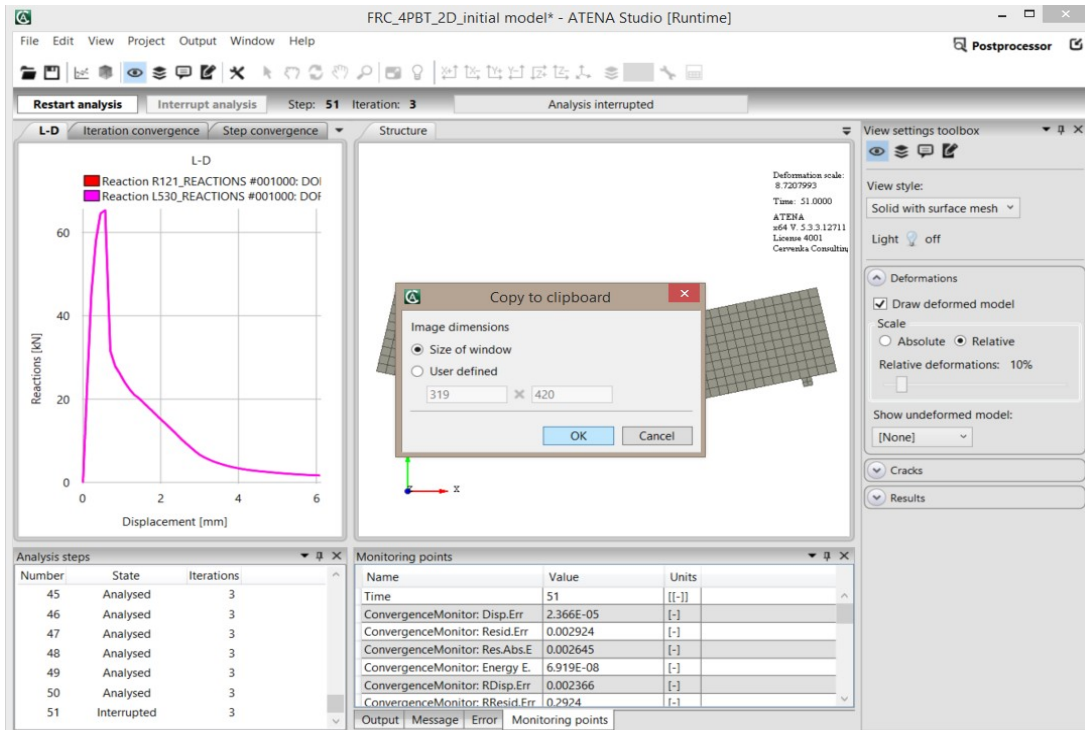


Figure 39: Dialog for the copy of data in the L-D diagram

For processing the copied data, **Microsoft Excel** or some similar program needs to be utilized. The Excel file named **LD_diagrams_empty.xlsx** is used in this tutorial and it can be found on following address: **%Public%\Documents\ATENA Examples\Science\Gid\Tutorial.FRC\LD_diagrams_empty.xlsx**. There are three lists, the first one contains data from laboratory tests and relevant L-D diagram (see Figure 40), the second list is prepared for the **ATENA** data and is empty at this moment, the third list serves to compare the results.

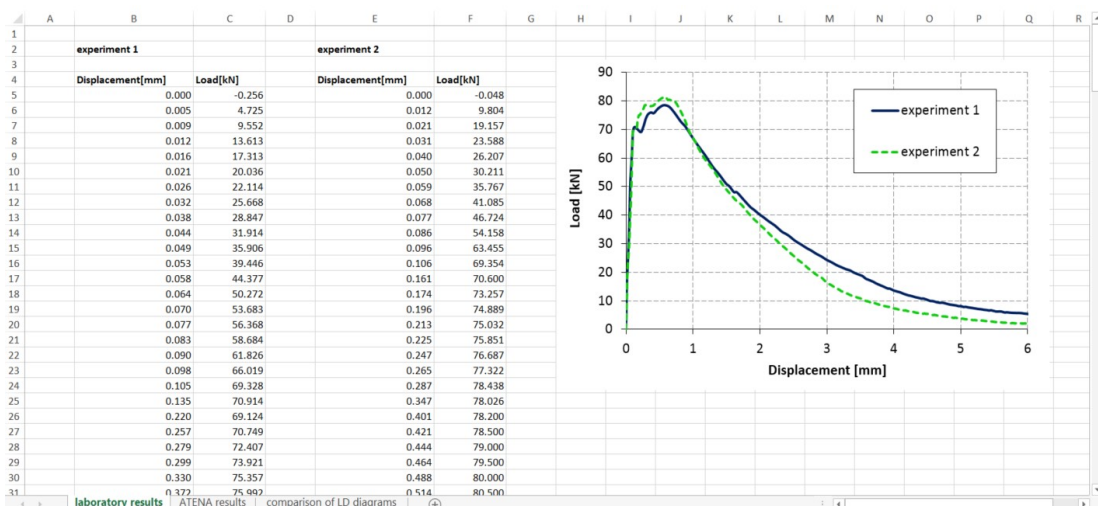


Figure 40: Excel file for comparison or results – List with the results of laboratory tests

The ATENA data can be inserted on the second list named ATENA results by Ctrl-V or by clicking right mouse button and choosing **Insert**. The data are organized in four columns. The first two columns belong to the diagram with the displacement on the horizontal axis and right reaction on the vertical axis. Other two columns belong to the diagram with the same horizontal axis but there is left reaction on the vertical axis, see Figure 41.

	A	B	C	D	E	F	G	H	I	J	K	L
1												
2		L-D										
3		Displacement [mm]	Reaction R121_REACTIONS	Displacement [mm]	Reaction L530_REACTIONS							
4		0	0	0	0							
5		0.108136845	23.43201794	0.108136845	23.43201794							
6		0.217519909	45.35819085	0.217519909	45.35819085							
7		0.332868948	57.97307494	0.332868948	57.97307494							
8		0.451889835	64.57322257	0.451889835	64.57322257							
9		0.570942668	65.34753354	0.570942668	65.34753354							
10		0.704446494	31.56758082	0.704446494	31.56758082							
11		0.826263645	27.94168221	0.826263645	27.94168221							
12		0.94756942	26.12057788	0.94756942	26.12057788							
13		1.069150623	24.10971036	1.069150623	24.10971036							
14		1.190068455	22.48220103	1.190068455	22.48220103							
15		1.310918999	21.10802051	1.310918999	21.10802051							
16		1.431233804	20.2617979	1.431233804	20.2617979							
17		1.551145041	19.20181037	1.551145041	19.20181037							
18		1.671007239	18.11055414	1.671007239	18.11055414							
19		1.790984906	17.05553734	1.790984906	17.05553734							
20		1.910837553	15.95083817	1.910837553	15.95083817							
21		2.030061646	14.91450537	2.030061646	14.91450537							
22		2.149568258	13.89193376	2.149568258	13.89193376							
23		2.270529811	12.80653536	2.270529811	12.80653536							
24		2.390783615	11.71572643	2.390783615	11.71572643							
25		2.509653435	10.57933753	2.509653435	10.57933753							
26		2.628059429	9.560663794	2.628059429	9.560663794							
27		2.747504465	8.591295	2.747504465	8.591295							
28		2.867360512	7.624224745	2.867360512	7.624224745							
29		2.986205935	6.733074302	2.986205935	6.733074302							
30		3.104933151	6.088578263	3.104933151	6.088578263							
31		3.224555016	5.553970017	3.224555016	5.553970017							
32		3.344553691	5.070120997	3.344553691	5.070120997							
33		3.46449905	4.678000291	3.46449905	4.678000291							
34		3.584621794	4.327312384	3.584621794	4.327312384							
35		3.7050191	4.001140669	3.7050191	4.001140669							
36		3.825600913	3.715846081	3.825600913	3.715846081							
37		3.945606885	3.484745395	3.945606885	3.484745395							
38		4.06549843	3.276463113	4.06549843	3.276463113							
39		4.185312304	3.092024475	4.185312304	3.092024475							
40		4.305111011	2.934074811	4.305111011	2.934074811							
41		4.424825875	2.803808256	4.424825875	2.803808256							

Figure 41: Excel file for comparison or results – List with the data from ATENA

The diagram comparable with the experimental results must be created from ATENA data. Both reactions must be summed up because the load in the experimental results expresses the overall force acting on the beam. Then the data are ready for making the diagram (see Figure 42) that can be put into one graph together with laboratory results and compared (see Figure 43).

	A	B	C	D	E	F	G	H	I	J
1										
2		L-D								
3		Displacement [mm]	Reaction R121_REACTIONS	Displacement [mm]	Reaction L530_REACTIONS		Summation of reactions [kN]			
4		0	0	0	0		0			
5		0.108136845	23.43201794	0.108136845	23.43201794		46.86403588			
6		0.217519909	45.35819085	0.217519909	45.35819085		90.71638169			
7		0.332868948	57.97307494	0.332868948	57.97307494		115.9461499			
8		0.451889835	64.57322257	0.451889835	64.57322257		129.1464451			
9		0.570942668	65.34753354	0.570942668	65.34753354		130.6950671			
10		0.704446494	31.56758082	0.704446494	31.56758082		63.13516165			
11		0.826263645	27.94168221	0.826263645	27.94168221		55.88336442			
12		0.94756942	26.12057788	0.94756942	26.12057788		52.24115576			
13		1.069150623	24.10971036	1.069150623	24.10971036		48.21942072			
14		1.190068455	22.48220103	1.190068455	22.48220103		44.96440206			
15		1.310918999	21.10802051	1.310918999	21.10802051		42.21604102			
16		1.431233804	20.2617979	1.431233804	20.2617979		40.5235958			
17		1.551145041	19.20181037	1.551145041	19.20181037		38.40362074			
18		1.671007239	18.11055414	1.671007239	18.11055414		36.22110828			
19		1.790984906	17.05553734	1.790984906	17.05553734		34.11107468			
20		1.910837553	15.95083817	1.910837553	15.95083817		31.90167634			
21		2.030061646	14.91450537	2.030061646	14.91450537		29.82901074			
22		2.149568258	13.89193376	2.149568258	13.89193376		27.78386752			
23		2.270529811	12.80653536	2.270529811	12.80653536		25.61307072			
24		2.390783615	11.71572643	2.390783615	11.71572643		23.43145287			
25		2.509653435	10.57933753	2.509653435	10.57933753		21.15867506			
26		2.628059429	9.560663794	2.628059429	9.560663794		19.12132759			
27		2.747504465	8.591295	2.747504465	8.591295		17.18259			
28		2.867360512	7.624224745	2.867360512	7.624224745		15.24844949			
29		2.986205935	6.733074302	2.986205935	6.733074302		13.4661486			
30		3.104933151	6.088578263	3.104933151	6.088578263		12.17715653			
31		3.224555016	5.553970017	3.224555016	5.553970017		11.10794003			
32		3.344553691	5.070120997	3.344553691	5.070120997		10.14024199			
33		3.46449905	4.678000291	3.46449905	4.678000291		9.356000582			
34		3.584621794	4.327312384	3.584621794	4.327312384		8.654624768			
35		3.7050191	4.001140669	3.7050191	4.001140669		8.002281338			
36		3.825600913	3.715846081	3.825600913	3.715846081		7.431692161			
37		3.945606885	3.484745395	3.945606885	3.484745395		6.969490789			
38		4.06549843	3.276463113	4.06549843	3.276463113		6.552926227			
39		4.185312304	3.092024475	4.185312304	3.092024475		6.18404895			
40		4.305111011	2.934074811	4.305111011	2.934074811		5.868149622			
41		4.424825875	2.803808256	4.424825875	2.803808256		5.607616512			

Figure 42: Excel file for comparison or results – Modification of the data from ATENA

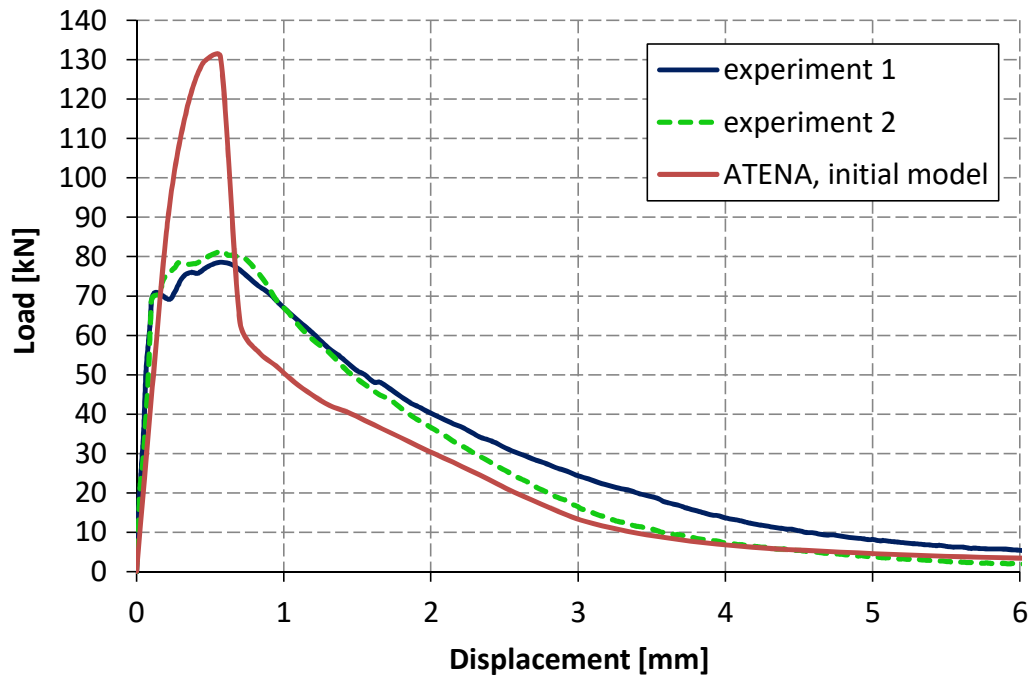


Figure 43: Comparison of L-D diagrams

5.2.4 Analysis of the results and subsequent material modification

It is obvious from the comparison of results in Figure 43 that material model does not describe behavior of FRC properly and needs modifications. As the beam is subjected to bending, the main attention should be paid to the tensile strength and tensile function.

By modification of the tensile strength, the whole L-D diagram moves up and down. The shape of the diagram can be adjusted through the tensile function. The position of the diagram peak is influenced both by the tensile strength and the tensile function, specifically by the slope of the first part of the diagram. The user can choose which parameter to modify to obtain the right position of the peak. Since the value of tensile strength is based on the formulas from previous chapter, the tensile function is adjusted.

It is useful to find fracture strains corresponding to point where the load should be changed. For example, at the peak of the L-D diagram, the displacement is 0.6 mm and the load is 131 kN while it should be 80 kN. The fracture strain at this step can be calculated by formula (5) using the crack width found in the postprocessor, see Figure 44. The fracture strain is 0.003, see Table 2. At this point, the relative stress should be decreased in the same proportion as is between the loads. The original position of the point is [0.003, 0.775] (the vertical coordinate is calculated from the first part of the tensile function, i.e. line beginning at the point [0, 1] and ending at [0.01, 0.25]). The new position of the point is [0.003, 0.473], the relative stress is decreased to 61 % based on the proportion between calculated and required load.

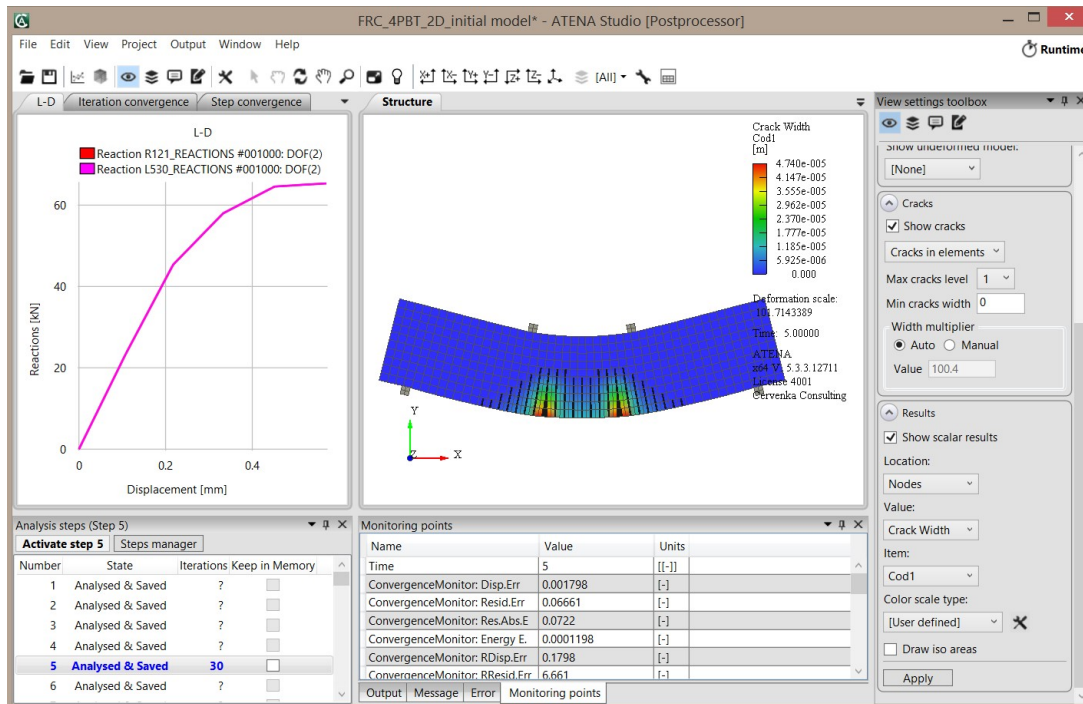


Figure 44: Crack width in postprocessor

Contrary to the peak of the diagram, the load corresponding to the displacement 1, 2, 3 and 4 mm should be increased by approximately 30 %. In the same proportion, the relative

stresses in the tensile function are increased. The corresponding fracture strains are summarized in the Table 2. According to the fracture strain at the displacement 6 mm, the maximal fracture strain in the tensile function is shifted from position [0.1, 0] to [0.15, 0]. Modified tensile function is depicted in Figure 45. Model with described modifications can be found at the location: **%Public%Documents\ATENA Examples\Science\GiD\Tutorial.FRC\FRC_4PBT_2D_modification_1.gid**.

Table 2: Fracture strain corresponding to different displacements in the beam analysis (initial model)

Displacement [mm]	Load [kN]	Step [-]	Crack width [mm]	Fracture strain [-]
0.6	131	5	0.047	0.0031
1	52	8	0.229	0.0153
2	30	17	0.610	0.0407
3	13	25	0.988	0.0659
4	7	33	1.400	0.0933
6	3	50	2.200	0.1467

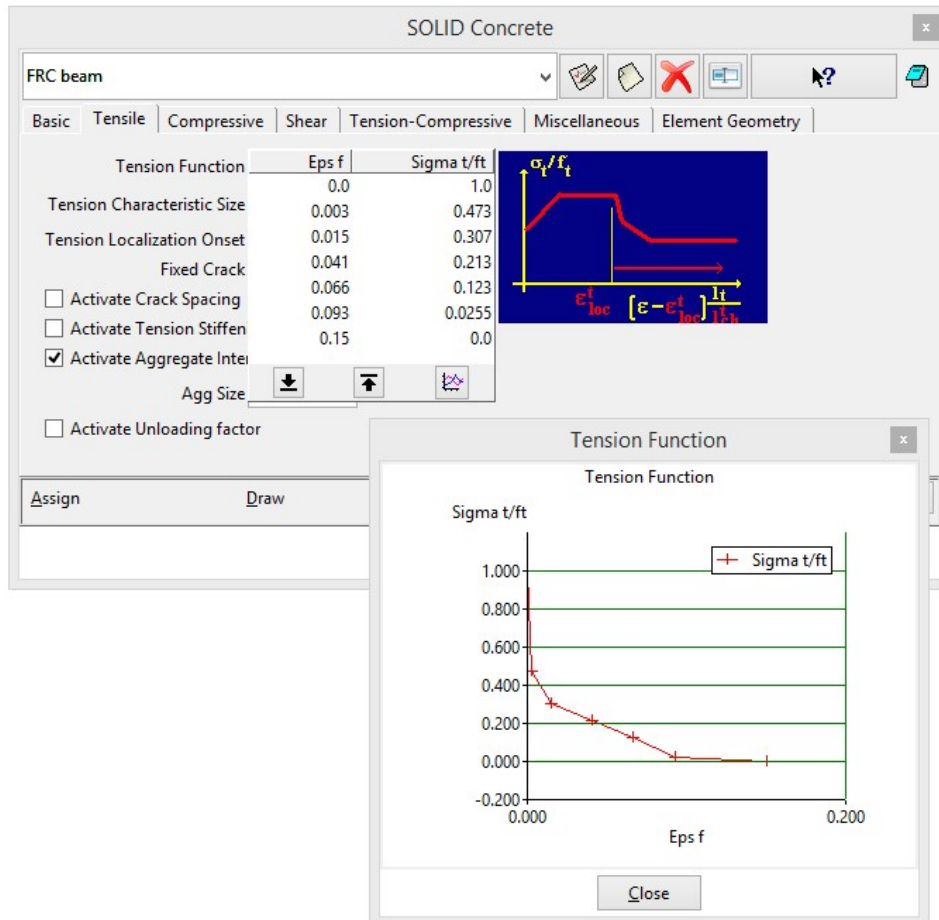


Figure 45: Modification of the tensile function no. 1

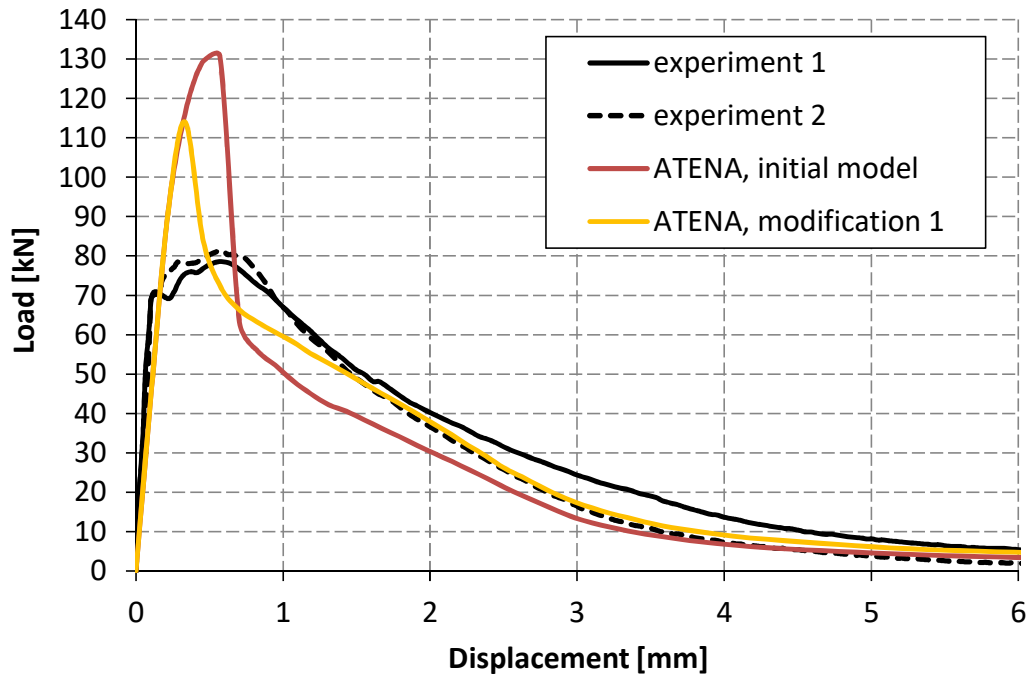


Figure 46: Comparison of L-D diagrams with new result for modification no. 1

Figure 46 shows that peak of the diagram decreases in comparison with the initial model but it still need further modifications. The number of subsequent modifications depends on the required accuracy of the material model. It is recommended to the user to do next modifications by him to find the way how the model works and how the different adjustments affect the model behavior. The procedure of model determination done by a developer is presented in the following part of the tutorial to help users as far as they do not know how to find the appropriate parameters.

Description of the modifications to find the suitable model:

- **Modification no. 2**

The result with modified curve no. 1 should be improved in the area around the maximum load (load is higher than in the experiment) and at the displacements 1, 3 and 4 mm (load is lower). The fracture strain corresponding to diagram peak is 0.0005, see Table 3, and at this point, the relative stress should be lower. Thus, the second point of the tensile diagram which original position was [0.003, 0.473] is shifted to [0.0005, 0.473], see Figure 47.

To find appropriate modifications around the displacements of 1, 3 and 4 mm, the fracture strains from Table 3 are utilized again. At the point corresponding to the displacement of 1 mm, the relative stress should be increased by approximately 14 % (it is defined by the relation between loads: the load is 58 kN and it should be 66 kN). The original point [0.015, 0.307] is shifted to position [0.015, 0.349].

The same procedure is done with tensile function in the area around displacement 3 and 4 mm, see Figure 47, the relative stresses at the corresponding fracture strains are increased.

Model with described modifications can be found at the location: **%Public%\Documents\ATENA**

Table 3: Fracture strain corresponding to different displacements in the beam analysis (modification no. 1)

Displacement [mm]	Load [kN]	Step [-]	Crack width [mm]	Fracture strain [-]
0.33	114	3	0.00748	0.0005
1	60	8	0.227	0.0151
3	17	25	0.981	0.0654
4	9	33	1.370	0.0913

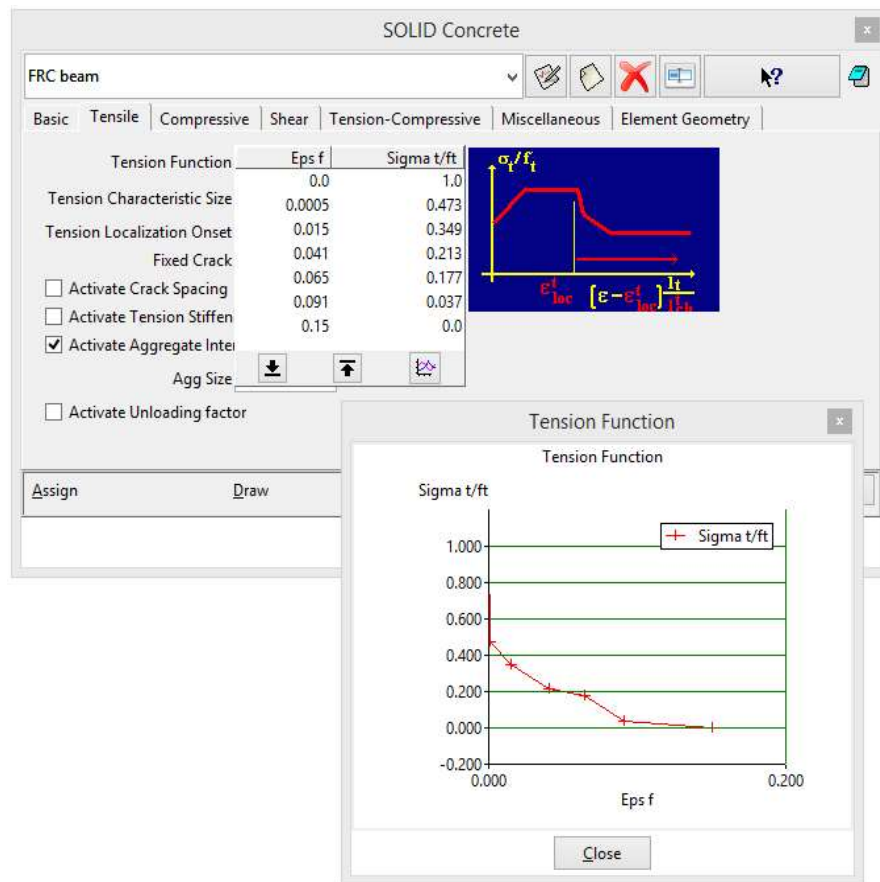


Figure 47: Modification of the tensile function no. 2

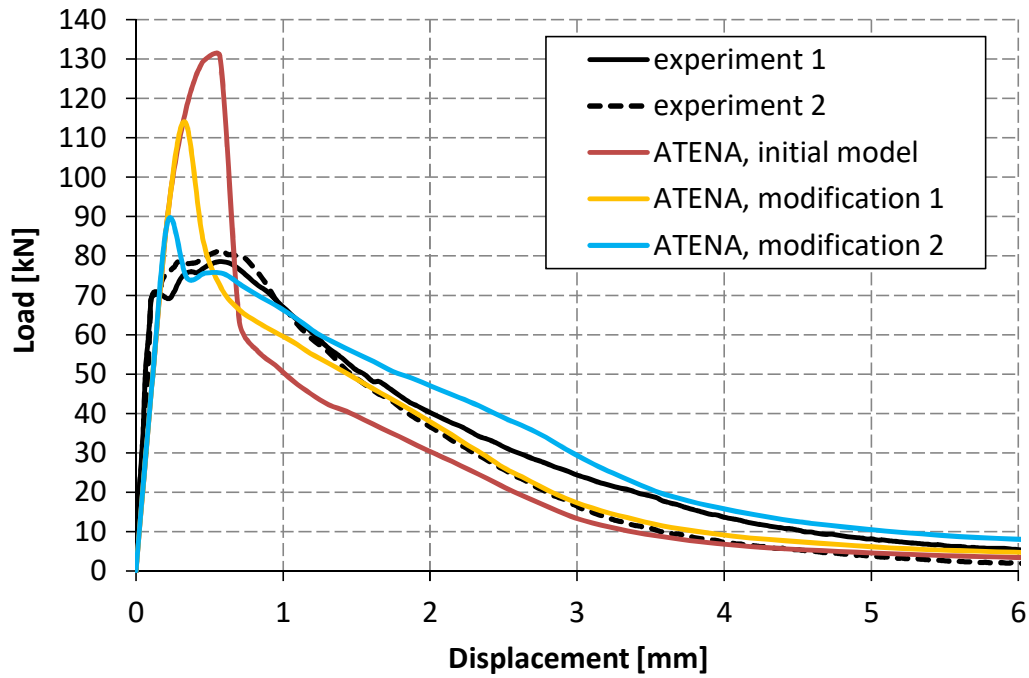


Figure 48: Comparison of L-D diagrams with new result for modification no. 2

- **Modification no. 3**

The result with modified curve no. 2 is shown in the Figure 48. The diagram peak is still higher than it is required. The load at the displacement 2 and 3 mm should be also lower. The fracture strains corresponding to these displacements are summarized in

Table 4.

The fracture strain corresponding to diagram peak is 0.0001 and the relative stress should be lower at this point. Thus, the second point of the tensile diagram which original position was [0.0005, 0.473] is shifted to [0.0001, 0.473], see Figure 48. The diagram can be also improved around the displacement of 0.5 mm (fracture strain 0.005). The load should be similar to the peak load at this area. For that reason, the new point is added to the tensile function and its coordinates are [0.005, 0.473].

At the fracture strains corresponding to the displacement of 2 and 3 mm, the relative stresses are decreased. The same procedure as during the previous modification is done and relative stresses are adjusted in the same proportion as is between loads, see Figure 49.

Model with described modifications can be found at the location: **%Public%\Documents\ATENA Examples\Science\GiD\Tutorial.FRC\FRC_4PBT_2D_modification_3.gid**.

Table 4: Fracture strain corresponding to different displacements in the beam analysis (modification no. 2)

Displacement [mm]	Load [kN]	Step [-]	Crack width [mm]	Fracture strain [-]
0.22	90	2	0.00209	0.0001
0.5	76	4	0.078	0.0052
2	47	16	0.547	0.0365
3	28	24	0.912	0.0608

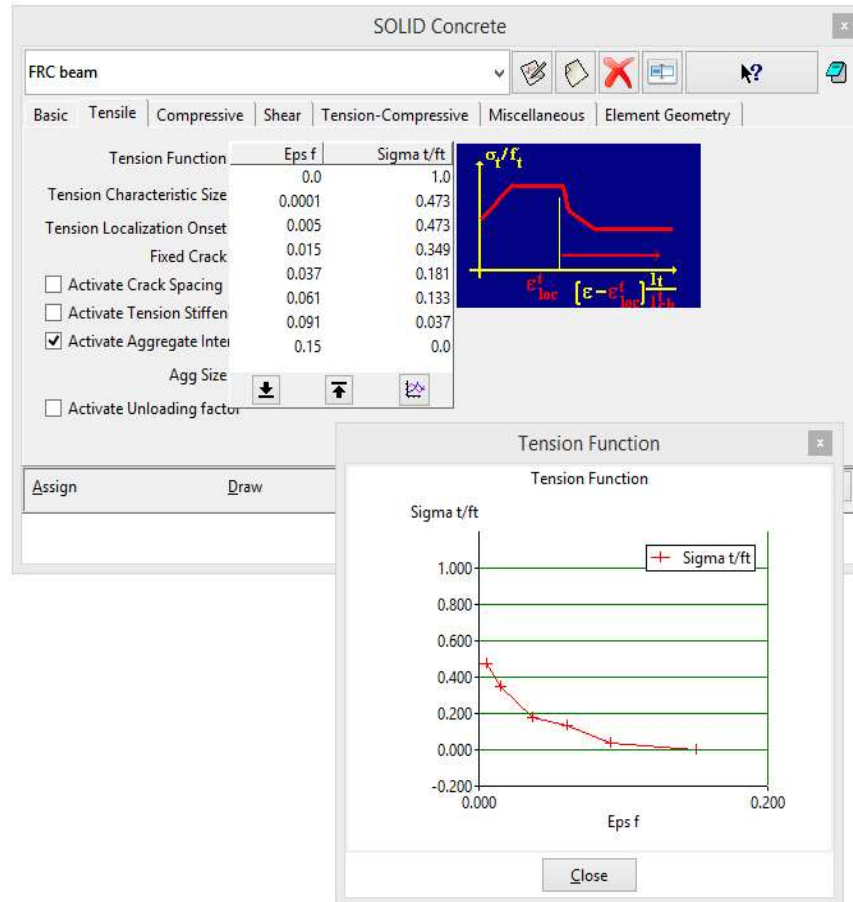


Figure 49: Modification of the tensile function no. 3

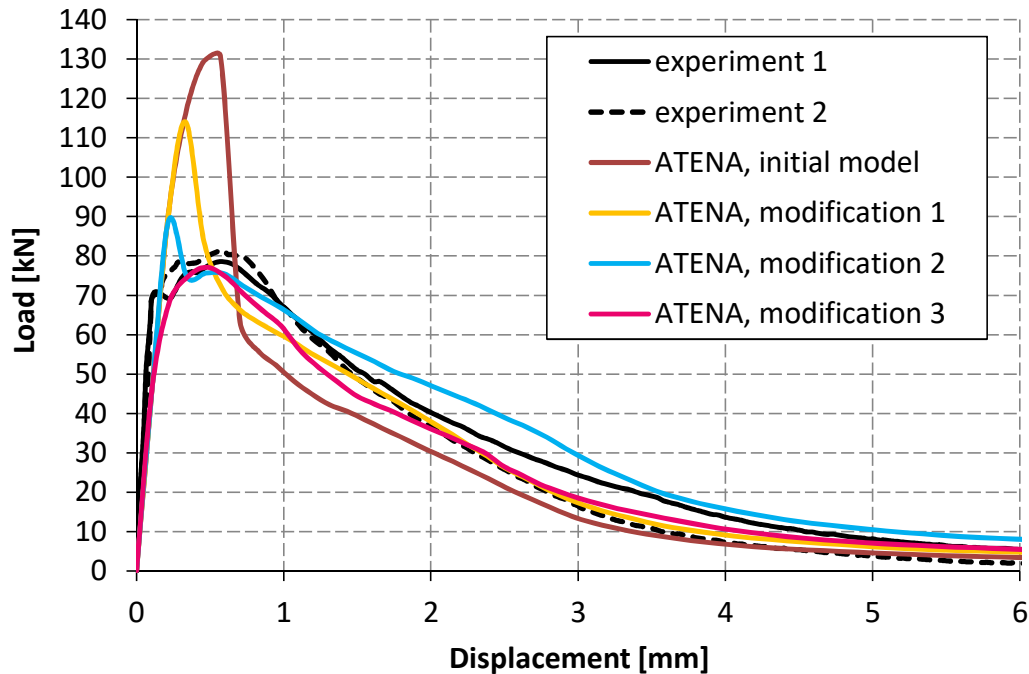


Figure 50: Comparison of L-D diagrams with new result for modification no. 3

- **Modification no. 4**

As the diagram in the Figure 50 shows, the L-D diagram with modified tensile function no. 3 described the FRC behavior very well. It is possible to accept this result as satisfactory or to slightly increase the peak load and load around displacement 1 to 3 mm to obtain more accurate response.

The relative stress at the peak points (fracture strains 0.0001 and 0.005) is increased by 4 %. Finally, the relative stress corresponding to displacement 1, 2 and 3 mm is also increased in the proportion that is between calculated and required load, see Figure 51.

The result of modification no. 4 is shown in Figure 52. The behavior of the FRC beam in four point bending test is in accordance with the experiments and this model can be designated as a final model. For better illustration, the final model is shown in comparison with test results without the other models in Figure 53.

Final model can be found at the location: **%Public%\ Documents\ATENA Examples\Science\GiD\Tutorial.FRC\FRC_4PBT_2D_modification_4.gid**.

Table 5: Fracture strain corresponding to different displacements in the beam analysis (modification no. 3)

Displacement [mm]	Load [kN]	Step [-]	Crack width [mm]	Fracture strain [-]
1	62	8	0.224	0.0149
2	36	16	0.559	0.0373
3	18	24	0.927	0.0618

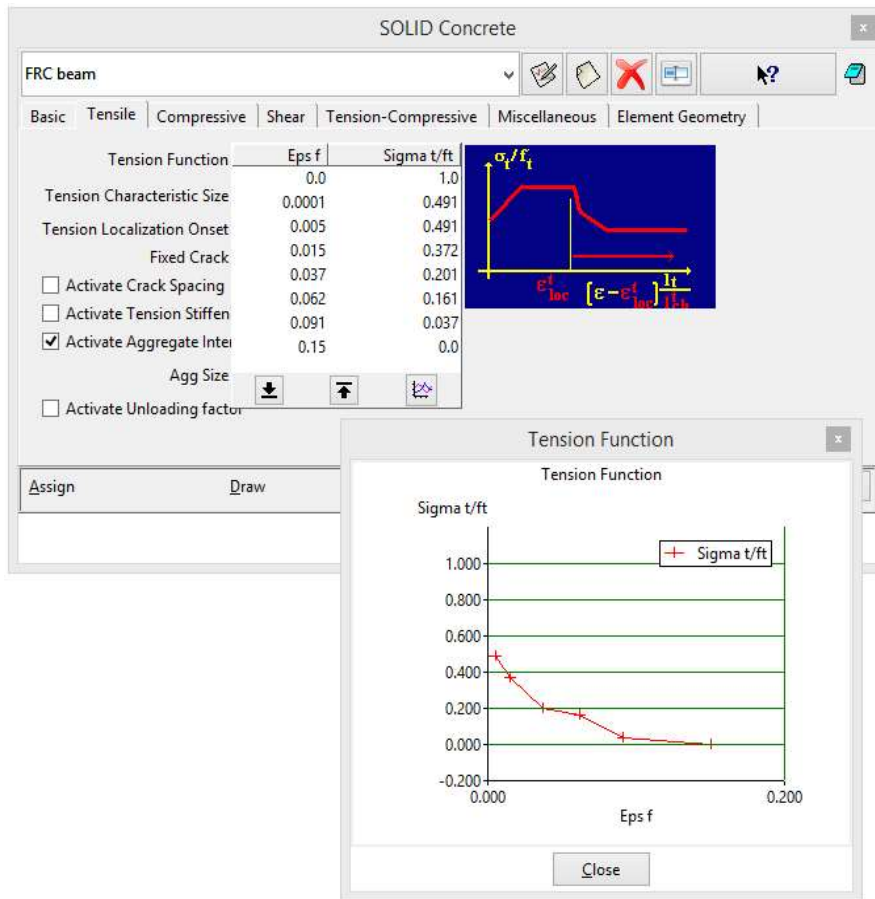


Figure 51: Modification of the tensile function no. 4

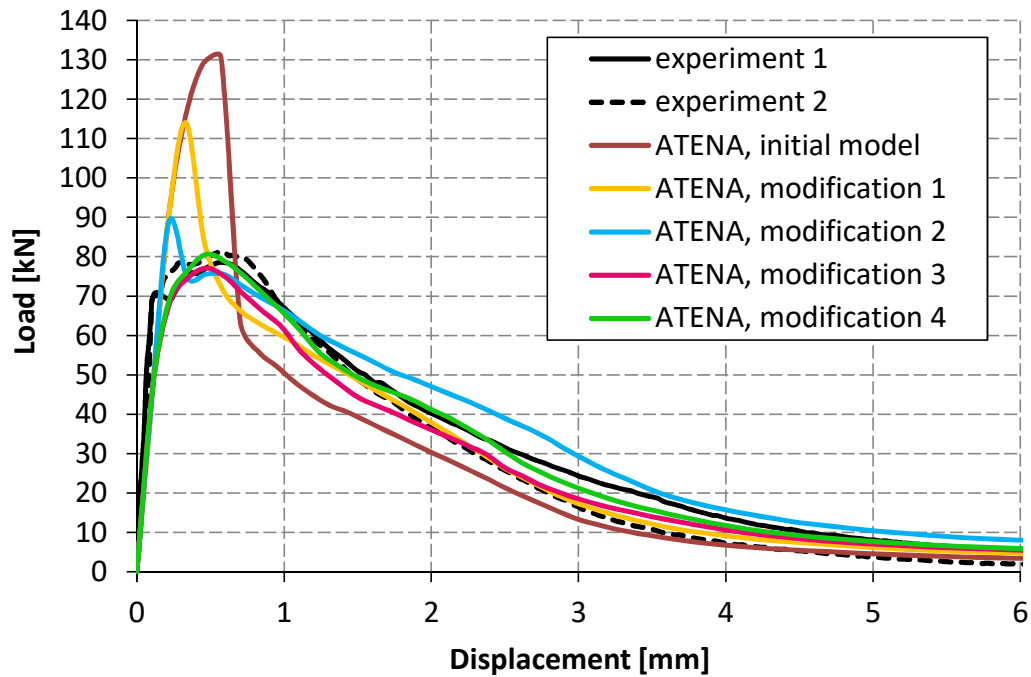


Figure 52: Comparison of L-D diagrams with new result for modification no. 4

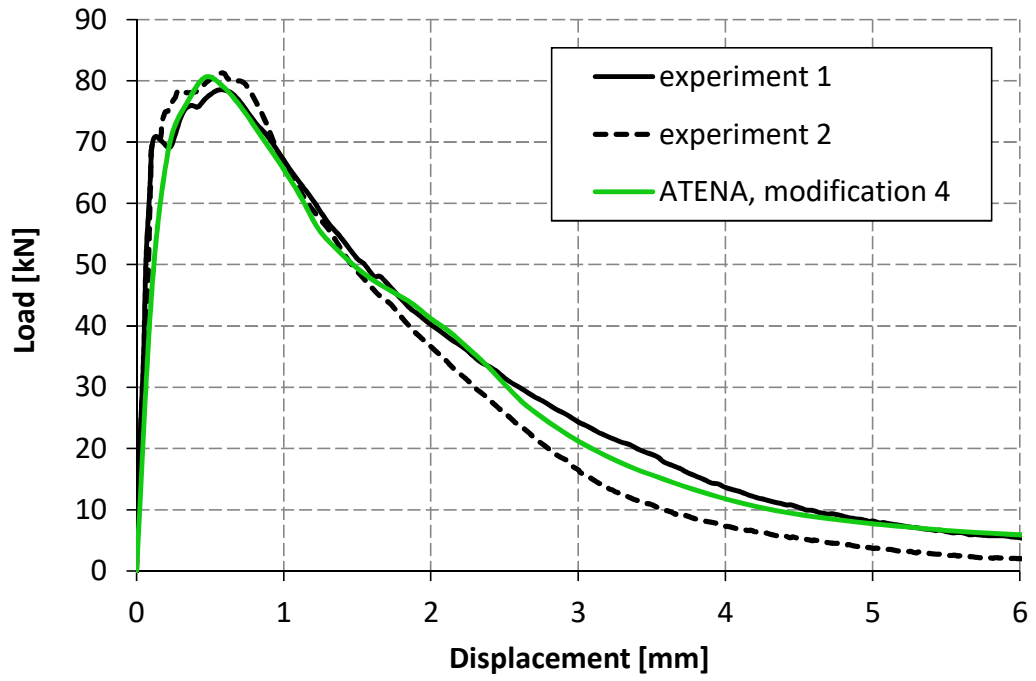


Figure 53: Load-displacement diagram with the final result

5.2.5 General Instructions for Inverse Analysis

During the inverse analysis described in the previous chapter, the user should learn how to work with the material model and how modification of each parameter affects the results. To conclude this section of tutorial, it is possible to say that important parameters for determination of FRC model are (in case of the model **CC3DNonLinCementitious2User**, i.e. **CC3DNonLinCementitious2FRC**):

- tensile strength,
- tension function,
- compressive function,
- Fc Reduction – COMPRED.

By adjusting tensile strength, the whole L-D diagram moves up and down. If the shape of the diagram needs to be modified, the tension function describing the ductility must be modified. For higher ductility in compression, the compressive function should be modified. The last parameter is Fc Reduction – COMPRED which says how the strength is reduced while the material is subjected to lateral tension. Based on developer's experience, it is useful to deactivate this parameter and suppose that for FRC the compressive strength do not decrease due to the lateral tension.

For more information about the material model and **ATENA** program, please read the documentation files ([1], [2], [4], [4] and[5]) or contact the support (following **ATENA** Troubleshooting [5], 2.1.1).

6 ANALYSIS OF SHORT TERM BEHAVIOR OF HIGH PERFORMANCE FIBER REINFORCED CONCRETE STRUCTURES

This section describes the use of material models specifically developed for FE analysis of short term behavior of high performance fiber reinforced concrete structures. It is assumed that the reader is familiar with creation of finite element models in Atena2D and GiD as well as with the ATENA input files syntax.

6.1 *Simulation of SHCC shear beam test*

6.1.1 Introduction

In this example, we demonstrate the application of material model CC3DNonLinCementitious2FRC for simulation of a shear beam test. The test was a part of the experimental study carried presented in ref. [11], which focused on clarifying the effect of fiber reinforcement on shear capacity of FRC structural elements. The tests were performed on beam specimens monotonically loaded by anti-symmetrical moment (so-called Ohno method), as shown in Figure 54. The authors also provided results of material tests in direct tension and compression. Beam specimen denoted as PVA20-00 is chosen for the present simulation. The central part of the beam consisted of strain hardening fiber reinforced cementitious composite (SHCC) with 2% by volume of short PVA fibres (PVA-ECC). The central part contained conventional reinforcement for bending, but no shear stirrups were used. The PVA-ECC material exhibited multiple cracking and significant pseudo-strain hardening behaviour in tension as shown in Figure 55.

The model, shown in Figure 54, is constructed assuming plane stress in Atena2D in a conventional way. One notable aspect is the representation of the connection between the load distribution beam and the specimen, which was in the experiment realized by rollers. In order to ensure that the distribution beam in the model does not constrain the specimen in the longitudinal direction, the connection is realized by reinforcement elements, which transfers only axial force. An attention has to be paid also to the choice of element size, which will be discussed later.

The PVA-ECC material is modeled using the individual-crack-based approach [12], where, even in the multiple-cracking state, each crack is represented on the finite element level and its response is characterized by the traction-separation law (i.e. in terms of bridging stress vs. crack displacement). When this approach is used for a strain hardening fibre reinforced composite, the finite element size in the domain where multiple cracking is anticipated (the central part of the beam) should correspond to the minimum spacing between cracks. We use the fixed crack model, i.e. the direction of cracks does not change once they form.

The traction-separation law represents the crack-bridging effect of matrix and fibers. In SHCC materials, the matrix usually exhibits tension softening (decreasing cohesive stress with increasing crack width) and fibres provide the hardening effect. The traction-separation relation for crack-opening mode can be determined experimentally or analytically. The former approach involves e.g. monitoring the response of a single crack in a tensile test - see e.g. [13]. The analytical approach is based on micromechanical modeling of fiber bridging – e.g. [12], [14]. To identify the micromechanical model, it is necessary to experimentally determine the micromechanical parameters of fibres, matrix and their interface, which may not be always feasible. Against this background, authors or

ref. [5] proposed a methodology which combines the micromechanical modeling with parameter identification from bending test on composite beams. Regardless of the way it is determined, the traction-separation law for the crack-opening mode can be input in the material model `CC3DNonLinCementitious2FRC` as piecewise linear function `TENSION_SOFT_HARD_FUNCTION`.

For the crack-tangential direction (crack sliding mode), it is rather difficult to obtain the traction-separation relationship experimentally. It is possible to use analytical models, e.g the crack sliding model (CSM) described in ATENA Program Documentation Part 1 – Theory, 2.2.11.3. The shear behavior of cracked FRC material is implemented in the `CC3DNonLinCementitious2FRC` material by means of variable shear retention factor β . Users can either select the CSM model or input their own dependence of β on the normal fracture strain through the piecewise linear `SHEAR_STIFF_FUNCTION`. In addition, it is possible to take into account damage of the fibre bridging due to shear by specifying the `SHEAR_STRENGTH_FUNCTION`. This function limits the shear strength of a cracked material based on the value of fracture strain.

6.1.2 Material parameters

In the present FE model we adopt most of the material parameters of PVA-ECC from ref. [12]. Calculations are performed with 2 sets of parameters denoted as PAR1 and PAR2. Set PAR1 fits the uniaxial tension test data (Figure 55) in terms of strength but it is on the lower side in terms of strain capacity. Set PAR2 corresponds to the lower bound of the uniaxial results. The shear retention is specified by the `SHEAR_STIFF_FUNCTION`, whose values are defined according to the CSM model. The fibre shear modulus, used in the CSM model, in PAR1 is adopted from ref. [16]. In set PAR2, the modulus is reduced to represent presumed damage of fibers by shearing according to ref. [12]. Parameters and functions are listed in Table 6 thru Table 9. No reduction of tensile strength due to transversal compression (`TENSILE_STRENGTH_RED_FUNCTION`), or limitation of shear strength (`SHEAR_STRENGTH_FUNCTION`) is considered in this example.

Table 6: Material parameters for PVA-ECC (set PAR1 and PAR2, units m, MPa)

Parameter set	PAR1	PAR2
TYPE	CC3DNonLinCementitious2FRC	CC3DNonLinCementitious2FRC
E	1.95E+04	1.95E+04
Mu	0.2	0.2
Ft	3.41E+00	2.75E+00
Fc	-3.91E+01	-3.91E+01
FT_MULTIP	2.50E+00	2.31E+00
TENSION_SOFT_HARD_FUNCTION	10	10
CHAR_SIZE_TENSION	0.002	0.001
X_LOC_TENSION	0.00E+00	0.00E+00

COMP_SOFT_HARD_FUNCTION	11	11
CHAR_SIZE_COMP	0.1	0.1
X_LOC_COMP	-3.00E-01	-3.00E-01
FC_REDUCTION_FUNCTION	12	12
SHEAR_STIFF_FUNCTION	13	13
X_LOC_SHEAR	0.00E+00	0.00E+00
SHEAR_STRENGTH_FUNCTION	14	14
TENSILE_STRENGTH_REDUCTION_FUNCTION	15	15
Exc	0.52	0.52
Beta	0	0
Rho	2.30E-02	2.30E-02
Alpha	1.20E-05	1.20E-05
Fixed	10	10

Table 7: Fiber parameters used for determination of the SHEAR_STIFF_FUNCTION by the CSM model (set PAR1 and PAR2, units m, MPa)

Parameter set	PAR1	PAR2
Vf	0.02	0.02
Fiber shear modulus Gf	1700	110
Fiber Young modulus Ef	40000	40000
Fiber shape factor k	0.9	0.9
Fiber diameter df	4.00E-05	4.00E-05

Table 8: Functions defining the cohesive crack behaviour of PVA-ECC (set PAR1)

FUNCTION								
id 10								
name "Function for Material ECC Value TENSION_SOFT_HARD_FUNCTION"								
type "CCMultiLinearFunction"								
xvalues	0	0.005865	0.02469	0.04352	0.06235	0.08117	0.1	1.137
yvalues	1	0.2883	0.5916	0.7854	0.9401	1.0727	1.1906	0

FUNCTION								
id 13								
name "Function for Material ECC Value SHEAR_STIFF_FUNCTION"								
type "CCMultiLinearFunction"								
xvalues	0	0.001	0.0025	0.00587	0.025	0.1	0.5	1.137
yvalues	1	0.9039	0.7897	0.6139	0.2544	0.0364	0.0003	0

Table 9: Functions defining the cohesive crack behaviour of PVA-ECC (set PAR2)

FUNCTION								
id 10								
name "Function for Material ECC Value TENSION_SOFT_HARD_FUNCTION"								
type "CCMultiLinearFunction"								
xvalues	0	0.01455	0.03804	0.06153	0.08502	0.1085	0.132	2.274
yvalues	1	0.3645	0.5895	0.7498	0.8813	0.9957	1.0982	0

FUNCTION										
id 13										
name "Function for Material ECC Value SHEAR_STIFF_FUNCTION"										
type "CCMultiLinearFunction"										
xvalues	0	0.0001	0.0005	0.001	0.002	0.005	0.01	0.05	0.1	2.274
yvalues	1	0.9242	0.709	0.5491	0.3784	0.1956	0.1082	0.0232	0.0113	0

6.1.3 Results

The results in terms of applied load vs. translational angle of simulations with parameters PAR1 and PAR2 are compared with experimental data in Figure 57. The fracture patterns can be compared in Figure 58 and Figure 59. It is evident that the result obtained with parameter set PAR1 overestimates the load and deformation capacity of the beam, while almost perfect fit is obtained with parameters PAR2. The latter calculation also fairly well captures the failure the fracture behavior with diagonal multiple cracking and fracture localization into a bond splitting horizontal crack. The fact that the matching results are obtained with the reduced set of parameters (PAR2) indicates that fiber bridging sustains damage under shear loads, which is consistent with other authors' observation, e.g. [17].

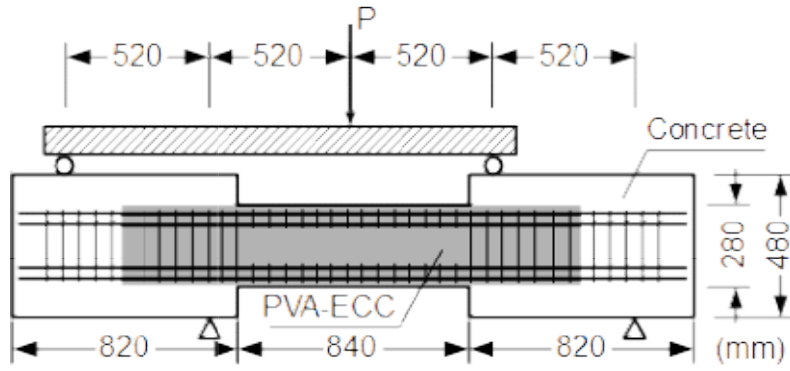


Figure 54: Configuration of shear beam test (reinforcement is shown schematically)

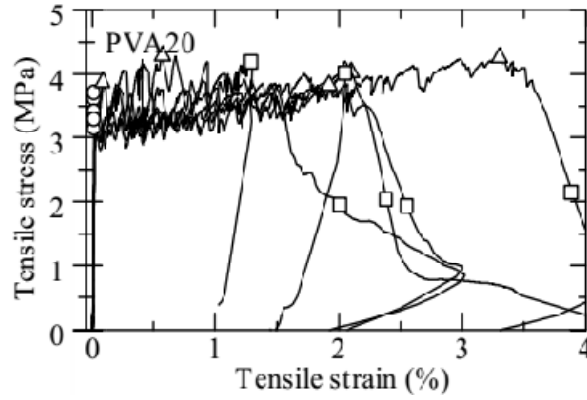


Figure 55: Results of direct tension tests on PVA-ECC with 2% by volume fiber content [1]

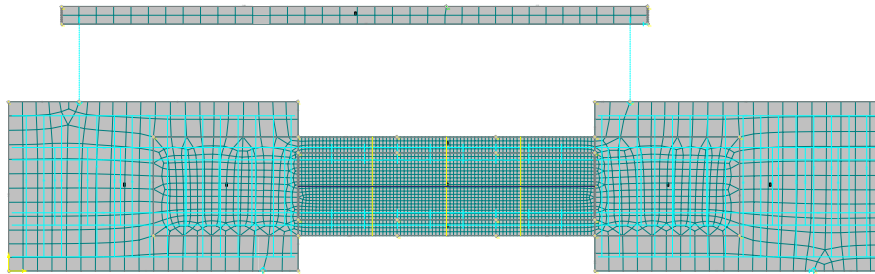


Figure 56: Finite element model of shear beam test

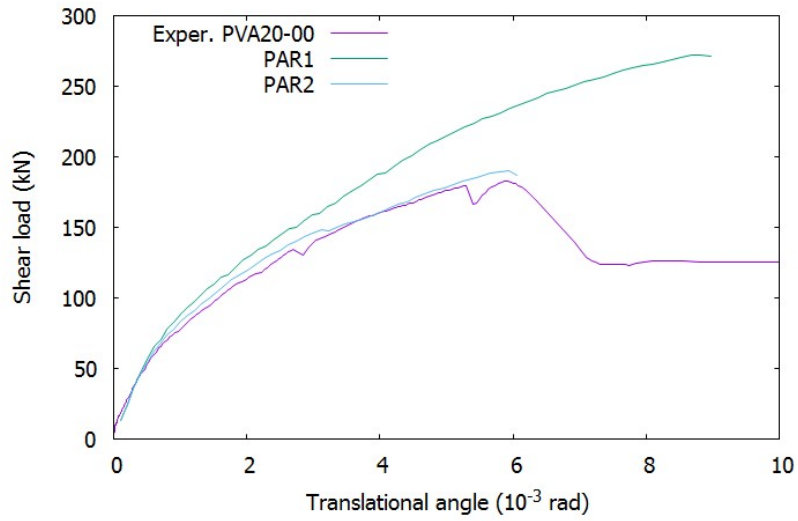


Figure 57: Experimental and numerical results of shear beam test

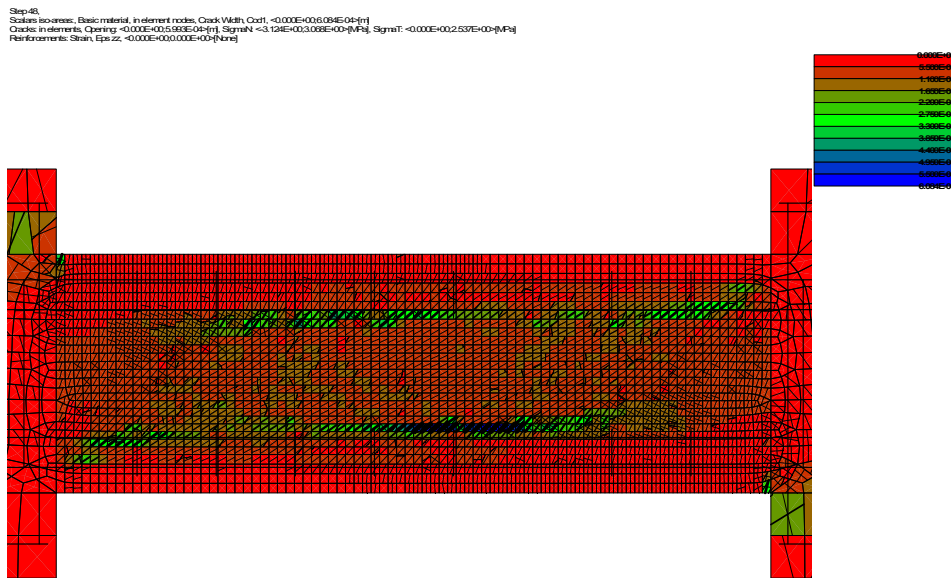


Figure 58: Fracture pattern of beam PVA20-00 obtained from the FE simulation with parameter set PAR2

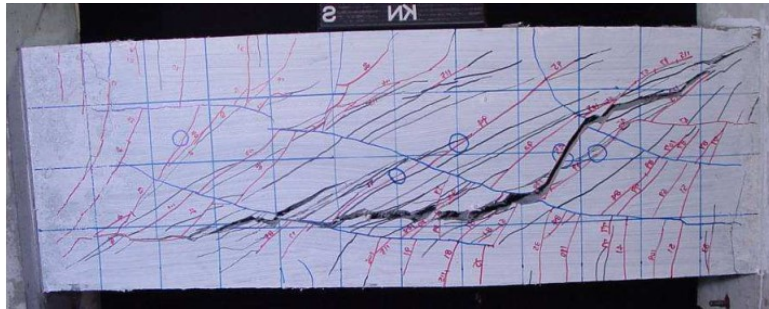


Figure 59: Fracture pattern of beam PVA20-00 observed in the experiment [8]

6.2 Simulation of HSFRC shear beam test

6.2.1 Introduction

In this example, we demonstrate the application of material model CC3DNonLinCementitious2SHCC for simulation of a shear beam test, which was conducted at the Klokner Institute of CTU in Prague in 2015. The test was performed on beam specimens monotonically loaded by anti-symmetrical moment (so-called Ohno method), as shown in Fig. 1. The beam was cast from high-strength fiber reinforced concrete (HSFRC), the same material, which was used for homogenous reference beams in the study by Kabele et al. [15]. The HSFRC material consisted of fine-grained cementitious matrix reinforced with 1.5% by volume of short steel fibers. It was found by inverse analysis of bending tests [5], that the material exhibited tension softening behavior. The beam was reinforced against bending failure by FRP sheets glued to the upper and lower surface. The experiment revealed both shear cracking in the area between the inner load point and inner support as well as bending cracks propagating from the bottom or top surface between supports or load points, respectively (Figure 64). This cracking resulted in reduction of the overall stiffness (Figure 62), but did not lead to the failure of the beam. The specimen eventually failed due to delamination of the upper FRP sheet.

The model, shown in Fig. 1, is constructed in GiD-Atena preprocessor. The problem is modeled by brick elements to test the capability of the material model in 3D. Nevertheless, since the experiment configuration does not impose any significant stress variation in direction perpendicular to the loading plane, only one layer of elements is used (in effect simulating plane stress conditions). The FRP reinforcement is modeled by the total of four reinforcement bars placed very close to the corners of the beam cross-section. As the objective of this example is to reproduce cracking of the HSFRC material (and not the failure of the FRP reinforcement), the FRP is considered to be elastic and perfectly bonded to the concrete. The connection between the load distribution beam and the specimen is realized by reinforcement elements as in example 6.1.

HSFRC is modelled using the individual-crack-based approach as in example 6.1. Thus each crack is represented on the finite element level and its response is characterized by the traction-separation relationship (i.e. in terms of stress vs. crack displacement). The direction of cracks does not change once they form (i.e. the fixed crack model is used).

6.2.2 Material parameters

The parameters and functions defining the HSFRC material model are adopted from [12]. The shear retention is specified through the CSM model. Relevant parameters and functions are listed in Table 10 and Figure 60. No reduction of the tensile strength due to transversal compression (TENSILE_STRENGTH_RED_FUNCTION), or limitation of the shear strength (SHEAR_STRENGTH_FUNCTION) is considered in this example.

Table 10: Material parameters for HSFRC (units m, MPa)

TYPE	CC3DNonLinCementitious2SHCC
E	50000
MU	0.2

RHO	0.0023
ALPHA	0.000012
FT	11.78
FC	-106
EXC	0.52
BETA	0
TENSION_SOFT_HARD_FUNCTION	10001
CHAR_SIZE_TENSION	0.005
X_LOC_TENSION	0
COMP_SOFT_HARD_FUNCTION	10002
CHAR_SIZE_COMP	1
X_LOC_COMP	-1
FIBER_VOLUME_FRACTION	0.015
FIBER_E_MODULUS	200000
FIBER_SHEAR_MODULUS	77000
FIBER_CROSS_SECTION_FACTOR	0.9
FIBER_DIAMETER	0.0002
FT_MULTIP	10
TENSILE_STRENGTH_RED_FUNCTION	10004
FIXED	0

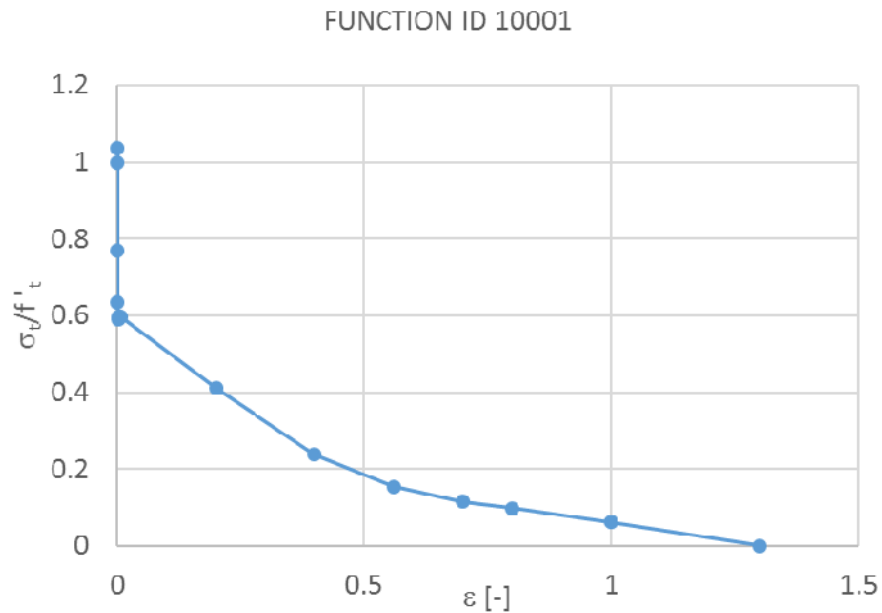


Figure 60: Function describing the tension softening relation for HSFRC material

6.2.3 Results

The calculation results in terms of applied load vs. vertical displacements under the inner and outer loading point are compared with experimental data in Figure 62. The fracture

patterns are shown in Figure 63 and Figure 64. It is evident that the FE model fairly well captures the tendency of the experimental load-displacement curve under the outer load point. However, under the inner load point, the slope of the calculated curve is steeper than that from the experiment. The points, where the simulation curves show a sudden drop and change of slope correspond to localization of the shear cracks in the central part of the beam. By comparing Figure 63 and Figure 64 it is evident that the calculation captures well the fracture pattern of the beam. Dominant cracking occurs in the form of inclined cracks between the inner load point and support, which form due to intense shearing. Secondary bending cracks between the load points and between the supports are represented as well.

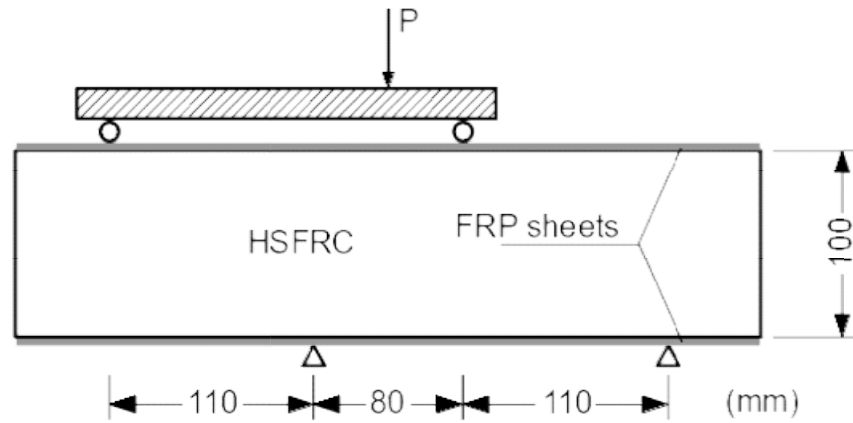


Fig. 1 Configuration of HSFRC shear beam test

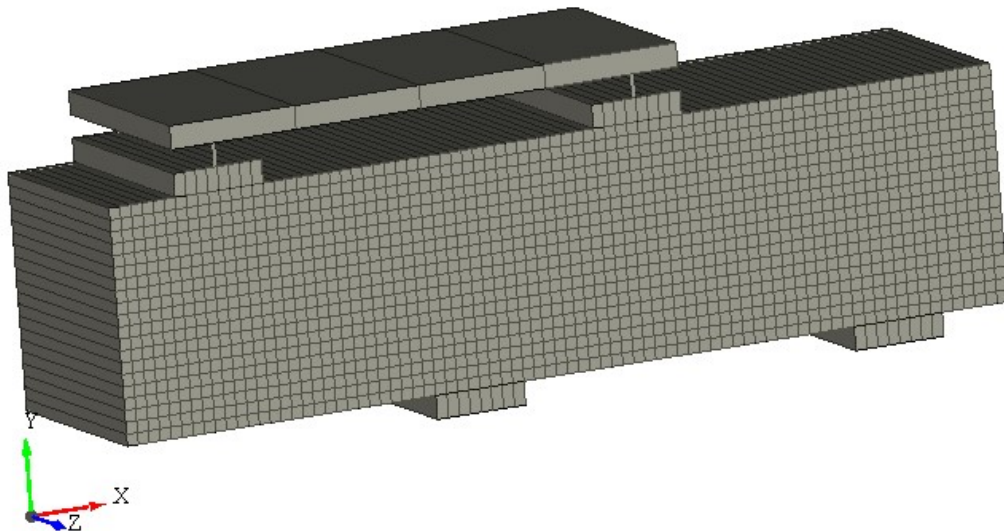


Figure 61: Finite element model of shear beam test

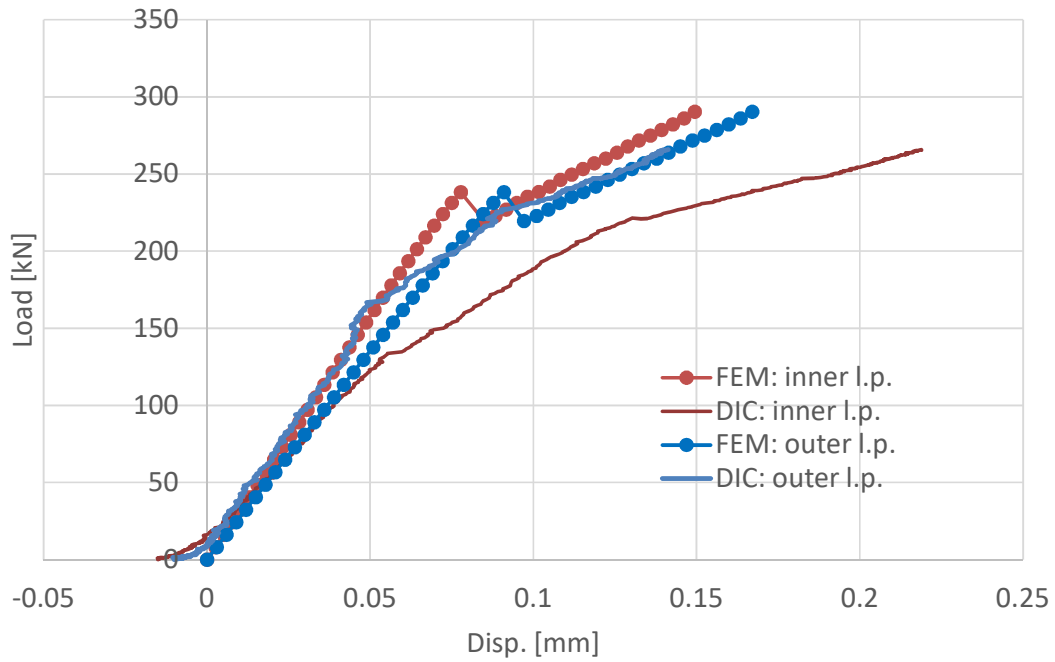


Figure 62: Experimental and numerical results of the HSFRc shear beam test

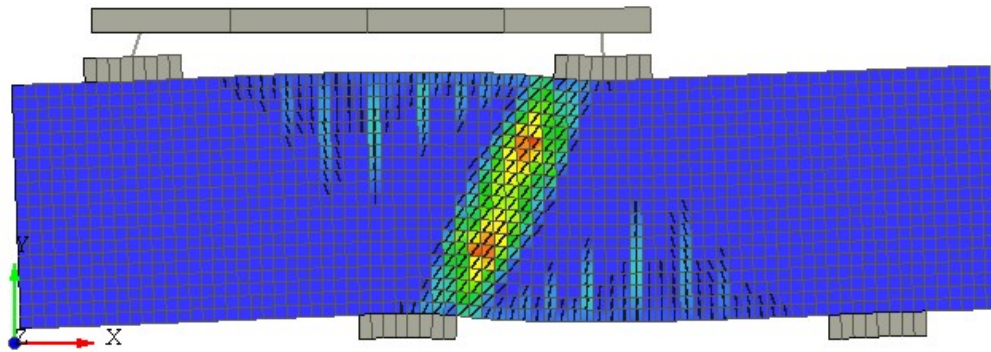


Figure 63: Fracture pattern of the shear beam obtained from the FE simulation (contours show crack opening displacement)

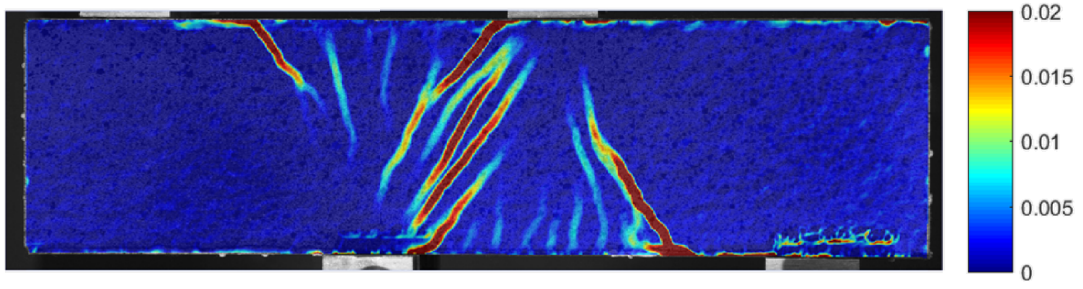


Figure 64: Fracture pattern of the shear beam obtained from the DIC analysis of the experiment

7 ANALYSIS OF LONG TERM BEHAVIOR OF HIGH PERFORMANCE FIBRE REINFORCED CONCRETE STRUCTURES

This section describes the use of material models specifically developed for FE analysis of long term behavior of high performance fiber reinforced concrete structures. It is assumed that the reader is familiar with creation of finite element models in Atena2D and GiD as well as with the ATENA input files syntax.

7.1 Simulation of ECC creep test – bending specimen under sustained load

7.1.1 Introduction

In this example, we demonstrate the application of material model CC3DNonLinCementitious2User for simulation of three point bending test according to Boshoff and van Zijl [19], see Figure 65. Displacement controlled bending test were carried out first to obtain specimen resistance for different testing rates. Afterwards, force controlled bending tests were performed at load level 85% and 95% of the ultimate loads determined by displacement controlled tests. Response of specimens is shown in Figure 66. Result for the highest and lowest load levels are shown together with two curves investigating creep deformation under sustained loads.

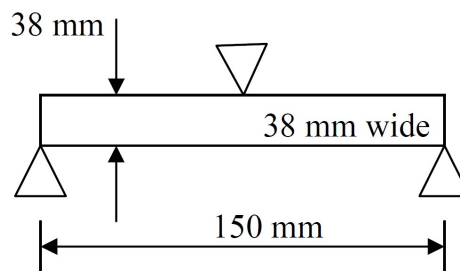


Figure 65: Load-displacement diagram of specimens in three point bending test [19]

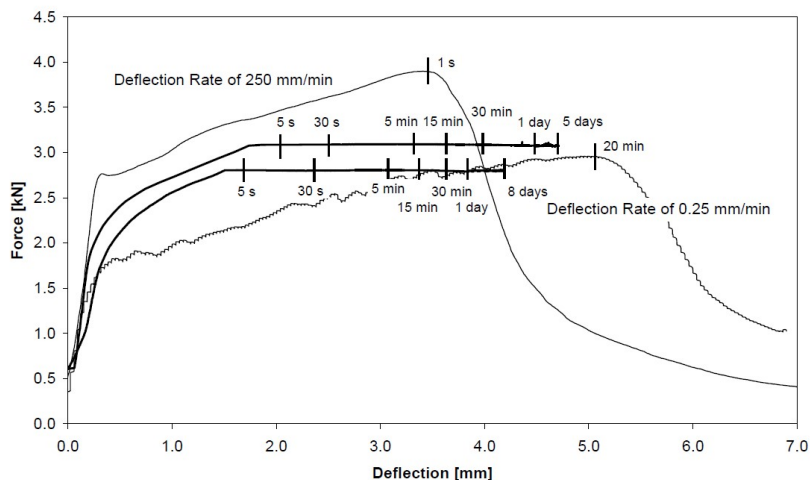


Figure 66: Load-displacement diagram of specimens in three point bending test [19]

The beam were casted from high-performance fiber reinforced concrete (HPFRC) with addition of PVA REC15-12 fibers (2% by volume), also called as ECC (engineering cement-based composite) material. Parameters of matrix are water:binder ratio of 0.4, aggregate to binder ration of 0.5, fly ash to binder ration of 0.5. Specimen were stripped from their moulds after three days, water cured for 11 days and then tested at the age of 14 days from casting. Casting and curing for the full 14 days were at controlled environmental temperature of 23°C.

The results in Figure 66 show that material exhibit tension hardening behavior. Force controlled tests revealed large creep deformation. High initial speed of creep deformation is indicated.

The model, shown in Figure 67, is constructed in GiD-ATENA pre-processor. The problem is modeled in 2D by quadrilateral elements. The connection between the load distribution plate or supporting plate and the specimen is realized by fixed contact condition.

ECC is modelled using the individual-crack-based approach. Thus each crack is represented on the finite element level and its response is characterized by the traction-separation relationship (i.e. in terms of stress vs. crack displacement). The direction of cracks does not change once they form (i.e. the fixed crack model is used).

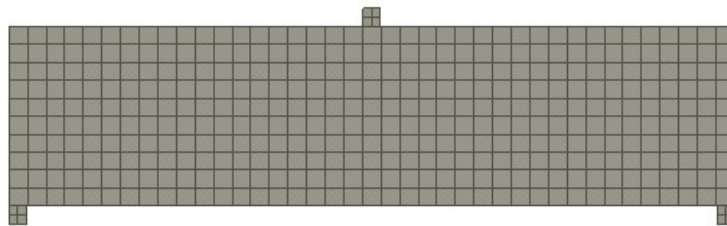


Figure 67: Specimen in three point bending test modelled in ATENA

7.1.2 Material parameters

To determine parameters and functions defining ECC material model, inverse analysis of results from three point bending test was performed in the same way as in chapter 5.2. Normal testing rate is 2.5 mm/min, therefore inverse analysis is done for this rate. Results for different rates are presented in [19] in graphs shown in Figure 68. According to these results, tensile function can be determined, see Figure 69. Results are shown in Figure 70 in comparison with load displacement diagrams for rate 0.25 and 250 mm/min. Results for rate 2.5 mm/min are shown as areas where the point of the first matrix crack and point of the peak resistance should be located.

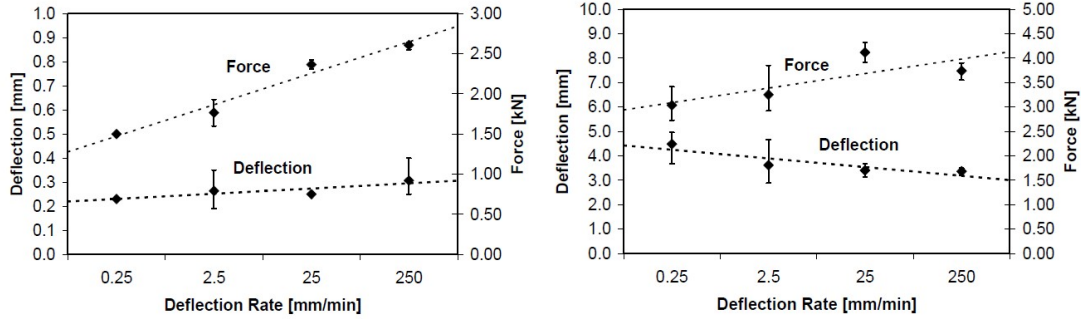


Figure 68: The deflection and force at the point of the first matrix crack (left), the deflection and force at the point of peak force resistance of the specimen (right) [19]

Other parameters that are not known from the paper [19] and cannot be determined by inverse analysis are based on results for similar material presented in Sajdlová and Kabele [20].

Relevant parameters and functions are listed in Table 11 and Figure 69. No reduction of the tensile strength due to transversal compression (TENSILE_STRENGTH_RED_FUNCTION) is considered in this example.

Table 11: Material parameters for ECC (units m, MPa)

TYPE	CC3DNonLinCementitious2User
E	18000
MU	0.2
RHO	0.0023
ALPHA	0.000012
FT	2
FC	-60
EXC	0.52
BETA	0
TENSION_SOFT_HARD_FUNCTION	20001
FT_MULTIP	4.62
CHAR_SIZE_TENSION	0.015
X_LOC_TENSION	0
COMP_SOFT_HARD_FUNCTION	20002
CHAR_SIZE_COMP	0.1
X_LOC_COMP	-0.0008411
SHEAR_STIFF_FUNCTION	20003
SHEAR_STRENGTH_FUNCTION	20006
X_LOC_SHEAR	0
FC_REDUCTION_FUNCTION	20005
TENSILE_STRENGTH_RED_FUNCTION	20004
FIXED	1
AGG_SIZE	0.02

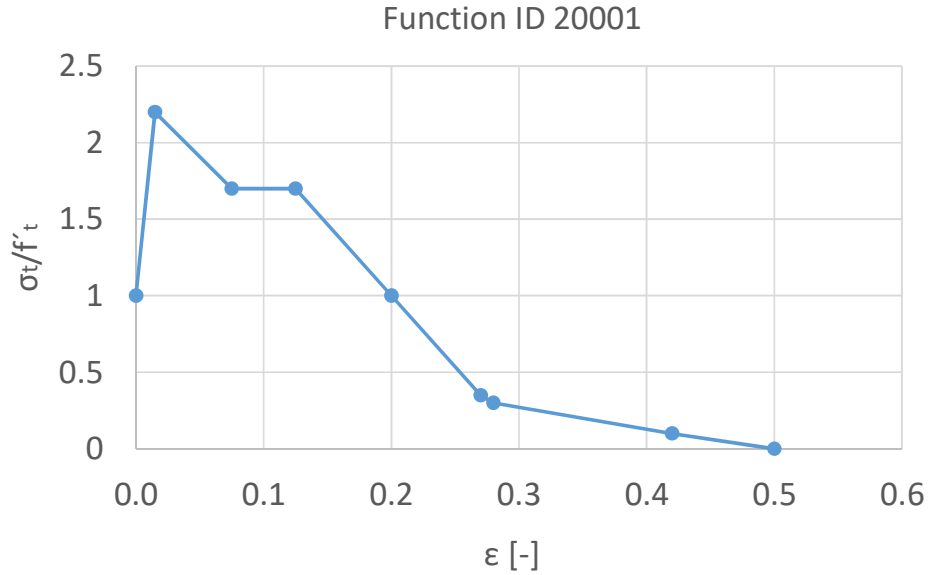


Figure 69: Function describing the tension softening relation for ECC material

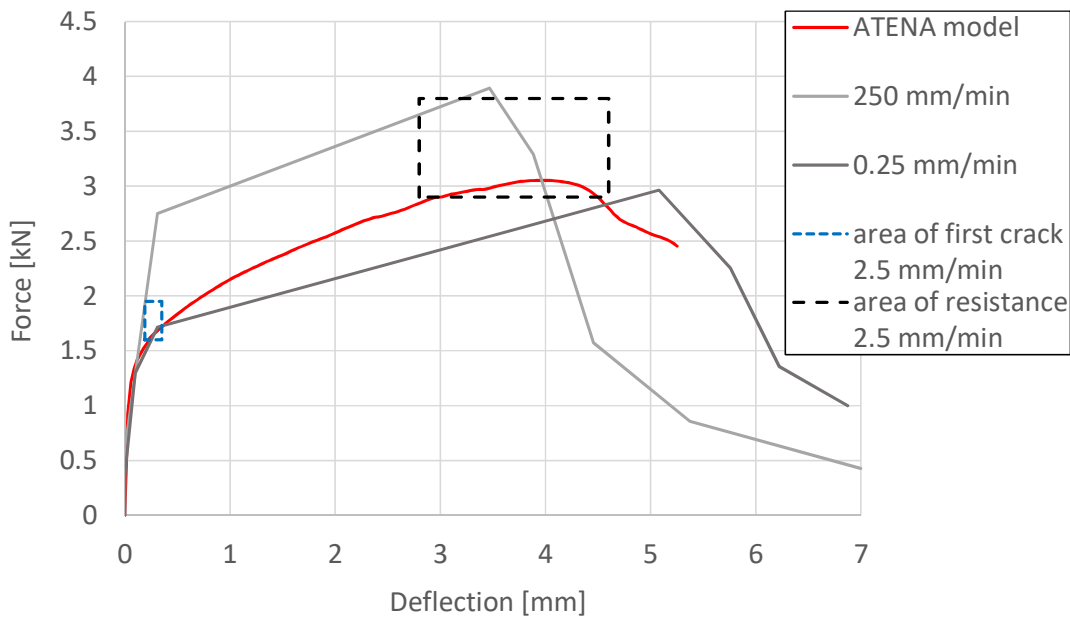


Figure 70: Load-displacement diagrams – comparison of experimental and numerical results

7.1.3 Results

The calculation results in terms of relative applied load vs. vertical displacements in the middle of the beam are compared with experimental data in Figure 71. The fracture patterns of model at different stages of calculation are shown in Figure 72 and Figure 73.

It is evident that numerical model fairly well describes creep deformation obtained during the experiment. During 8 days deformation of beam under sustained load increased by 2.8 mm.

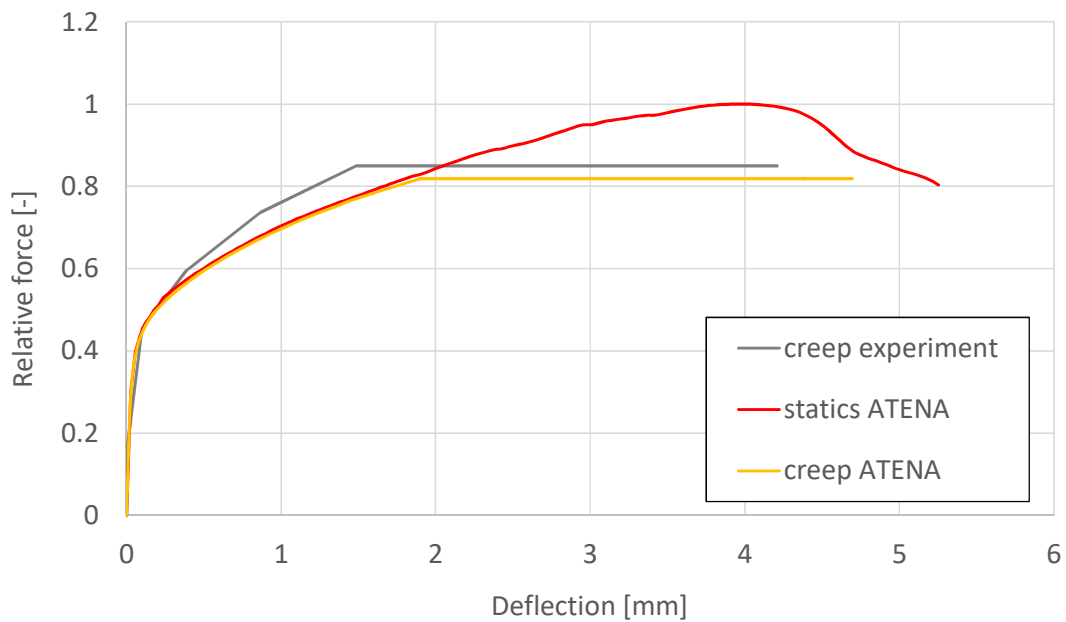


Figure 71: Load-displacement diagrams – comparison of experimental and numerical results

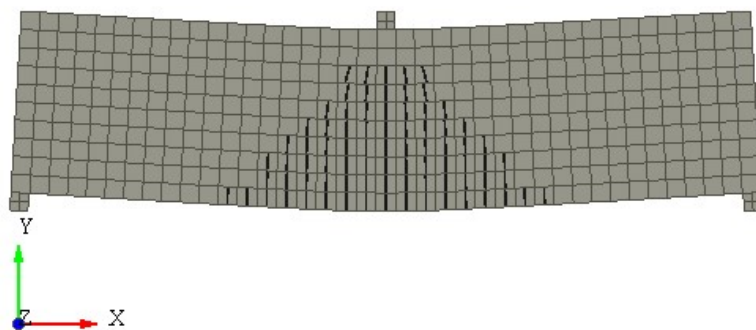


Figure 72: Cracks in specimen before application of sustained load, cracks wider than 0.05 mm are shown

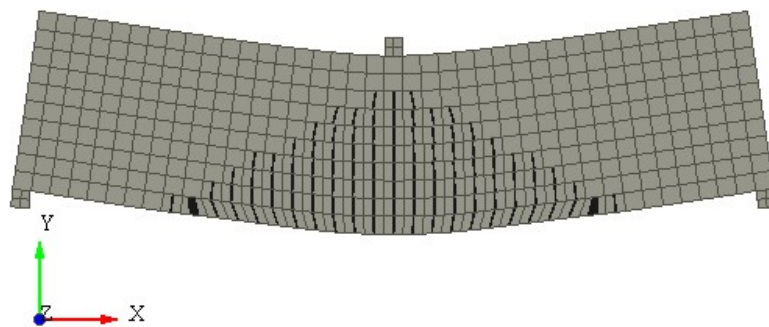


Figure 73: Cracks in specimen at the end of creep test, cracks wider than 0.05 mm are shown

8 SIMULATION OF MOISTURE TRANSPORT AND DRYING SHRINKAGE PROPERTIES OF STEEL FIBER REINFORCED CONCRETE

In this example, we demonstrate the application of material model CC3DNonLinCementitious2User for simulation of tests dealing with moisture transport and drying shrinkage according to Jafarifar et al. [21].

Two mixes (CC and RCC) are tested, both with (60 kg/m^3) and without steel fibers. Components of each mix are shown in Table 12. Compressive strength in 28 days obtained from 150 mm cubes is 61 MPa for CC mix and 51 MPa for RCC mix.

Table 12: Composition of concrete mixes [21]

Mix	Cement (kg/m^3)	W/C	Crushed aggreg. (kg/m^3)	River aggreg. (kg/m^3)	Sand (kg/m^3)	Superplasticizer ^a	Air-entrainer ^a
CC	380	0.35	-	1004	833	0.85%	0.135%
RCC	300	0.54	2084	-	-	-	-

^a % by cement mass

Two types of tests were performed. The first test include prisms $180 \times 150 \times 150 \text{ mm}$ that are sliced in two segments at different depths, see Figure 74. The sides of segments are sealed. This approach provides one-dimensional drying conditions. After cutting, two segments were put back together and the joint was also sealed, see Figure 75. By measuring the moisture transport on these segments, it is possible to define moisture content in different depth of specimen.

Evolution of moisture content in different depths during 84 days is shown in Figure 76. Results show that after 84 days drying at 40% humidity, the moisture content at a depth of 10 mm from the drying surface only dropped in the range of 65-70%, whereas, at a depth of 35 mm the moisture content remained above 90%. The fastest rate of drying occurs at early ages and then it decreases with time.

Tests were performed after 90 days of curing in water. During tests, the specimens were placed in a chamber with relative humidity of $40 \pm 3\%$ and temperature of $25 \pm 3^\circ\text{C}$.

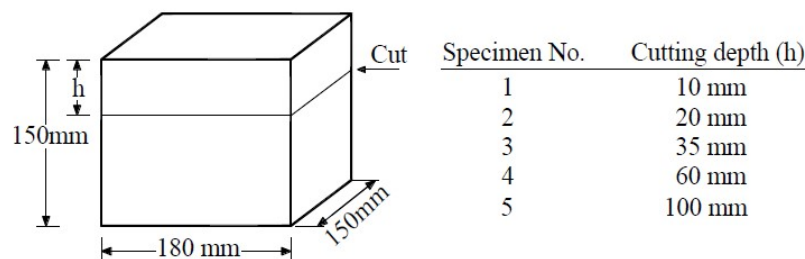


Figure 74: Specimen for moisture measurements – list of cutting depths Chyba! Nenalezen zdroj odkazů.

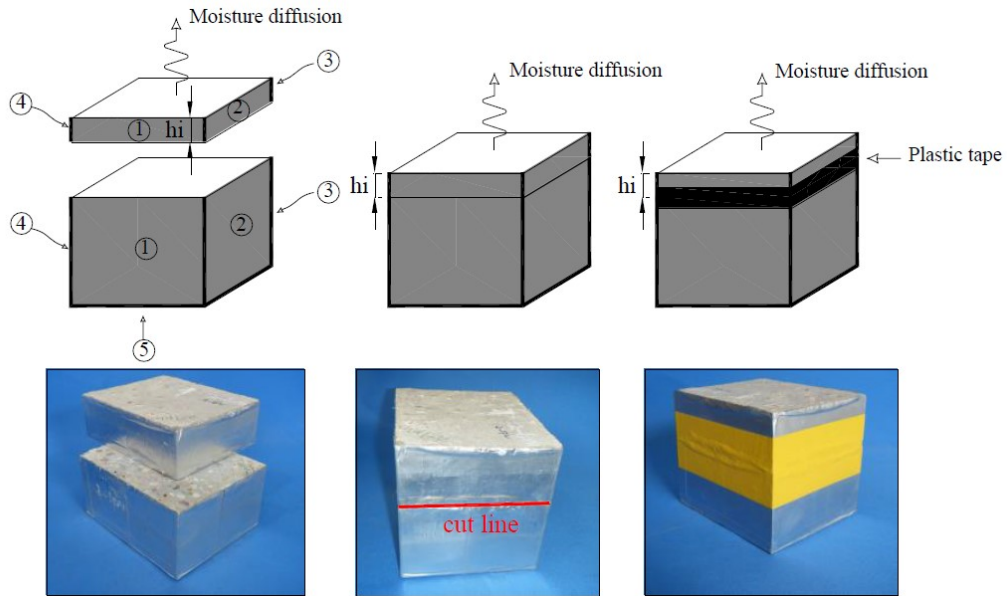


Figure 75: Preparation of specimen for moisture measurements [21]

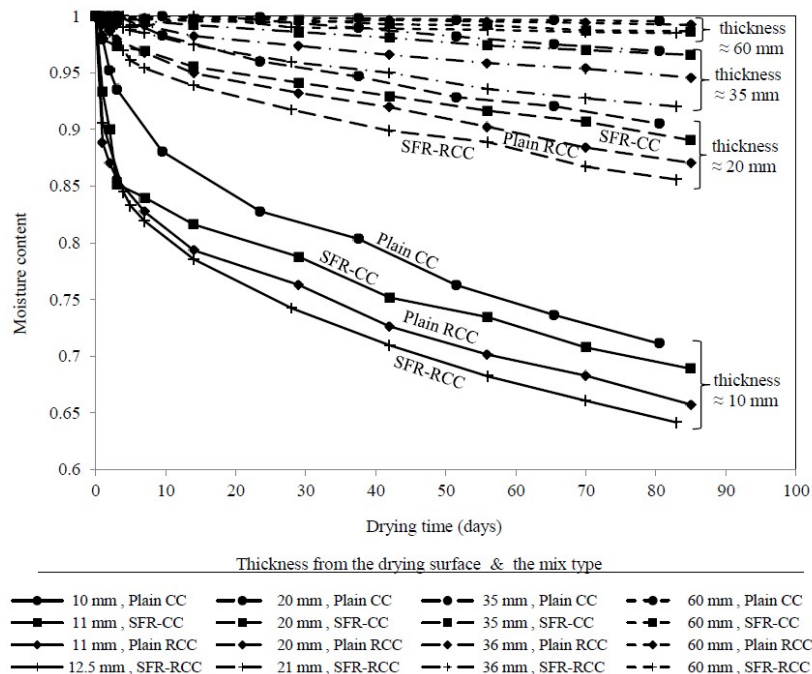


Figure 76: Results of moisture experiments [21]

The second test contains prisms with dimensions 150x150x550 mm for free shrinkage measurements. The two end sides of the specimen were sealed thus moisture transport was only allowed from the exposed sides according to Figure 77. To provide uniform drying and unrestrained conditions, the specimens were rested on two sharp edges whilst drying. The environmental conditions were the same as in the first test.

Results are shown in Figure 78. For RCC mixes, shrinkage occurs at a relatively uniform rate. For CC mixes, shrinkage occurs at a fast rate at early ages and then the rate decreases.

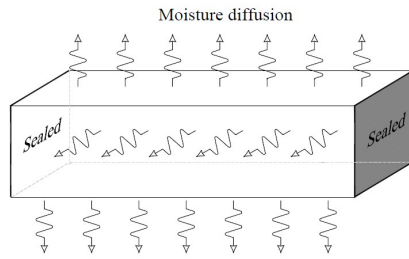


Figure 77: Scheme of specimen for free shrinkage measurements (left), beams during the test (right) [21]

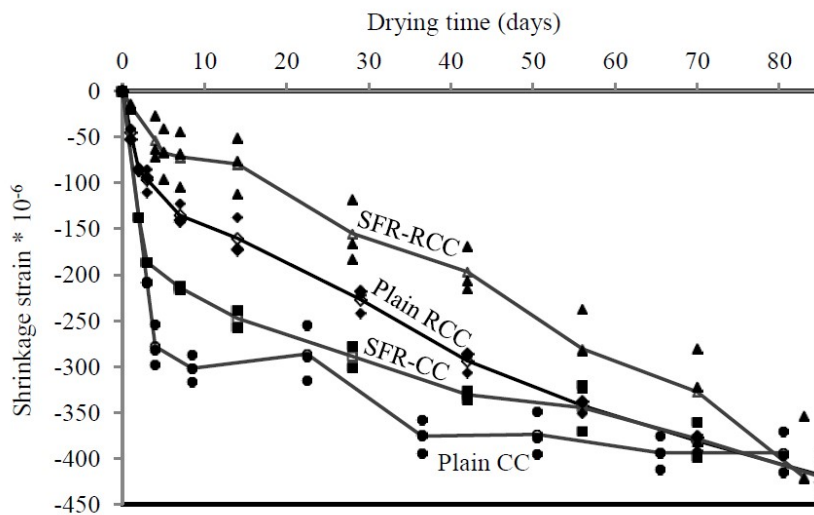


Figure 78: Strain history curves for free shrinkage specimens [21]

The models, shown in Figure 79, are constructed in GiD-ATENA pre-processor. The specimens are modeled in 3D by hexahedra elements. For moisture tests, model consists of elements 5 mm thick to capture each moisture profile according to Figure 74. In the x-y plane, there is one finite element in the whole specimen because only one-dimensional drying in z-axis direction is measured. Therefore, there is no need to divide structure into more finite elements. Model for free shrinkage consists of brick elements with size 15 mm. In contrary to the previous model, this beam has finer mesh to capture cracking that can occur during the shrinkage test.

Steel fiber reinforced concrete is modeled using the individual-crack-based approach. Thus each crack is represented on the finite element level and its response is characterized by the traction-separation relationship (i.e. in terms of stress vs. crack displacement). The direction of cracks does not change once they form (i.e. the fixed crack model is used).

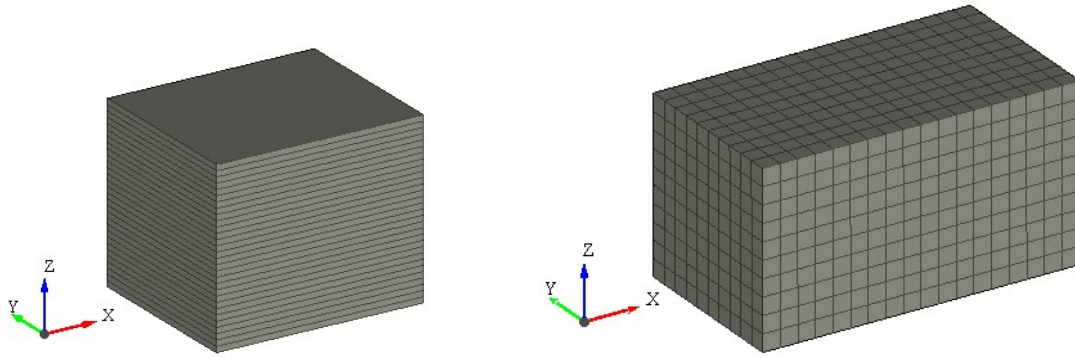


Figure 79: Specimen for moisture measurements (left), specimen for free shrinkage test (right) modelled in ATENA

8.1 Material parameters

Material model for moisture transport and drying shrinkage test is based on the compressive strength and composition of matrix that are only parameters we know about material used in the study. Compressive strength is 61 MPa for CC mix and 51 MPa for RCC mix. Matrix is reinforced by steel fibers recycled from tires. Fibers has diameter in the range of 0.1 to 0.23 mm and a tensile strength of around 2000 MPa. 60 kg of fibers per each cubic meter of concrete (approx. 2.5% by weight) is utilized.

According to these parameters, similar model as is presented as a result of inverse analysis in the chapter 5.2 is applied in these calculations. Only compressive strength is set to 60 MPa and tensile strength and Young's modulus are adjusted to this value, see Table 13. Tensile and compressive functions remain the same as in chapter 5.2.

Table 13: Material parameters for steel fibre reinforced concrete (units m, MPa)

TYPE	CC3DNonLinCementitious2User
E	38000
MU	0.2
RHO	0.0023
ALPHA	0.000012
FT	6
FC	-60
EXC	0.52
BETA	0
TENSION_SOFT_HARD_FUNCTION	10001
FT_MULTIP	2.1
CHAR_SIZE_TENSION	0.015
X_LOC_TENSION	0
COMP_SOFT_HARD_FUNCTION	10002
CHAR_SIZE_COMP	0.1
X_LOC_COMP	-0.0008411
SHEAR_STIFF_FUNCTION	10003
SHEAR_STRENGTH_FUNCTION	10006

X_LOC_SHEAR	0
FC_REDUCTION_FUNCTION	10005
TENSILE_STRENGTH_RED_FUNCTION	10004
FIXED	1
AGG_SIZE	0.02

Material parameters for moisture transport are based on the measured values presented by Jafarifar et al.[21]. Initial humidity is set to 1 and temperature to 20°C. Moisture diffusivity is in model defined by function based on Figure 80. Surface factor (3-10 mm/day) defined by inverse analysis in [21] is applied in the model as moisture convection (boundary condition).

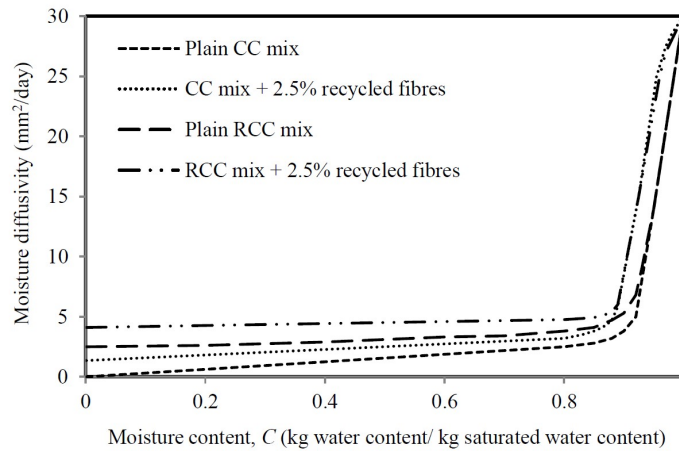


Figure 80: Moisture diffusivity for different mixes [21]

Material model for drying shrinkage is based on water/cement ratio (0.35 or 0.54), aggregate/cement ratio (4.83 or 6.95), humidity calculated by separate model (with the same parameters as in model for moisture transport), curing type (water) and length of curing (90 days).

8.2 Results

Result of one-dimensional drying in ATENA is shown in Figure 81. It is obvious that moisture significantly decreases only in eight top elements, i.e. in depth 40 mm. Below this depth, moisture is in the range of 0.91 to 0.98. Numerical results are compared with experimental ones in Figure 82. Moisture profile in depth 10 mm is in accordance with experimental results. For other profiles, moisture content is lower than in experiments by approx. 6 %.

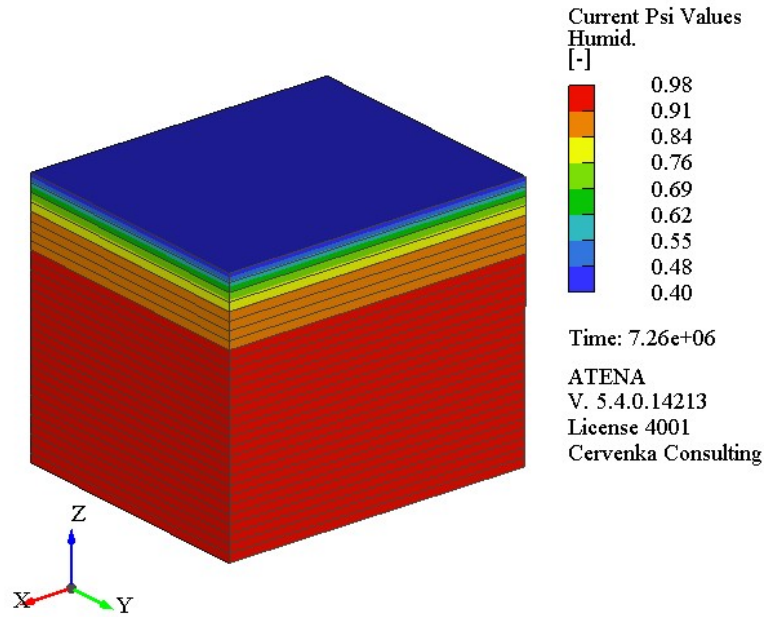


Figure 81: Result of one-dimensional drying in ATENA model

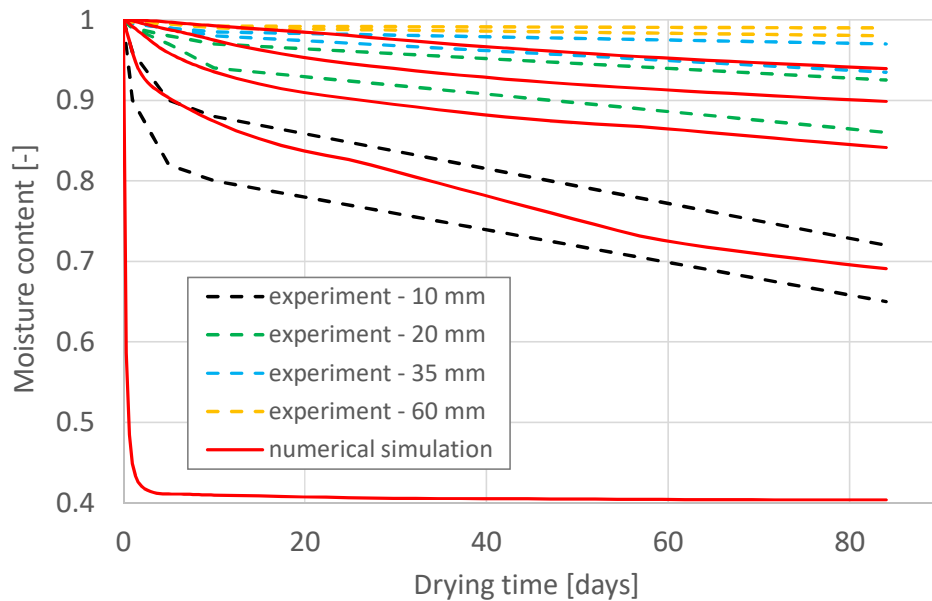


Figure 82: Comparison of moisture profiles from experiments and numerical simulations

For calculation of drying shrinkage, moisture content in the beam must be determined. Based on the calculation of moisture transport in previous model, same parameters are used here. As a result, we get moisture gradient in the beam, see Figure 83. Afterwards, these values are used to calculate drying shrinkage. Numerical results of drying shrinkage are shown in Figure 84 where displacement in x-axis direction is presented. From these values, shrinkage strain is calculated by dividing by 0.275 m (length of modeled part of beam). Strain are compared with experimental results in Figure 85.

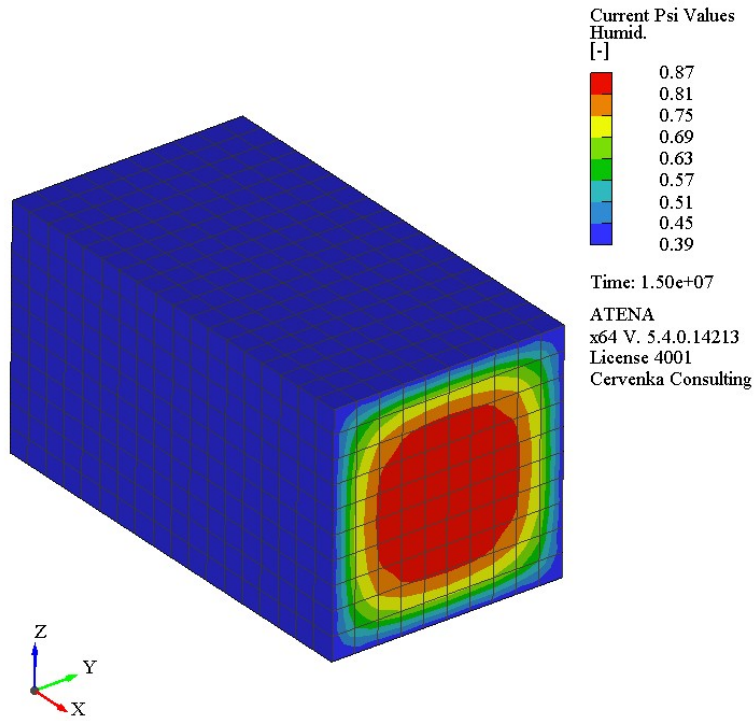


Figure 83: Results of moisture transport used for the calculation of drying shrinkage

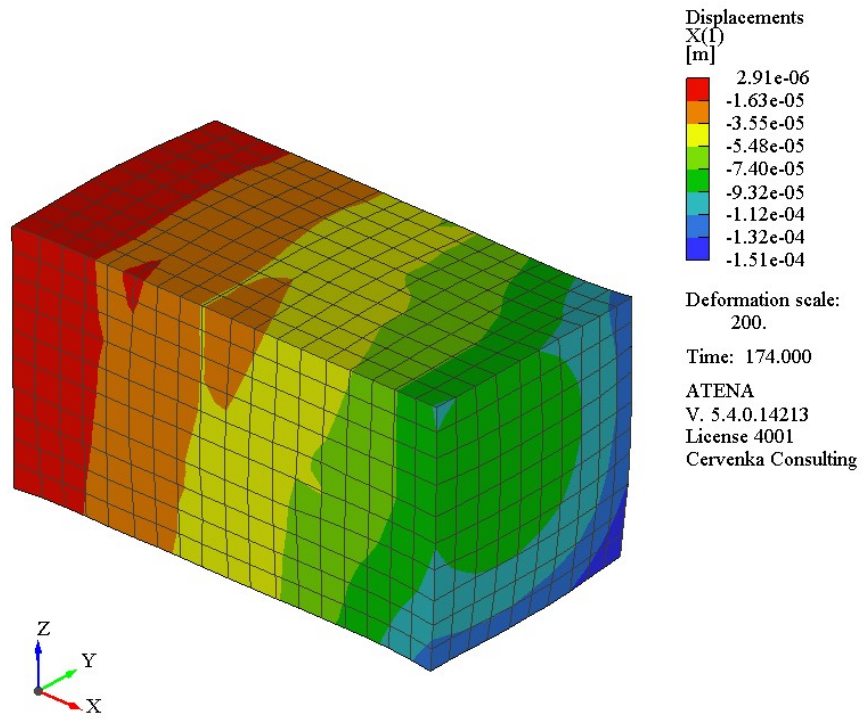


Figure 84: Result of drying shrinkage in ATENA model

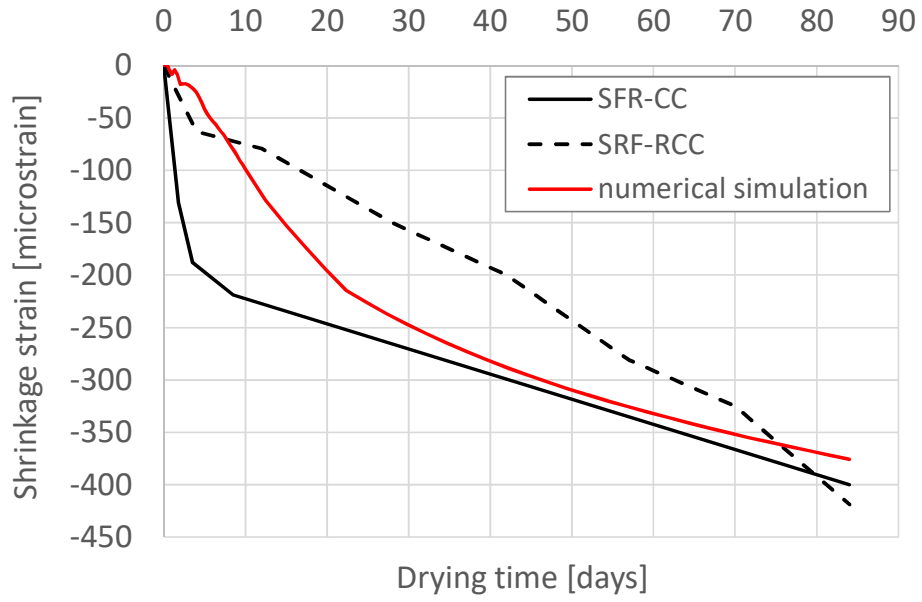


Figure 85: Comparison of shrinkage strain

9 THERMAL ANALYSIS OF HIGH PERFORMANCE FIBER REINFORCED CONCRETE STRUCTURES

This section describes the use of material models specifically developed for FE analysis of long term behavior of high performance fiber reinforced concrete structures. It is assumed that the reader is familiar with creation of finite element models in Atena2D and GiD as well as with the ATENA input files syntax.

9.1 Introduction

In this example, we demonstrate the application of material model CC3DNonLinCementitious2SHCC for simulation of Fire thermal analysis. Set-up of the experiment is shown described in Figure 86. The experiment takes cca 90 minutes, and furnace temperature curve is shown in Figure 89.

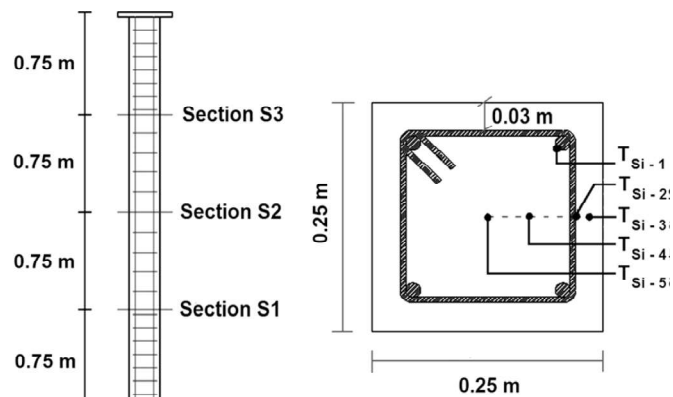


Figure 86: Scheme of the column [22]

The tested column was square section 250 mm x 250 mm with 3 m high. The longitudinal steel reinforcing bars are 4x16mm, stirrups 8mm and 27.24kg steel fibers per m³ of concrete. Total amount of steel was 46,20kg per m³ of concrete.

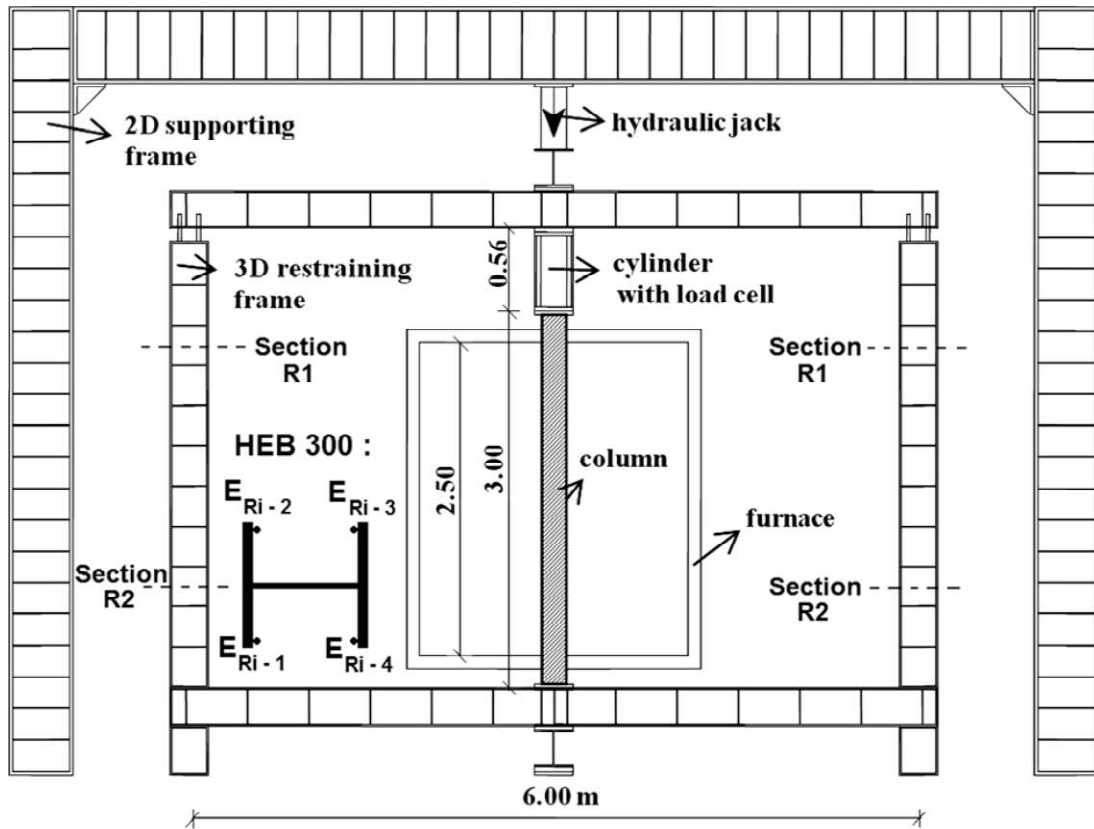


Figure 87: Scheme of the test set-up for fire resistance tests on columns [22]

The model is constructed in GiD-ATENA pre-processor. The problem is modeled with 3D linear brick elements. Only quarter of the model is considered.

9.2 Thermal analysis

The material parameters for the fiber reinforced concrete material are not given in the paper so they are assumed based on the provided amount of fibers and from the previously performed inverse analysis as described in Session 5 and paper [19] and [20].

The relevant parameters and functions for the thermal analysis are listed in Table 14.

Table 14: Material parameters for the thermal analysis

TYPE	CCTransportMaterial	
K_TEMP_TEMP	10 J/(sec C m)	
C_TEMP_TEMP	$4.5 \cdot 10^6$ J/(m ³ C)	
K_TEMP_TEMP_FNC_TEMP_ID		10204
C_TEMP_TEMP_FNC_TEMP_ID		10216

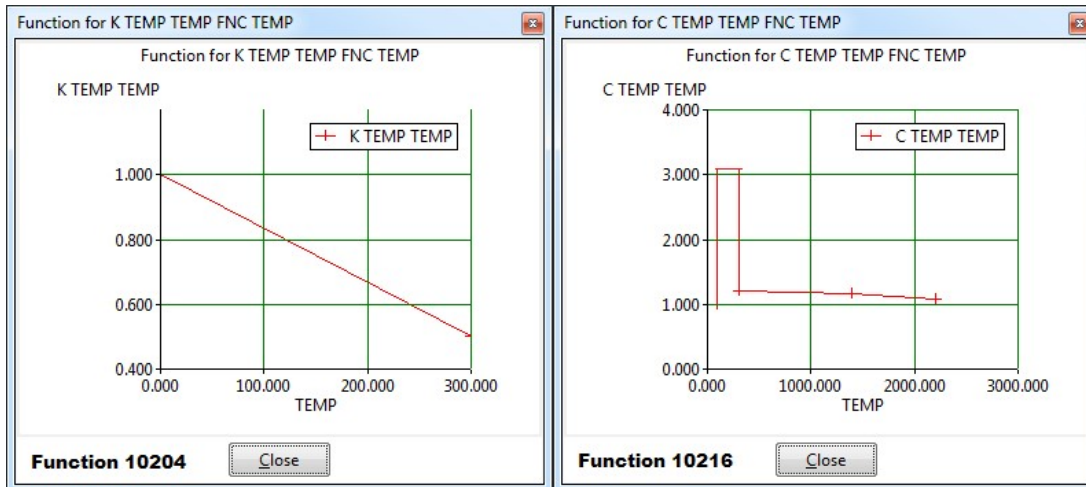


Figure 88: Functions 10204 and 10216 describing the function parameters of CCTransportMaterial

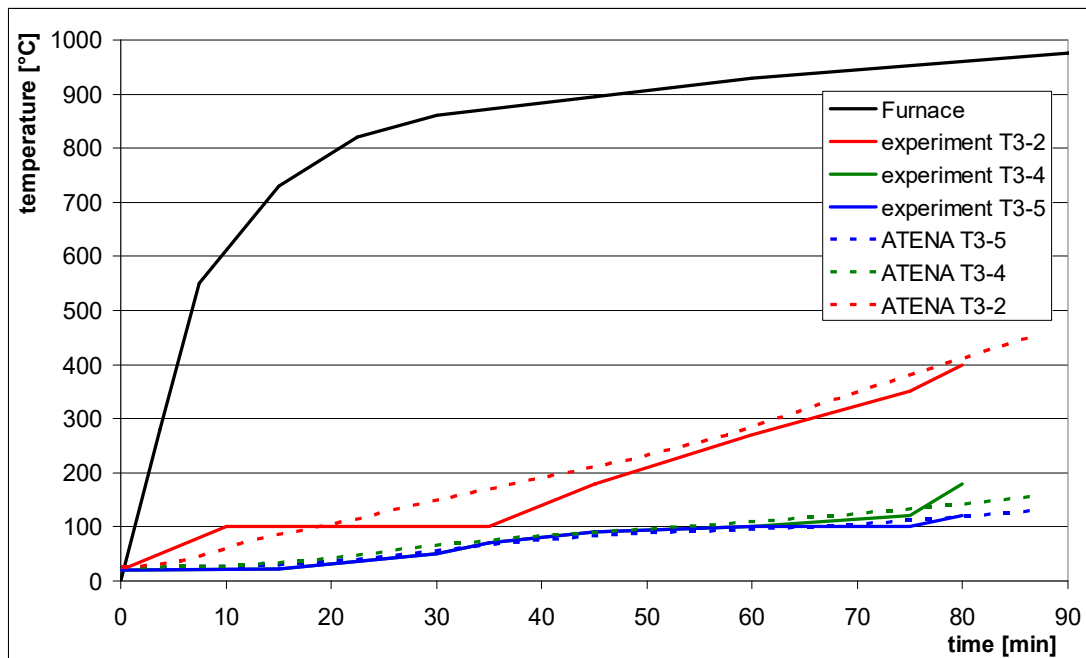


Figure 89: Evolution of temperature in section S3 for experiment and calculation by ATENA [22]

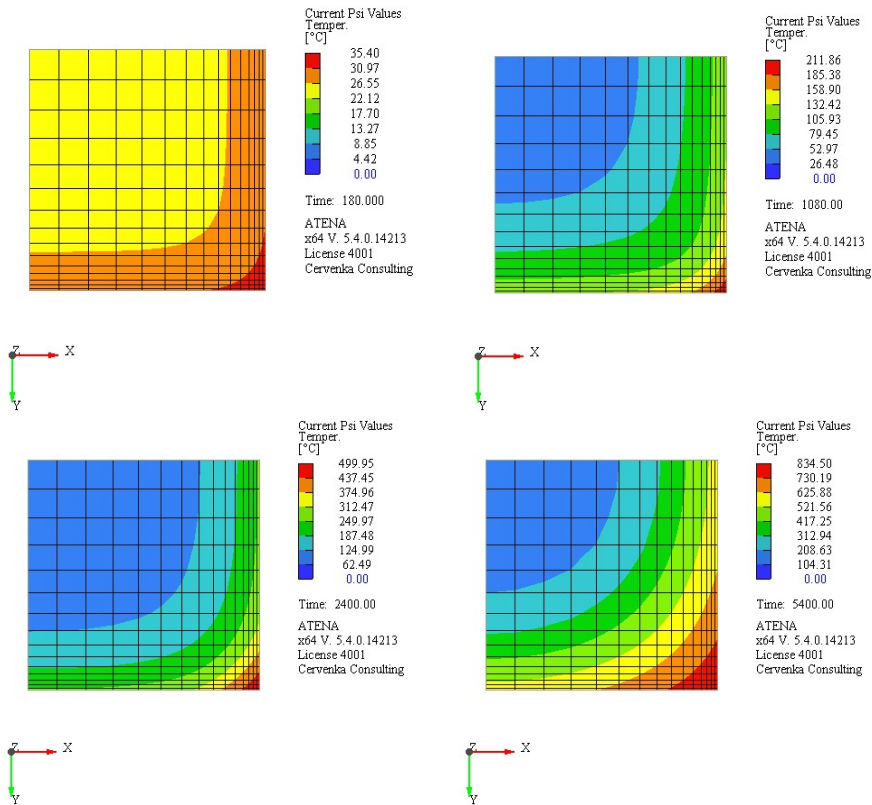


Figure 90: Result in cross-section of column at different times

9.3 Stress analysis

After the thermal analysis is completed the calculated temperature fields are used to perform a stress analysis. The material type CC3DNonLinCementitious2SHCC, i.e. HPCFRC was used for static analysis. The relevant parameters and functions are listed in Table 15. The material parameters are dependent on the temperature as described in Figure 92.

Table 15: Material parameters for stress analysis (units m, MPa)

TYPE	CC3DNonLinCementitious2HPFRC
E	2.993800e+04
MU	2.000000e-01
RHO	2.300000e-03
FT	2.140000e+00
FC	-2.700000e+01
EXC	5.200000e-01
BETA	5.000000e-01
TENSION_SOFT_HARD_FUNCTION	40021
FT_MULTIP	2.100000e+00
CHAR_SIZE_TENSION	1.500000e-02
X_LOC_TENSION	0.000000e+00

COMP_SOFT_HARD_FUNCTION	40022
CHAR_SIZE_COMP	2.500000e-01
X_LOC_COMP	-8.411000e-04
FIBER_VOLUME_FRACTION	3.440000e-03
FIBER_E_MODULUS	3.000000e+04
FIBER_SHEAR_MODULUS	1.500000e+02
FIBER_CROSS_SECTION_FACTOR	9.000000e-01
FIBER_DIAMETER	4.000000e-05
FT_MULTIP	1.100000e+00
TENSILE_STRENGTH_RED_FUNCTION	40024
FIXED	1.000000e+00
AGG_SIZE	2.000000e-02
IDEALISATION	3D

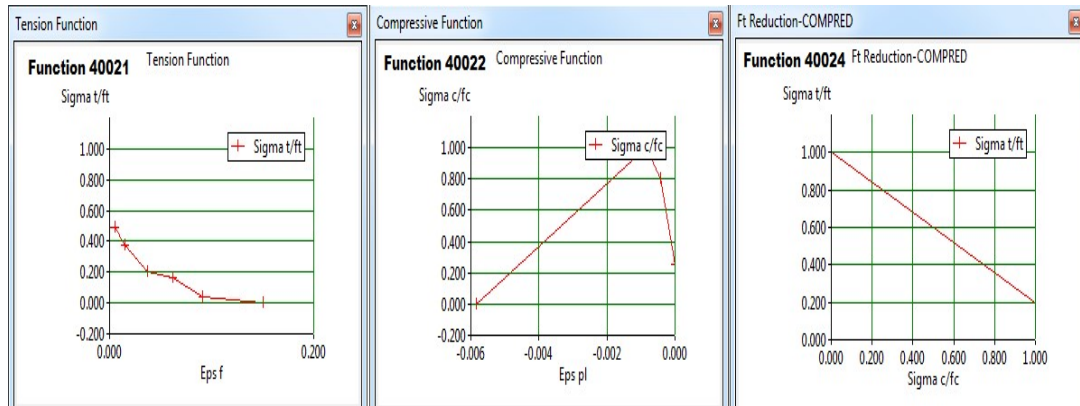


Figure 91: Functions describing the function parameters of CC3DNonLinCementitious2HPFRC

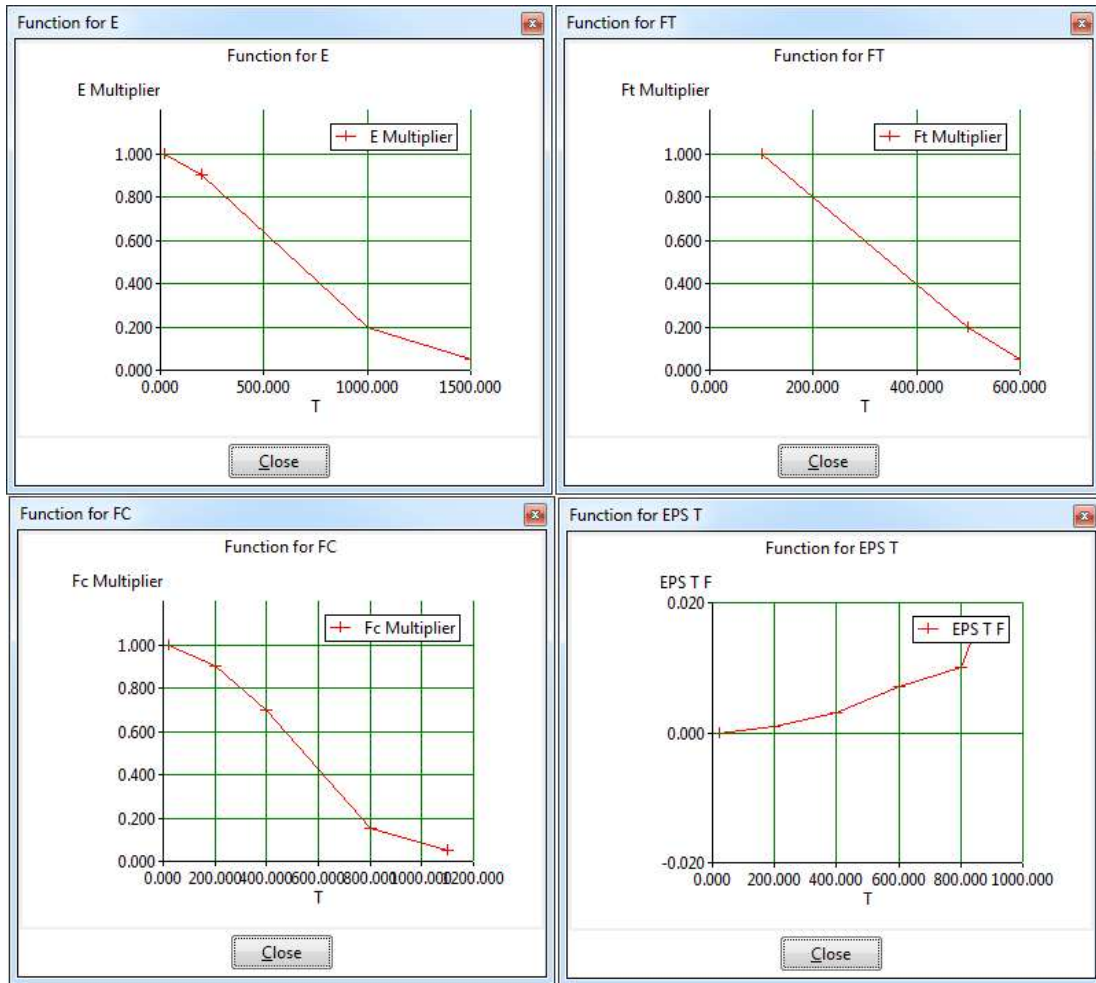


Figure 92: Temperature dependent functions for material CC3DNonLinCementitious2HPFRC

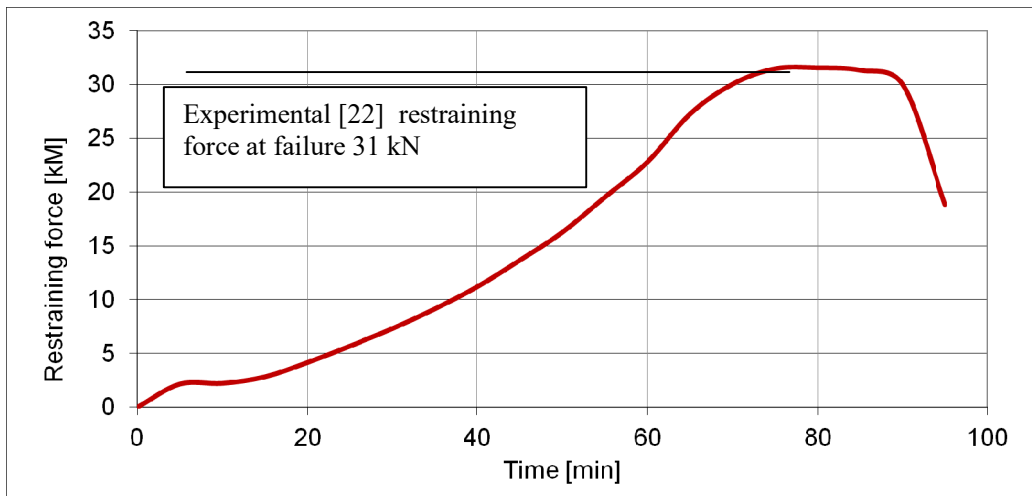


Figure 93: Evolution of the restraining force

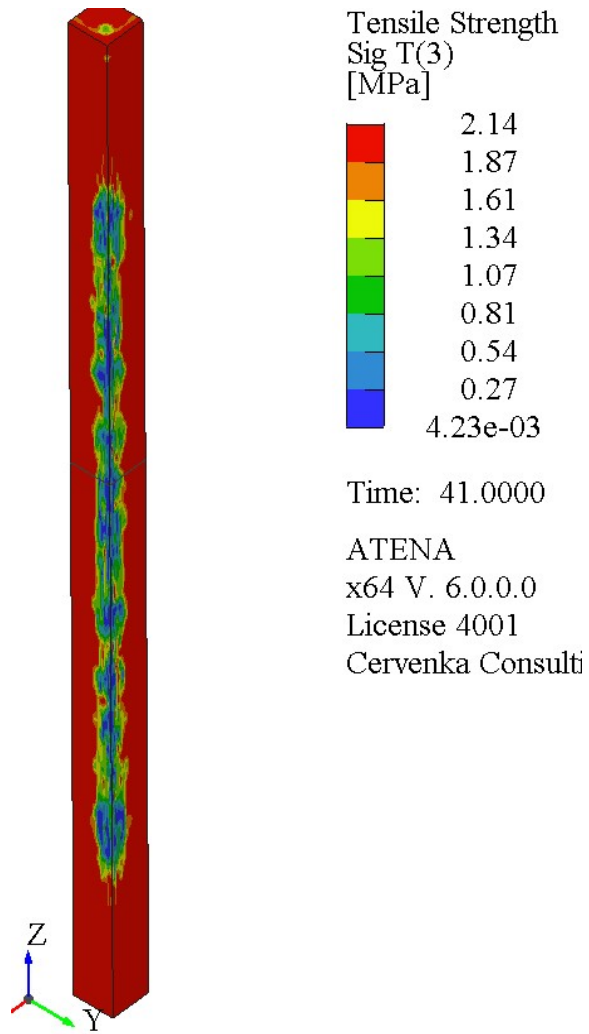


Figure 94: Comparison of damage pattern by extensive spalling near the corners in the experiment and in the numerical analysis

8 APPLICATION OF FRC MATERIAL MODEL

Current significant application of FRC material in the Czech Republic is segmental tunnel lining installed by TBM (tunnel boring machine) during tunnel excavation. Utilization of FRC with steel fibres for segmental tunnel lining promises potential advantages in comparison to the traditionally reinforced concrete structures - efficient manufacturing, lower risk of corrosion, less damage during transport, etc. Červenka Consulting took a part in the project designing precast tunnel segments used in the underground and railway tunnels, see [9] and [10]. Some of the obtained results are presented in this section as a practical example of FRC material model application.

8.1 Vault Bending Tests

Vault bending tests were performed on the whole segments or on a part of the segments. Subject of this experiment was to clarify behavior of the segment under local lateral load. If the laboratory results are known before the numerical modeling, they can be used for inverse analysis instead of three or four point bending tests on beams, described in the previous chapters, in case these tests are not available. The behavior of the segment is similar to the three point bending test.

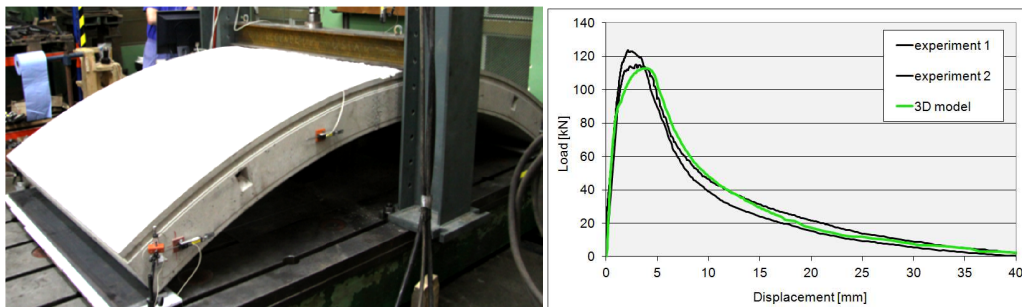


Figure 95: Vault bending test of the whole segment – laboratory test (left), comparison of L-D diagrams of laboratory tests and 3D model

Development of bending cracks in the model is very close to the structural behavior in experiment. Comparison of the final crack in the experiment and the model is shown in Figure 96; the significant cracking areas are marked. The cracks in both experiment and numerical analysis are here strongly localized even in the SFRC material.

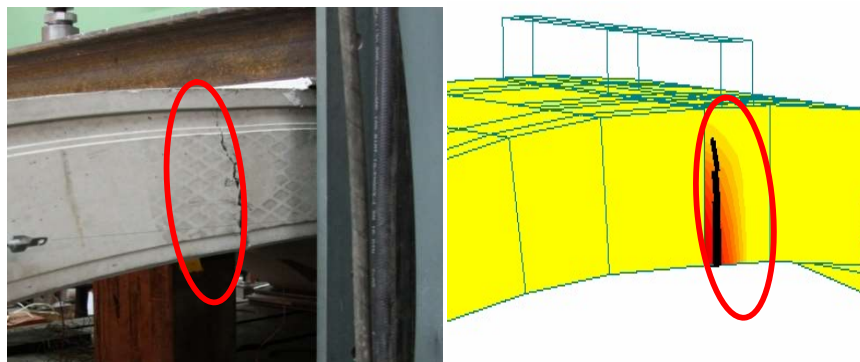


Figure 96: Cracks in SFRC segment – vault bending: experiment (left), numerical simulation (right)

Another vault bending test is presented in Figure 97 and it is performed just on part of the segment. In this case, the experimental results were used for inverse analysis to find appropriate parameters of FRC material model.

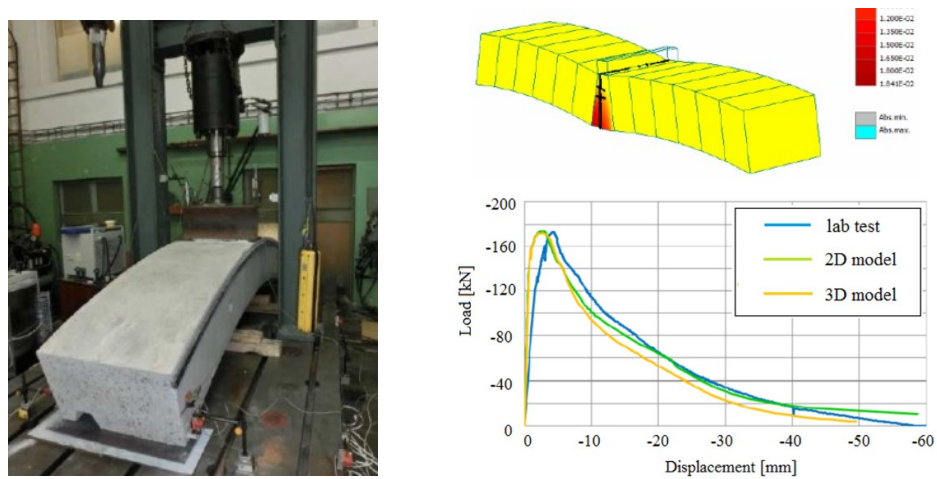


Figure 97: Vault bending test in lab (left), failure of numerical model (top right), load-displacement diagram of test and models (bottom right)

8.2 Model of Segment (Keystone) in Compression

The next analysis contains keystone segment subjected to compression test. The keystone is loaded by concentrated pressure in the central part according to conditions during installation of segments by TBM. Comparison of results and failure mode between the laboratory test and the model (see Figure 98) confirmed that the FRC model works in accordance with the reality.

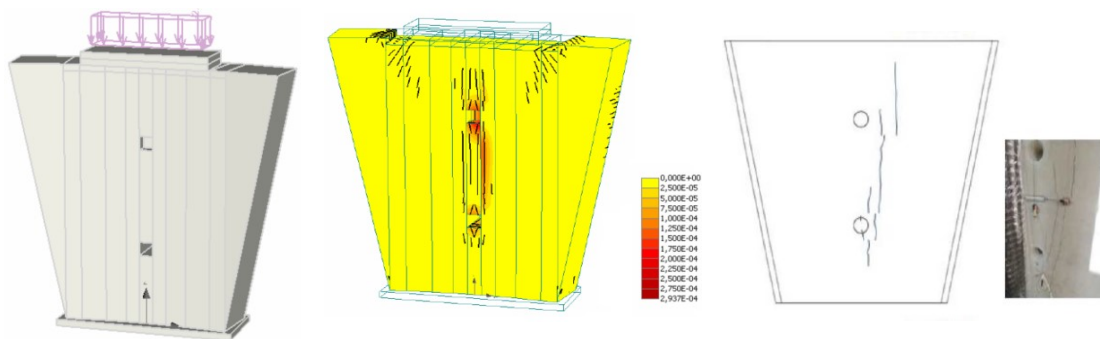


Figure 98: Model of keystone, crack pattern in the model and results of laboratory test

9 CONCLUSION

This first part of this manual provides a step by step instructions for determination of fiber reinforced concrete material model in **ATENA-GiD** interface. In the second part of the manual other examples with other loading types are included.

The important issue in the modeling of FRC material is the appropriate definition of tensile parameters. The measured response of direct tensile test could serve for direct input of the parameters into the material model. Unfortunately, preparation of test sample is complicated and the test is not performed very often. The three or four point bending tests are more common. Results can be also used for the material model, but they cannot be directly input into the model. Inverse analysis of the results must be performed to identify model parameters correctly. Step by step tutorial for such an inverse analysis is provided in Chapter 5.2.

The objective of this tutorial is to provide the user basic principles of FRC modeling and understanding of the material model behavior. For more information about the program the user should consult the ATENA documentation (e.g. [1], [2],[4] or [4]) or contact the program distributor or developers. Our team is ready to answer your questions and help you to resolve your problems.

The theoretical derivations and formulations that are used in the program are described in the Theory manual[4].

10 PROGRAM DISTRIBUTORS AND DEVELOPERS

Program developer: **Červenka Consulting s.r.o.**
Na Hrebenkach 55, 150 00 Prague 5, Czech Republic
phone: +420 220 610 018
fax: +420 220 612 227
website: www.cervenka.cz
email: cervenka@cervenka.cz

The current list of our distributors can be found on our websites:
<http://www.cervenka.cz/company/distributors/>

11 LITERATURE

- [1] ATENA Program Documentation, Part 4-6, ATENA Science – GiD Tutorial, CERVENKA CONSULTING, 2016
- [2] ATENA Program Documentation, Part 8, User’s Manual for ATENA-GiD Interface, CERVENKA CONSULTING, 2015
- [3] ATENA Program Documentation, Part 12, User’s Manual for ATENA Studio, CERVENKA CONSULTING, 2016
- [4] ATENA Program Documentation, Part 1, ATENA Theory Manual, CERVENKA CONSULTING, 2015
- [5] ATENA Program Documentation, Part 11, ATENA Troubleshooting Manual, CERVENKA CONSULTING, 2016
- [6] Consoft - software documentation. Available at: <http://bauwesen.htwk-leipzig.de/nc/de/fakultaet-bauwesen/personen/name/slowik/>
- [7] *fib* Model Code 2010 - Final draft, Volume 1., Lausanne: International Federation for Structural Concrete (*fib*), 2012
- [8] EN 14651, Test method for metallic fibre concrete - Measuring the flexural tensile strength (limit of proportionality (LOP), residual). European Committee for Standardization, B-1050 Brussels, September 2007
- [9] Sajdlová, T. and Pukl, R., (2014): "Optimization of input parameters for material model of fibre reinforced concrete and application on the numerical simulation of tunnel lining", FRC 2014 - Fibre Reinforced Concrete: from Design to Structural Applications, Joint ACI-*fib* International Workshop, Montreal, Canada, p. 13
- [10] Marek, M.; Gramblička, M.; Baláž, D.; Pukl, R. and Sajdlová, T., (2016): "Steel fiber reinforced concrete precast tunnel segments: Design using nonlinear analysis", Podzemní stavby 2016, Prague, Czech Republic
- [11] K. Shimizu, T. Kanakubo, T. Kanda, and S. Nagai, "Shear behavior of steel reinforced PVA-ECC beams," in 13th World Conference on Earthquake Engineering, Conference Proceedings DVD, Paper, Sapporo, Japan, 2004.
- [12] P. Kabele, "Finite element fracture analysis of reinforced SHCC members," in Advances in Cement-Based Materials, Stellenbosch, South Africa, 2009, pp. 237–244.
- [13] E. B. Pereira, "Processes of Cracking in Strain Hardening Cementitious Composites," Ph.D. thesis, University of Minho, 2012.
- [14] P. Kabele, "Multiscale framework for modeling of fracture in high performance fiber reinforced cementitious composites," Eng. Fract. Mech., vol. 74, no. 1–2, pp. 194–209, Jan. 2007.
- [15] P. Kabele, T. Sajdlová, M. Rydval, and J. Kolísko, "Modeling of High-Strength FRC Structural Elements with Spatially Non-Uniform Fiber Volume Fraction," J. Adv. Concr. Technol., vol. 13, no. 6, pp. 311–324, 2015.

- [16] T. Peijs, R. J. M. van Vught, and L. E. Govaert, "Mechanical properties of poly(vinyl alcohol) fibres and composites," *Composites*, vol. 26, no. 2, pp. 83–90, Feb. 1995.
- [17] B. Suryanto, K. Nagai, and K. Maekawa, "Modeling and analysis of shear-critical ECC members with anisotropic stress and strain fields," *J. Adv. Concr. Technol.*, vol. 8, no. 2, pp. 239–258, 2010.
- [18] P. Kabele and T. Kanakubo, "Experimental and numerical investigation of shear behavior of PVA-ECC in structural elements," in *Fifth International Workshop on High Performance Fiber Reinforced Cementitious Composites (HPFRCC5)*, Mainz, Germany, 2007, pp. 137–145.
- [19] W. P. Boshoff and G. P. A. G. van Zijl, "Time-dependent response ECC: Characterisation and modelling of creep and creep fracture," in *International RILEM Workshop on High Performance Fiber Reinforced Cementitious Composites in Structural Applications*, 2006, pp. 125-134.
- [20] T. Sajdlová and P. Kabele, "Numerical analysis of layered UHPFRC-SHCC structural elements," in *3rd International RILEM Conference on Strain Hardening Cementitious Composites (SHCC3-Delft)*, Dordrecht, The Netherlands, 2014.
- [21] N. Jafarifar, K. Pilakoutas and T. Bennett, "Moisture transport and drying shrinkage properties of Steel-Fibre-Reinforced-Concrete," *Construction and Building Materials*, vol. 73, no. 10, pp. 41-50, Dec. 2014.
- [22] J. P. C., Rodrigues, L. Laim., A. M. Correia, Behaviour of fiber reinforced concrete columns in fire, *Composite Structures*, 92 (2010) 1263-1268